

Università degli Studi di Pavia

Physics Colloquia

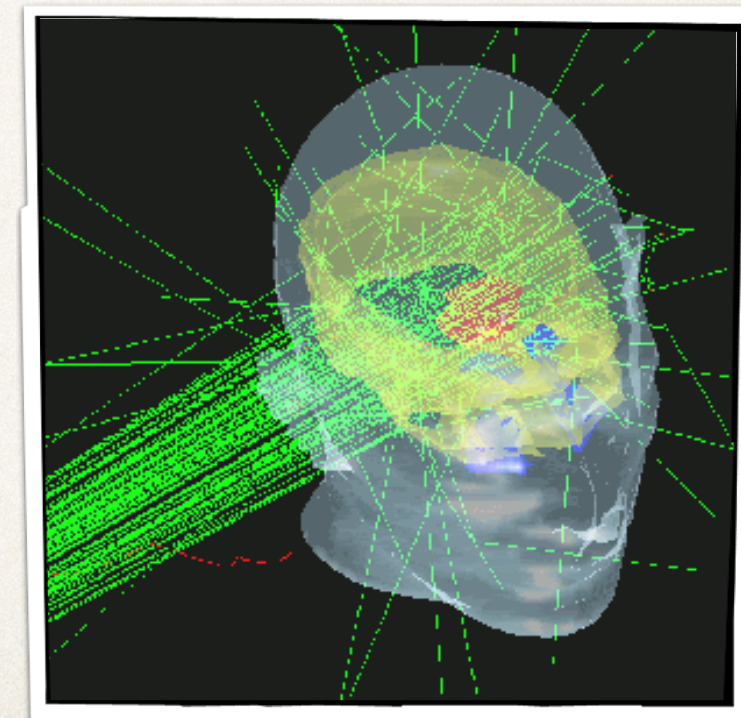
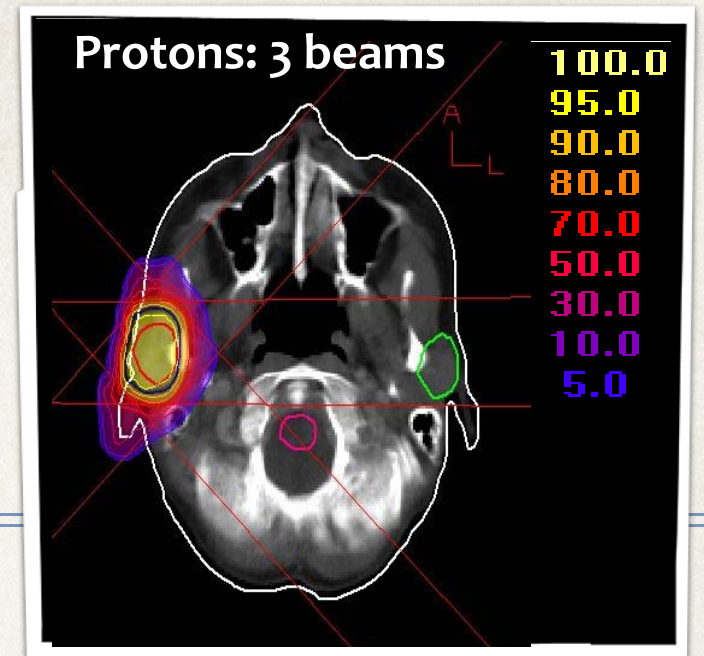
Ilaria Mattei

Recent development on range monitoring in Particle Therapy

22-11-2021

Outline

- ❖ Introduction to **Particle Therapy**
- ❖ **Range Monitoring:**
 - ❖ The Dose Profiler detector
 - ❖ The PAPERICA project
- ❖ **MonteCarlo nuclear DataBase:**
the FOOT experiment
- ❖ **Upcoming Activities**



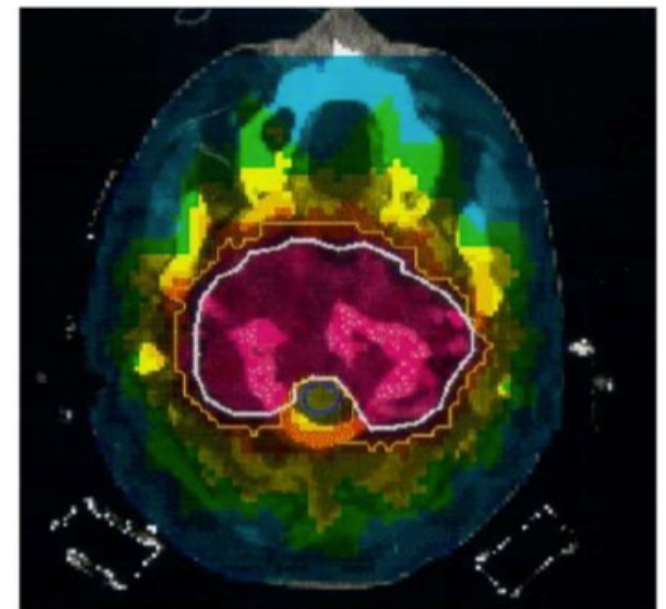
Introduction to Particle Therapy

Tumor Treatment with Radiotherapy

- Mainly **photons** and electrons
- Useful for ~65% of all cancer patients (**localized tumors**), together with surgery
- **Sophisticated imaging (CT)**, superimposition of **several beams**, computed **optimization** and **multi-leaves collimators (IMRT)**
- **Not so expensive** and reliable

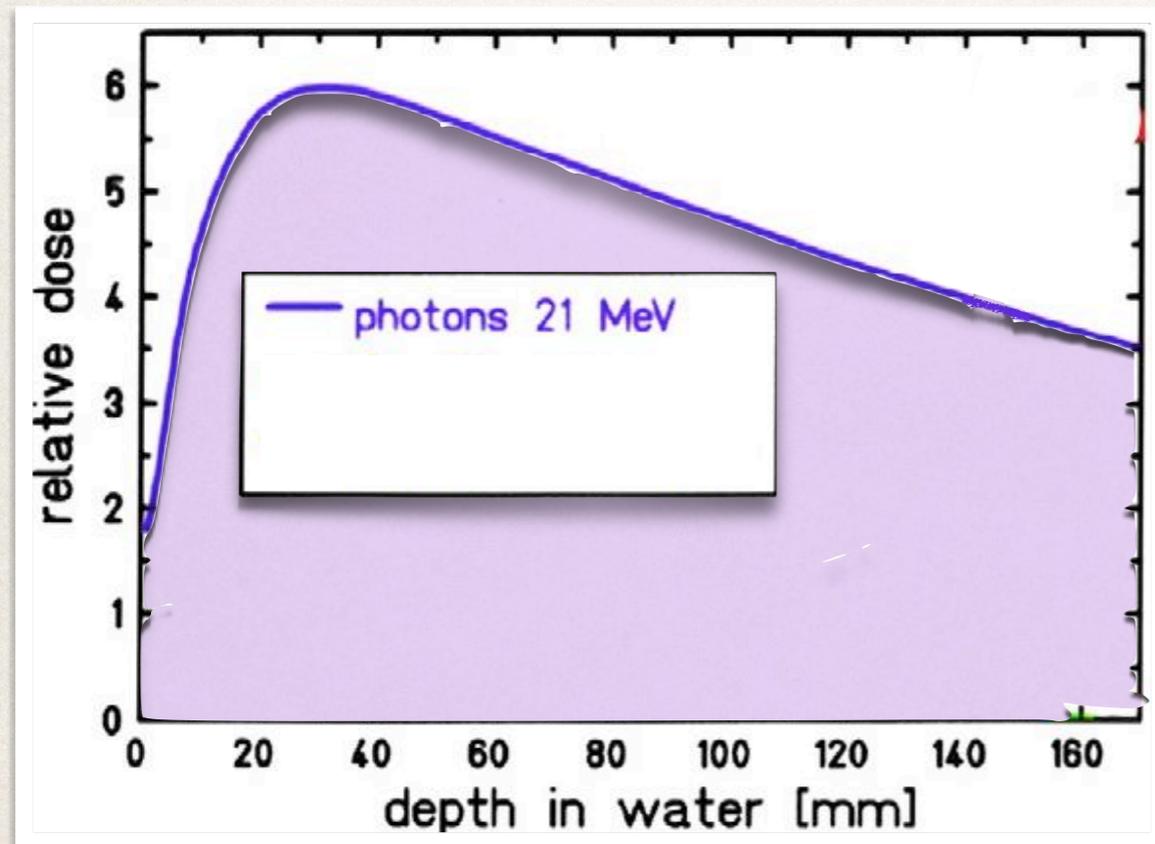
...BUT...

DOSE RELEASED
more CONFORMAL to
the TUMOR volume



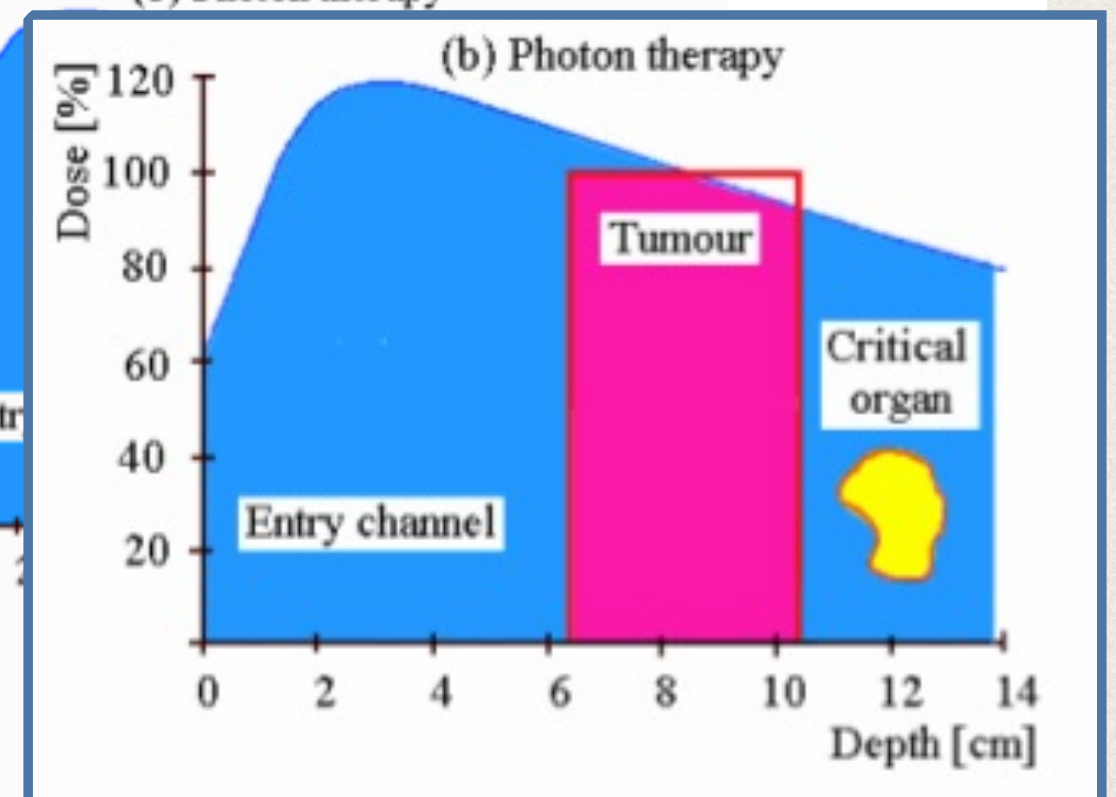
Radiotherapy: Dose Deposition

...**BUT** the energy release is not sparing healthy tissues.



$$Dose = \frac{dE_{abs}}{dm} [Gray]$$

The RT dose distribution implies a large and unwanted dose delivered to healthy tissues.



Tumor treatment in EU

Many tumors are not treated...

- ❖ Anatomy does not permit surgery
- ❖ Radioresistant tumors
- ❖ Tumor position close to Organs At Risk (OAR)

EU Report 2000

- No cure non regional
- Surgery
- RadioTherapy
- SU+RT combined
- Other (chemo)
- No cure loco-regional



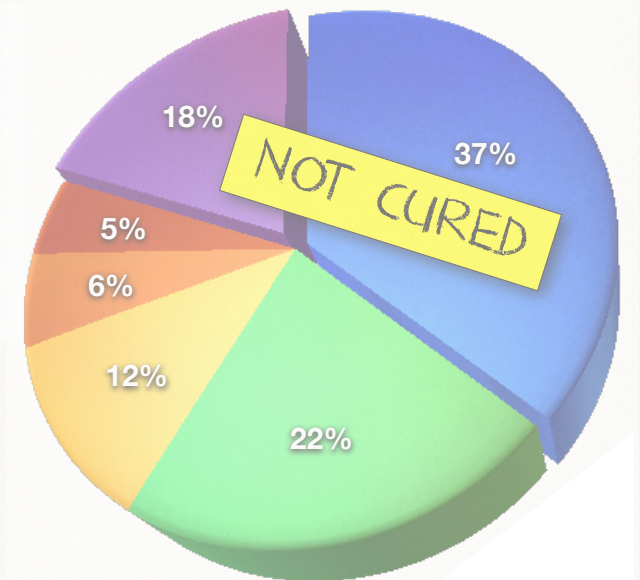
Tumor treatment in EU

Many tumors are not treated...

- ❖ Anatomy does not permit surgery
- ❖ Radioresistant tumors
- ❖ Tumor position close to Organs At Risk (OAR)

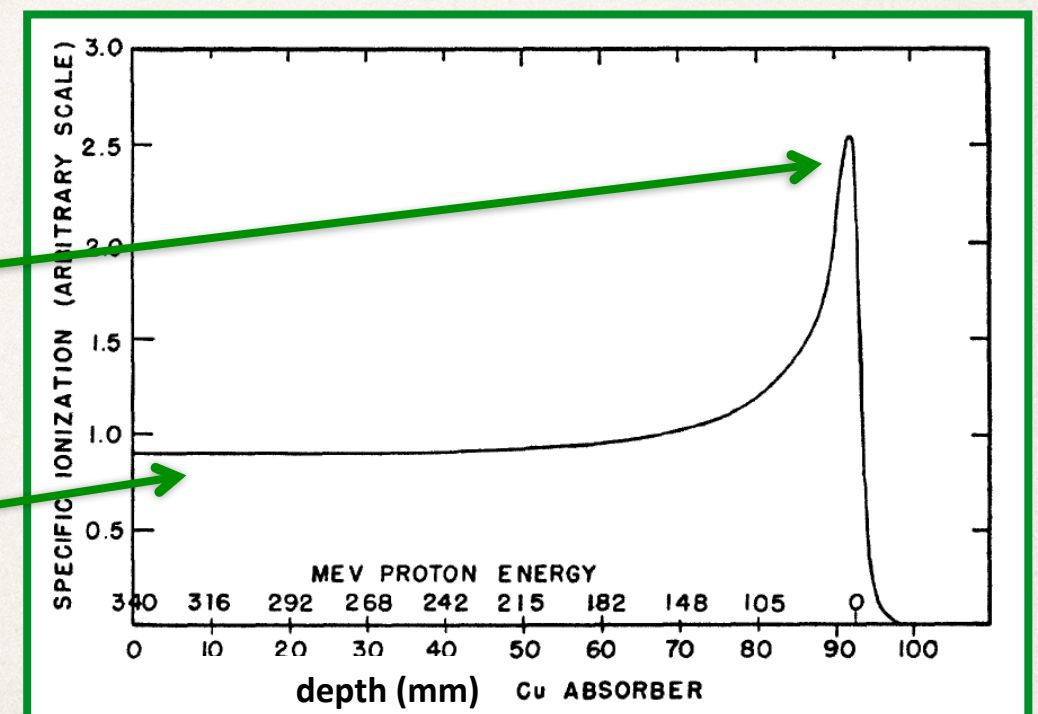
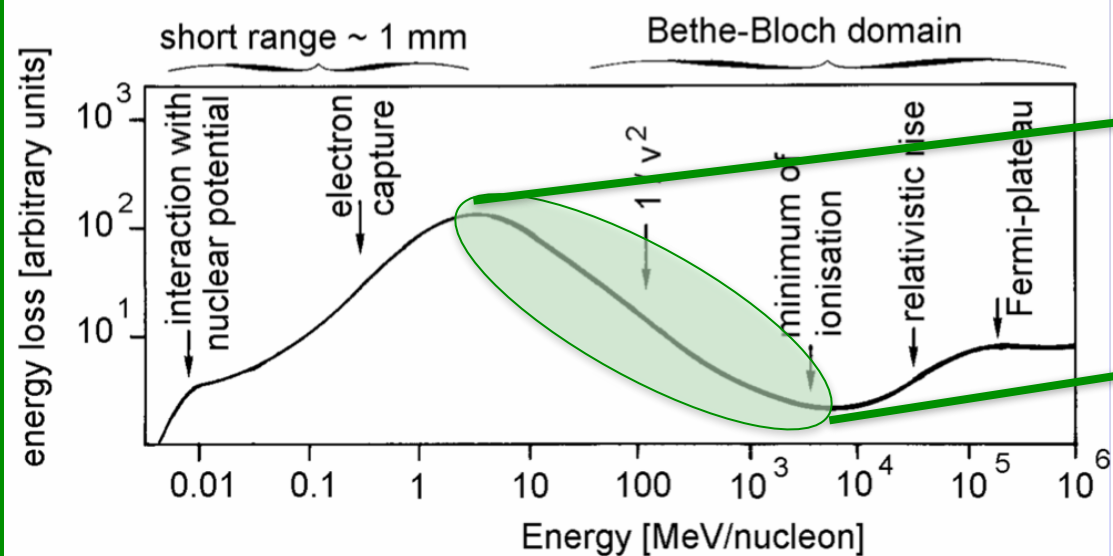
EU Report 2000

- No cure non regional
- Surgery
- RadioTherapy
- SU+RT combined
- Other (chemo)
- No cure loco-regional



...BUT PHYSICS CAN HELP (Wilson 1964)

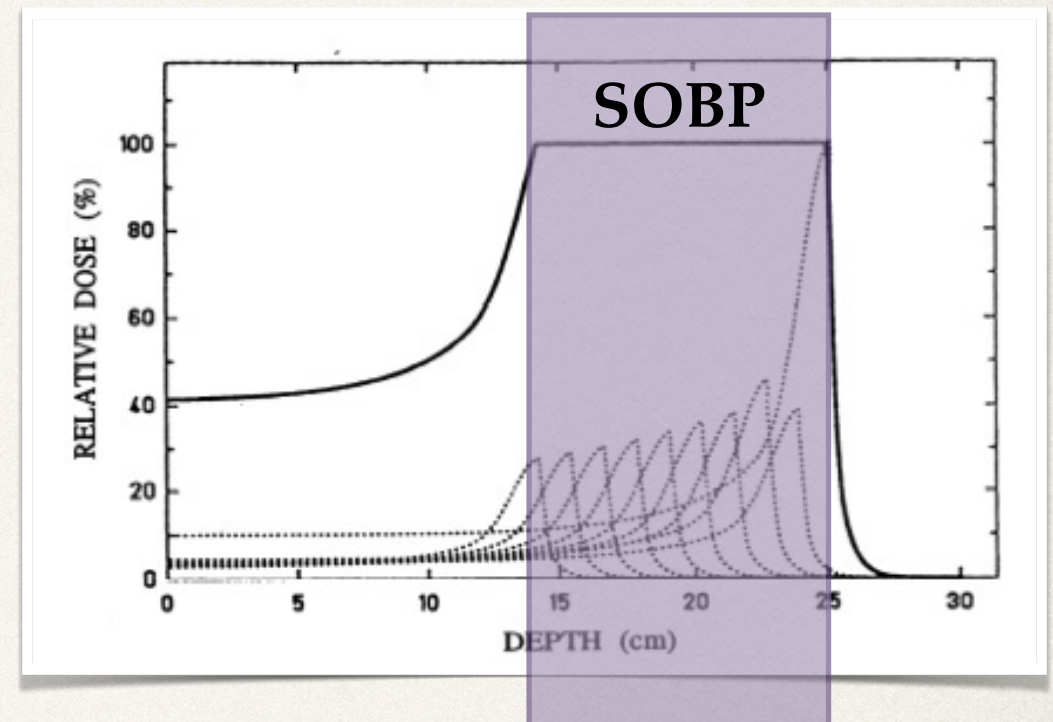
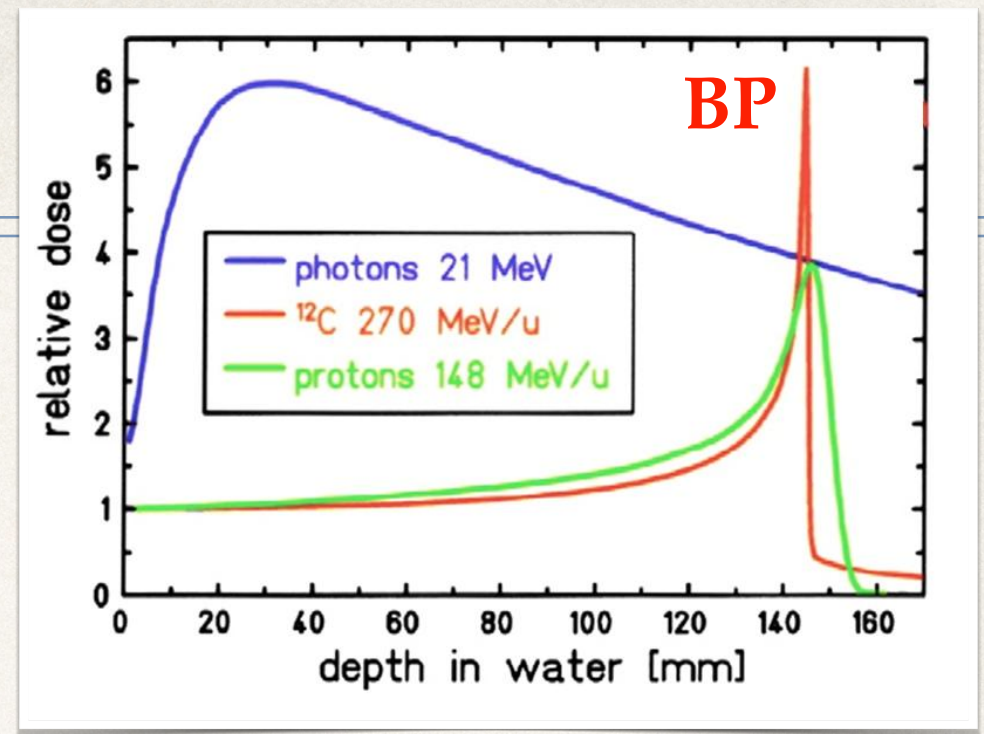
CHARGED PARTICLES (HADRONS) ENERGY LOSS in MATTER



Particle Therapy

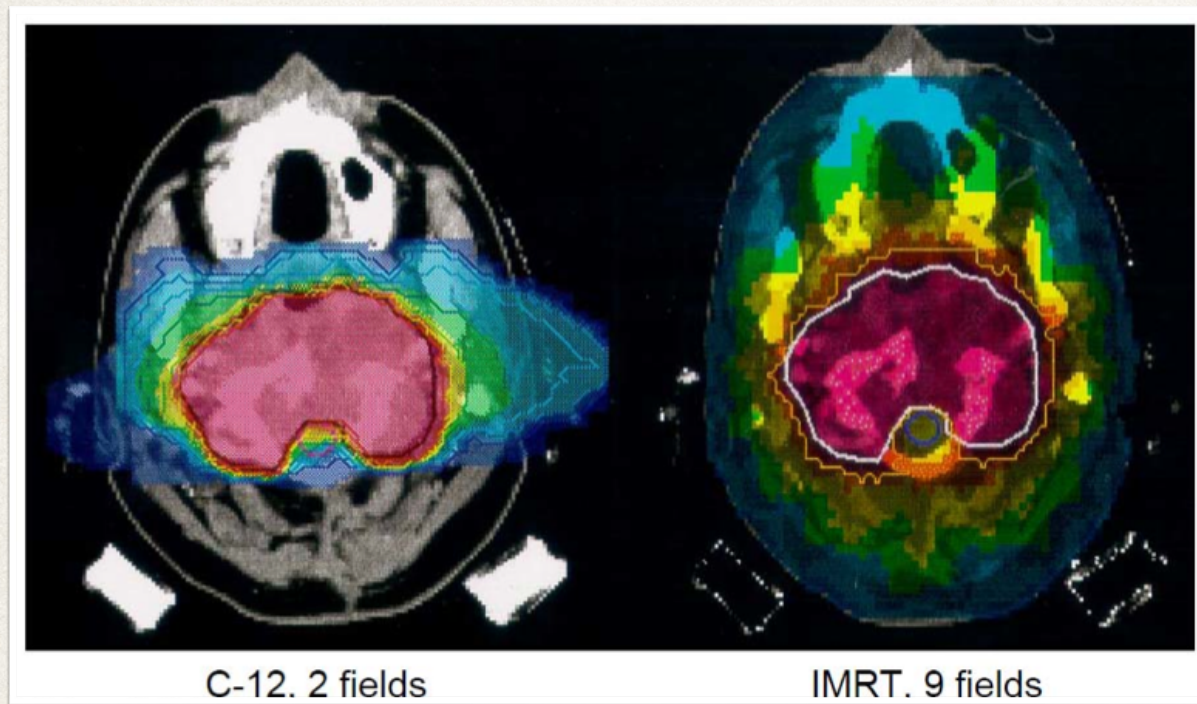
- ❖ Hadron beams (p, ^{12}C , ^{16}O , ^4He ..)
- ❖ Highest dose release (Bragg peak) at the end of the particle range, sparing normal tissues
- ❖ Particle range function of the beam energy and density of crossed material
- ❖ Dose decrease rapidly after the BP
- ❖ Several pencil beams can be combined in order to “shape” the maximum dose release region
=> Spread Out Bragg Peak (SOBP)

Localized Dose Distribution



Particle Therapy: Dose Deposition

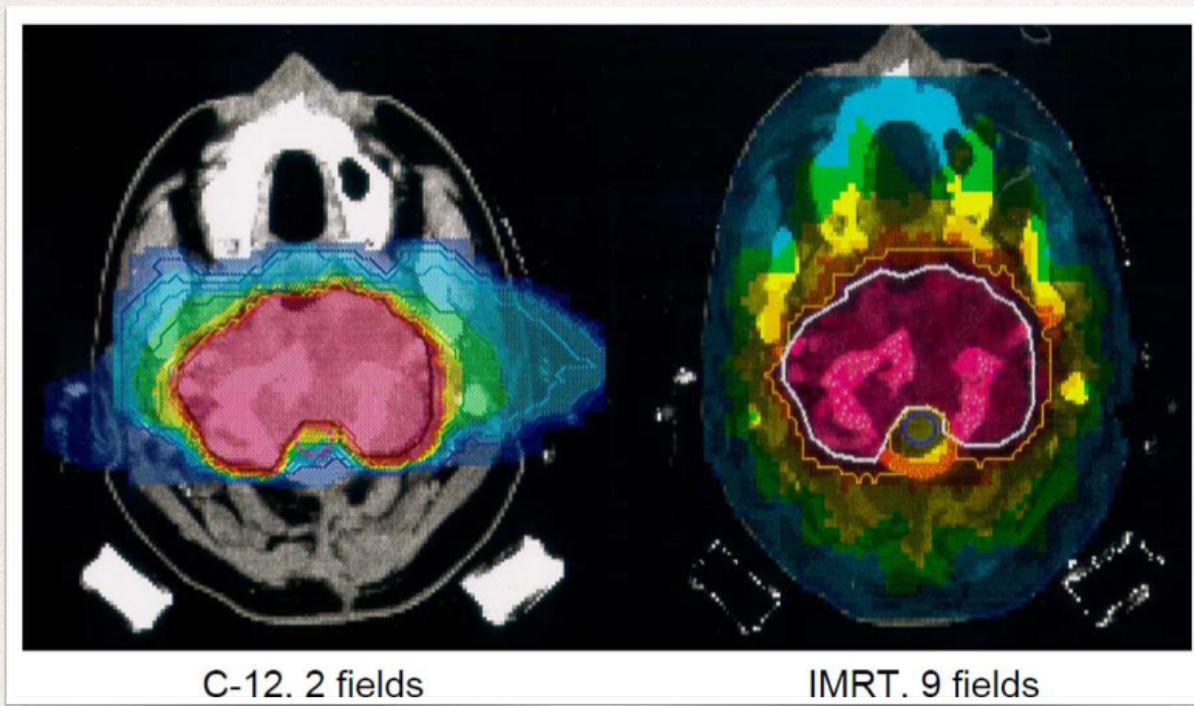
^{12}C (PT) vs IMRT



The dose deposition can be very conformal to the tumor volume both for PT and RT, but with PT healthy tissues and critical organs are better saved.

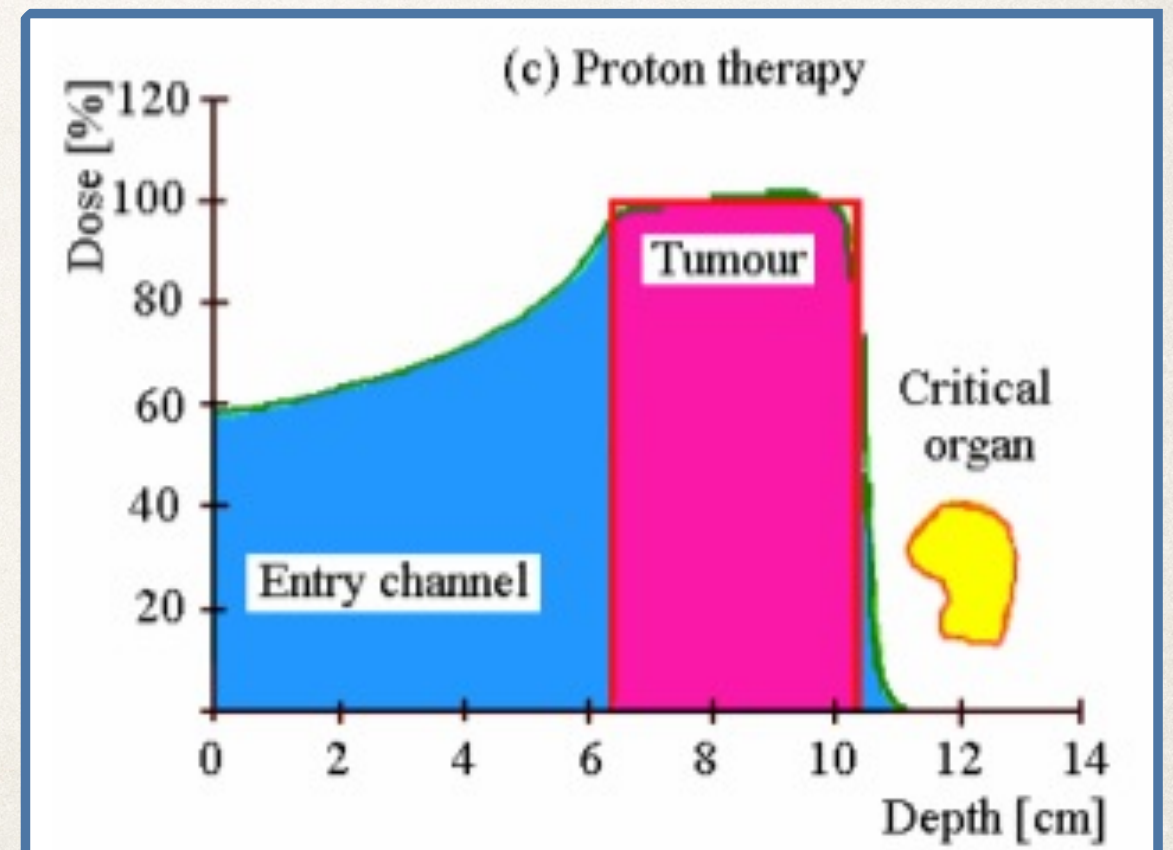
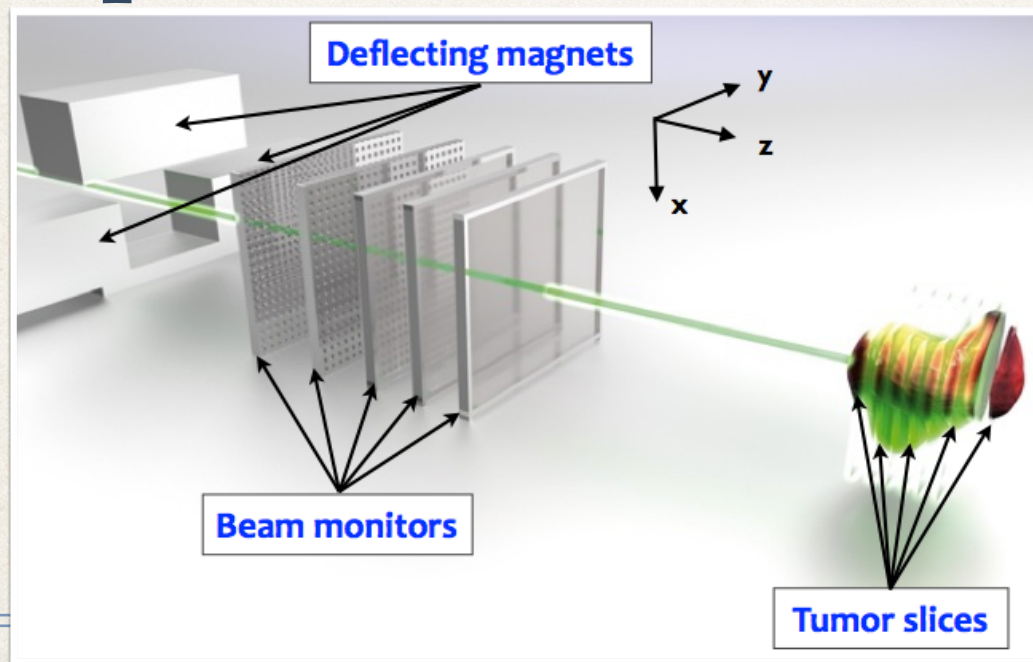
Particle Therapy: Dose Deposition

^{12}C (PT) vs IMRT



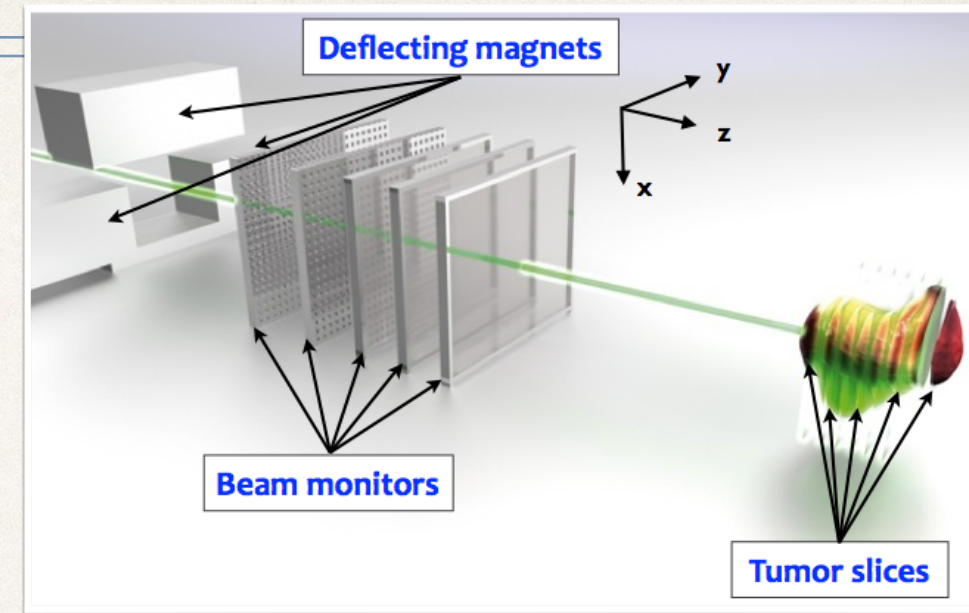
The dose deposition can be very conformal to the tumor volume both for PT and RT, but with PT healthy tissues and critical organs are better saved.

PT pencil beam scanning

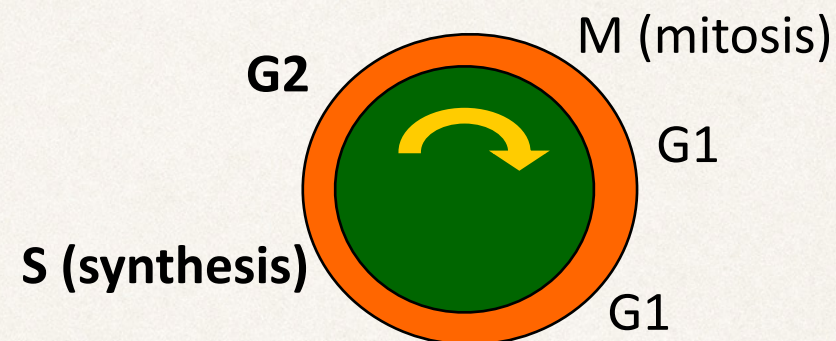


Particle Therapy: Treatment

- ❖ p: 50 - 250 MeV
- ❖ ^{12}C : 80 - 400 MeV / u
- ❖ Total Dose: 20 - 70 Gy
- ❖ Treatment delivered in 2 Gy fractions



- => 4R:
- ◆ Reoxygenation
 - ◆ Redistribution
 - ◆ Repopulation
 - ◆ Repair



Radiations: Biological Damage

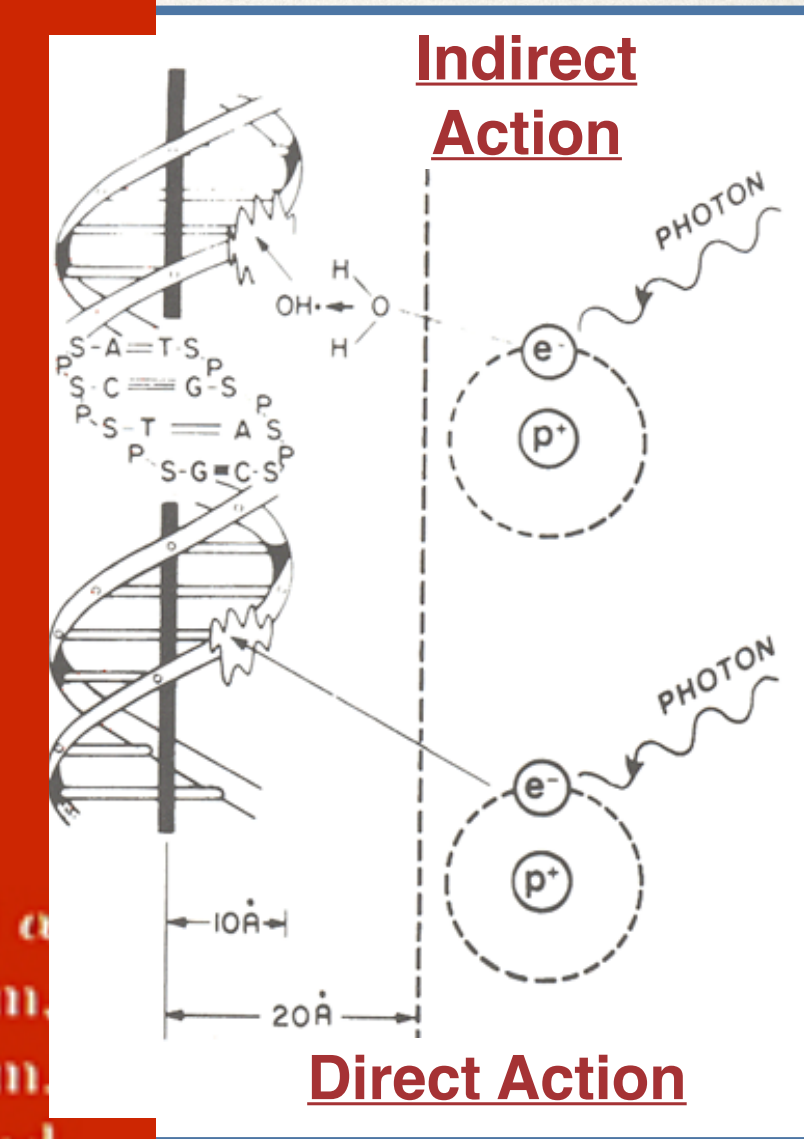
Directly related to the DNA damage:

- ❖ **Indirect Action:** by free radicals
- ❖ **Direct Action:** the radiation breaks directly the DNA helix (SSB, DSB)

Cells are able to repair DNA damages induced by radiations, **EXCEPT** for DSB.

The Linear Energy Transfer (LET) gives an estimation of the radiation biological damage

$$LET = \frac{\Delta E}{\Delta x} \text{ (keV}/\mu\text{m)}$$



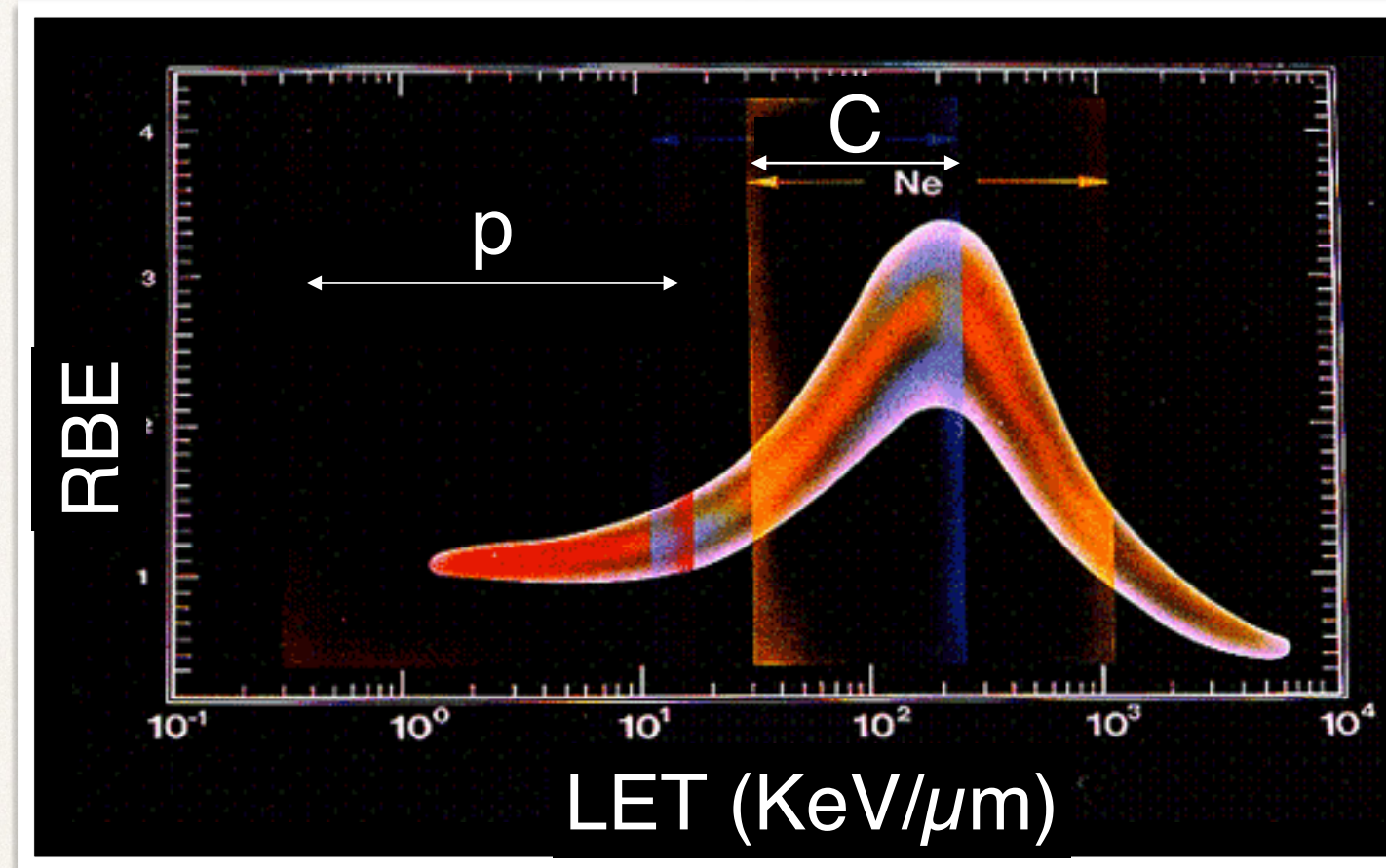
PT: Biological Damage

❖ Relative Biological Effectiveness

$$RBE = \frac{D_{\gamma}}{D_{ch}} \Big|_{iso}$$

PT allows the use of higher LET particles with respect to photons (RT) inducing more direct DNA damages:

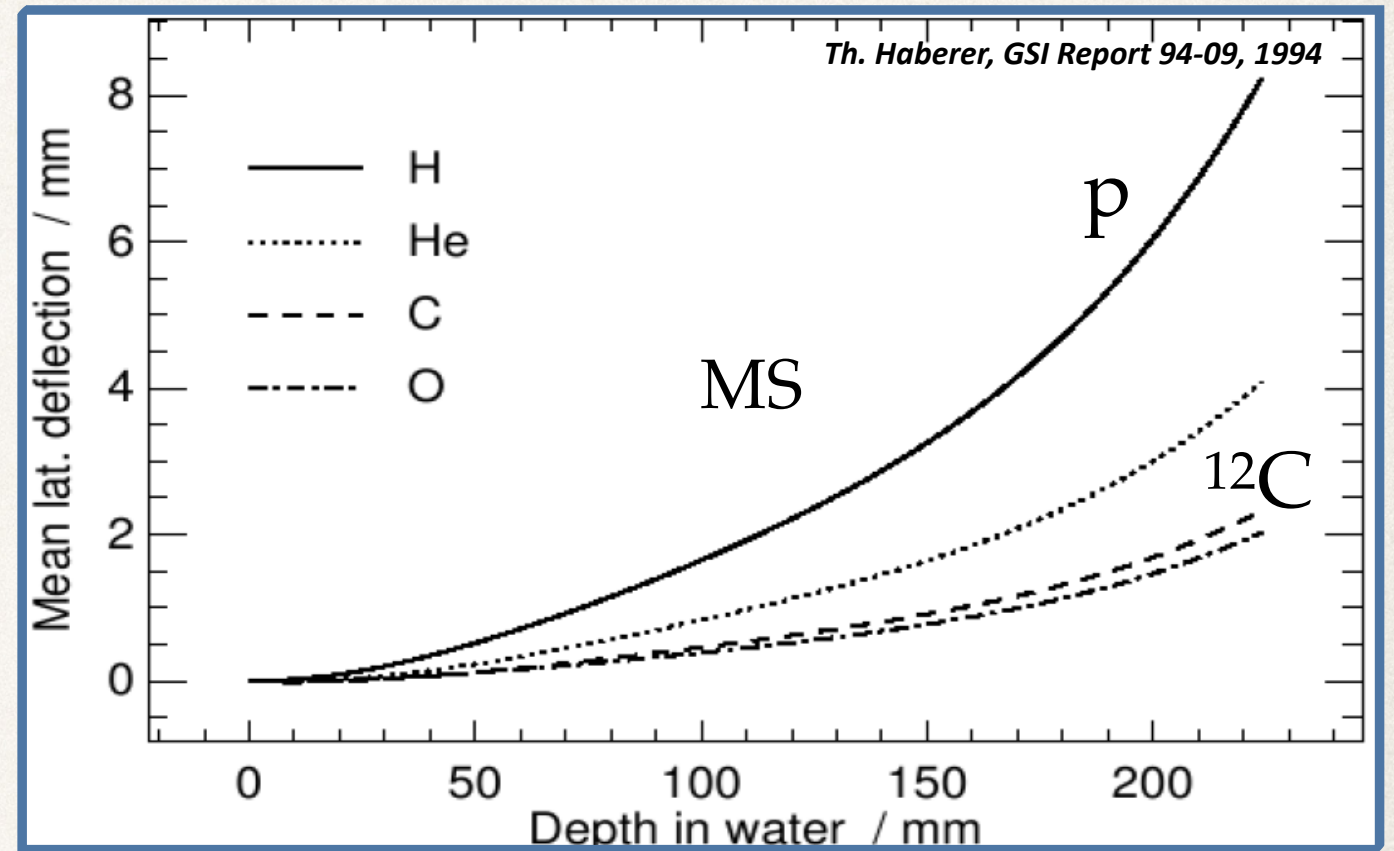
- ❖ **high RBE**
- ❖ **not sensitive to oxygen** => same effect on hypoxic/well oxygenated tumor regions



PT has a higher radiobiological effectiveness with respect to RT.

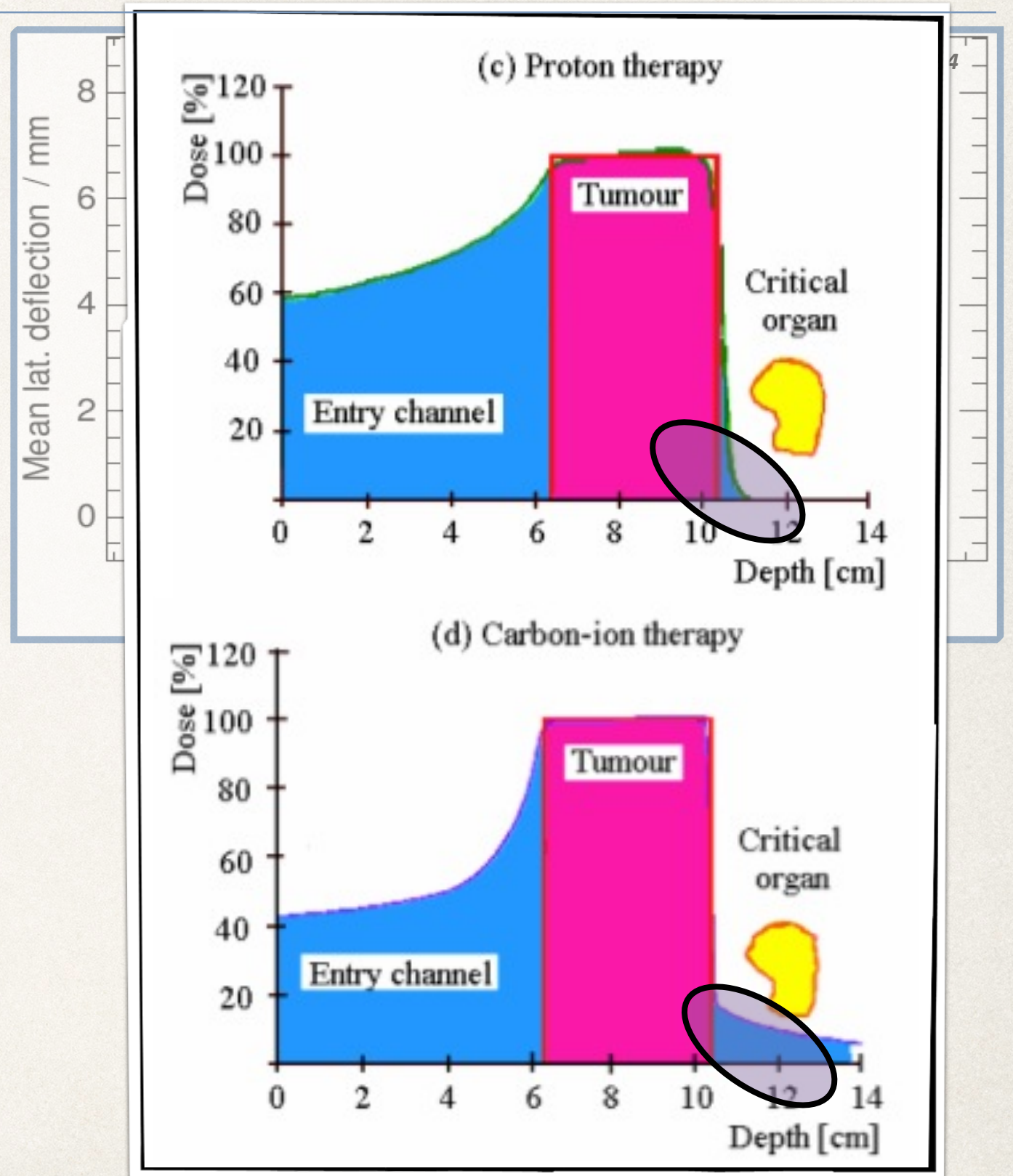
Particle Therapy: features

- ❖ Charged particles suffer multiple scattering
=> lateral beam spread
($\propto Z_{\text{mat}}, (p\beta c)^{-1}, \sqrt{x}$)



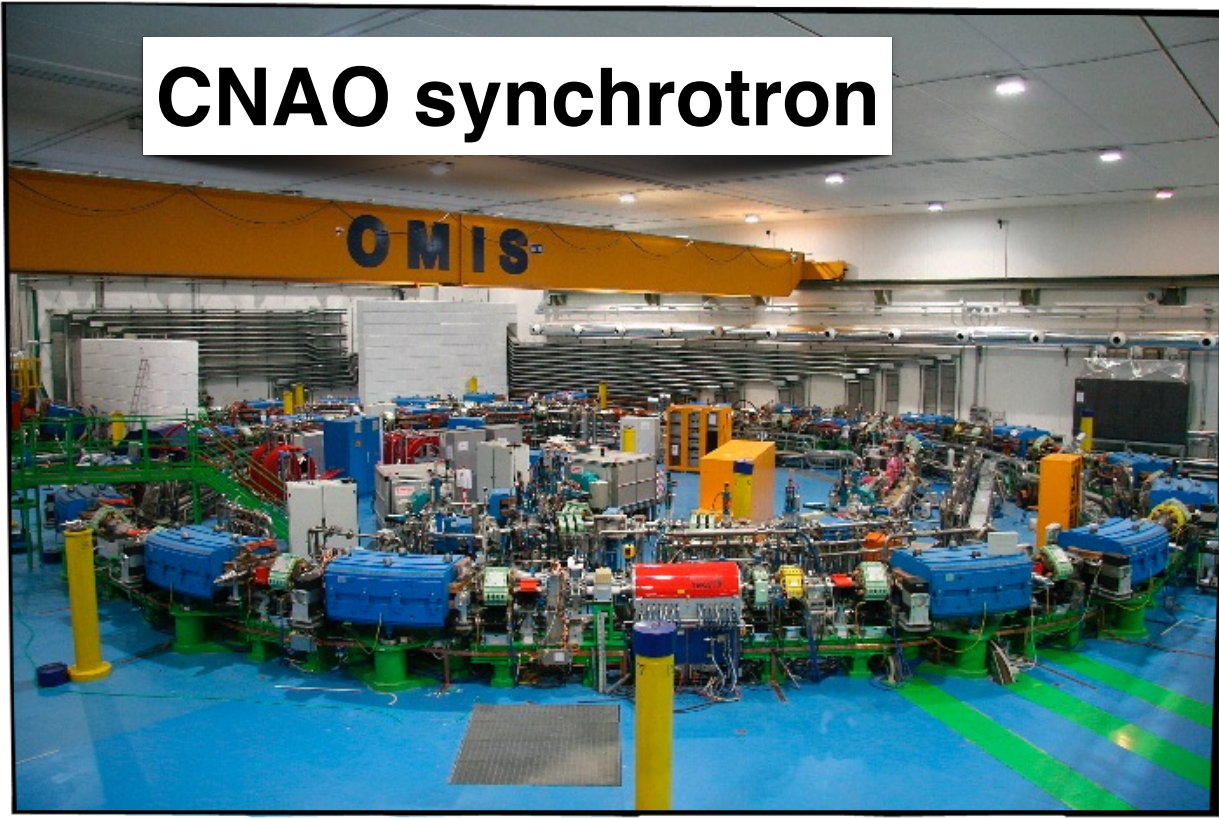
Particle Therapy: features

- ❖ Charged particles suffer multiple scattering \Rightarrow lateral beam spread ($\propto Z_{\text{mat}}, (p\beta c)^{-1}, \sqrt{x}$)
- ❖ Particles with $A > 1$ undergo **nuclear fragmentation** \Rightarrow BP tail

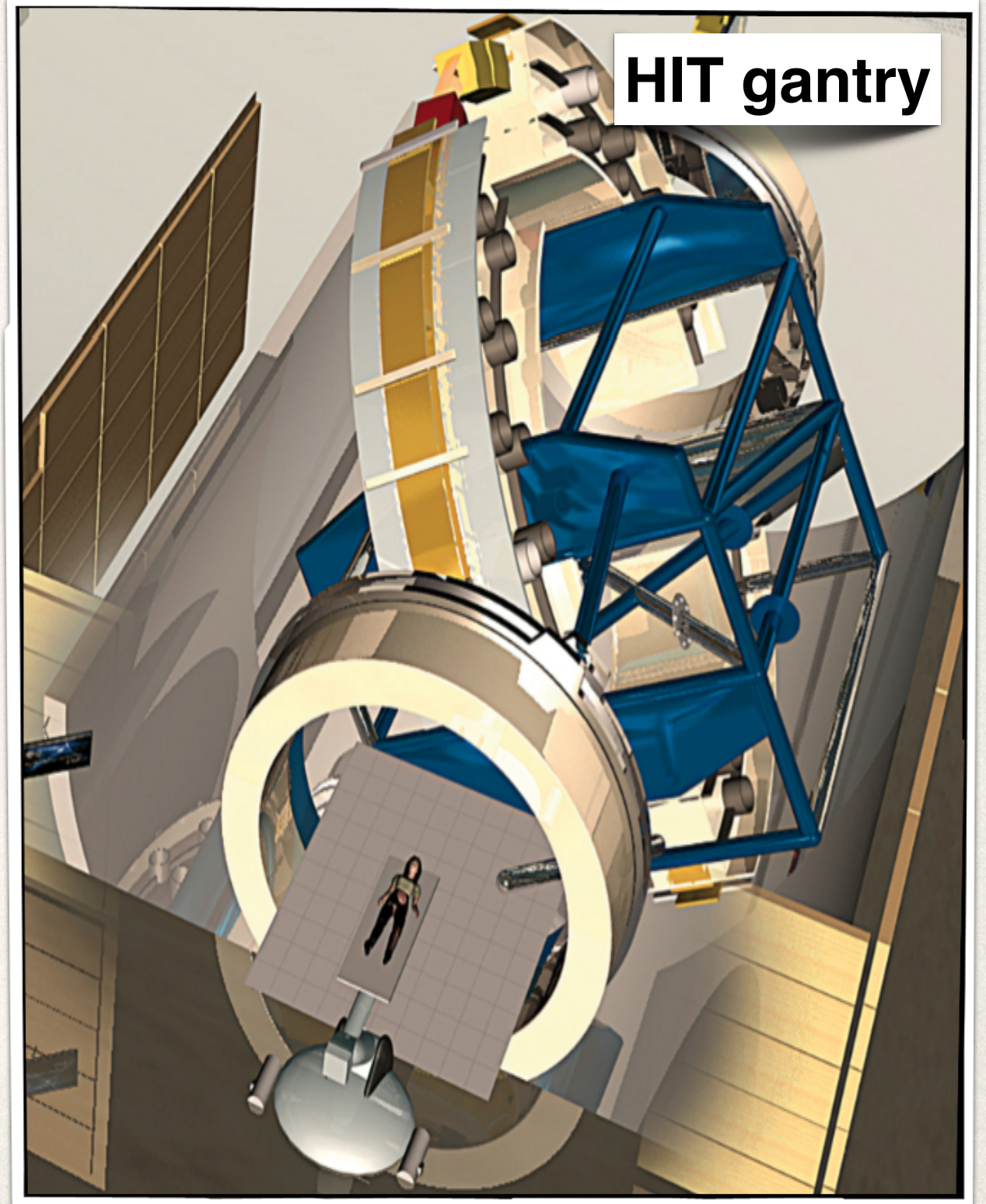


Particle Therapy: features

CNAO synchrotron



HIT gantry



- ❖ PT is more expensive than RT: the beam delivery is a complex work of engineering

Particle Therapy in the World

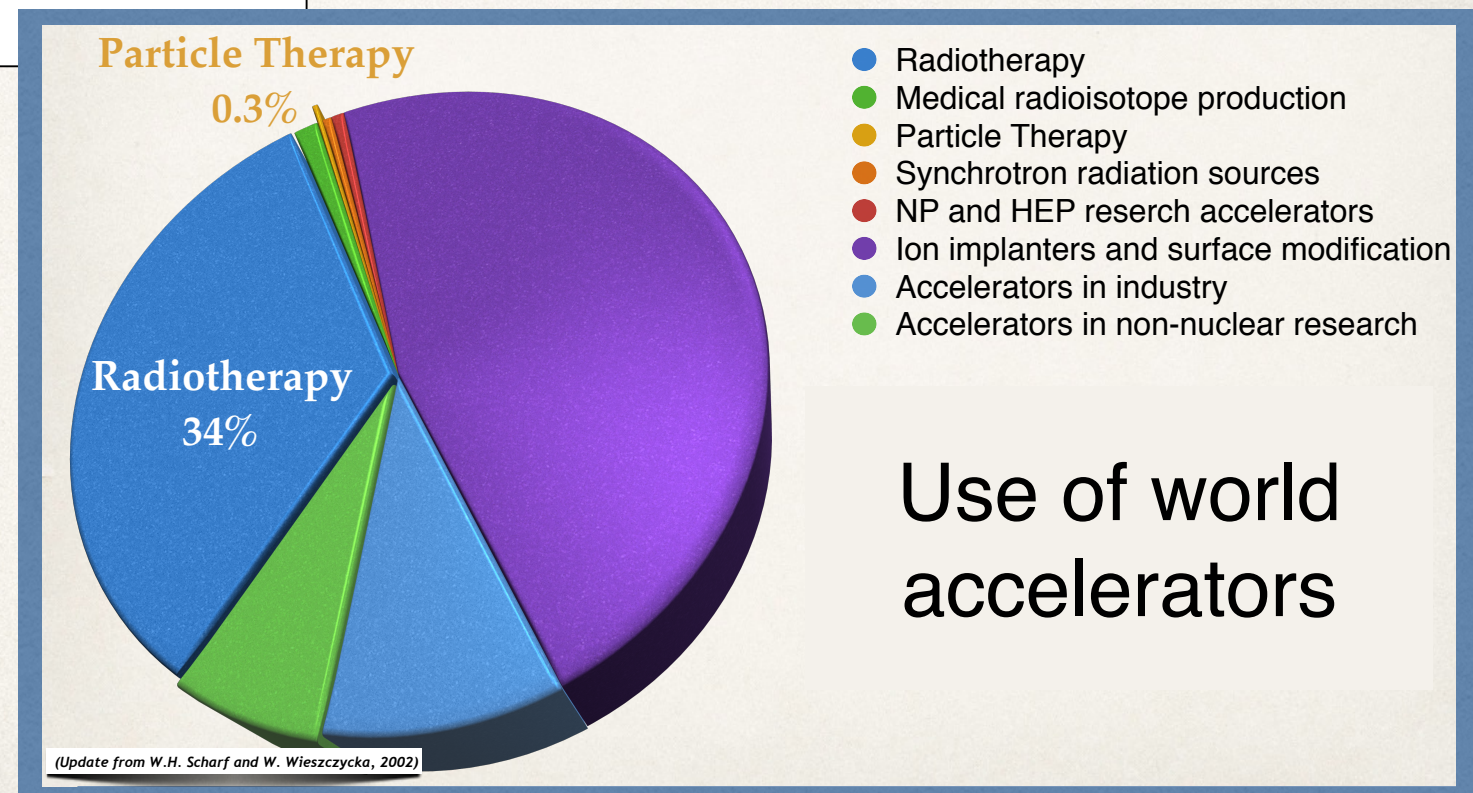
Country	Facilities in operation		Facilities planned (or under construction)		Patients treated (operative facilities)	
	Protons	Light ions	Protons	Light ions	Protons	Light ions
USA	16	0	15	0	44458	
Europe	13	2	15	1	27479	1473
Japan	9	4	3	1	13859	11055
Russia	3	0	2	0	6701	
China	1	2	2	1	1078	249
South Korea	1	0	1	1	1158	
South Africa	1	0	0	0	521	
Canada	1	0	0	0	175	
Taiwan	0	0	2	0		
Saudi Arabia	0	0	1	0		
India			1			

More than 50 PT facilities and others under construction, more than 100000 patients treated...

PT in Italy

- ❖ CATANA - Catania
- ❖ CNAO - Pavia
- ❖ ATreP - Trento

...But only a 0.3% with respect to the 34% of RT.

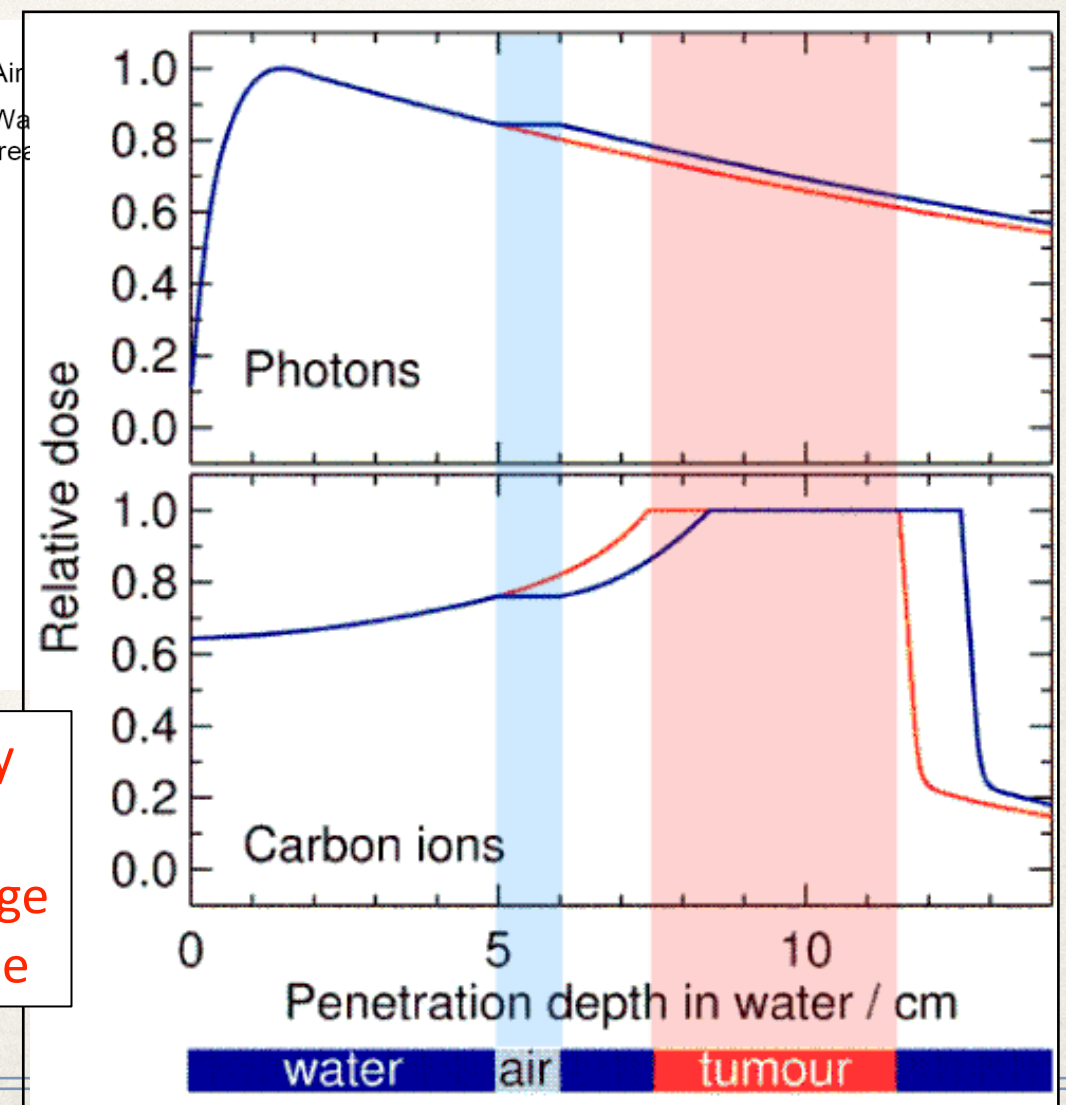


Range Monitoring

**Why it is so crucial to monitor the beam range in PT?
It is like firing with a precision rifle!**

- TPS dose calculation errors
 - Inhomogeneities, metallic implants
 - Conversion HU ion range
 - CT artifacts
- Difference TP / delivery
 - Daily setup variation
 - Internal organ motion
 - Anatomical / physiological changes

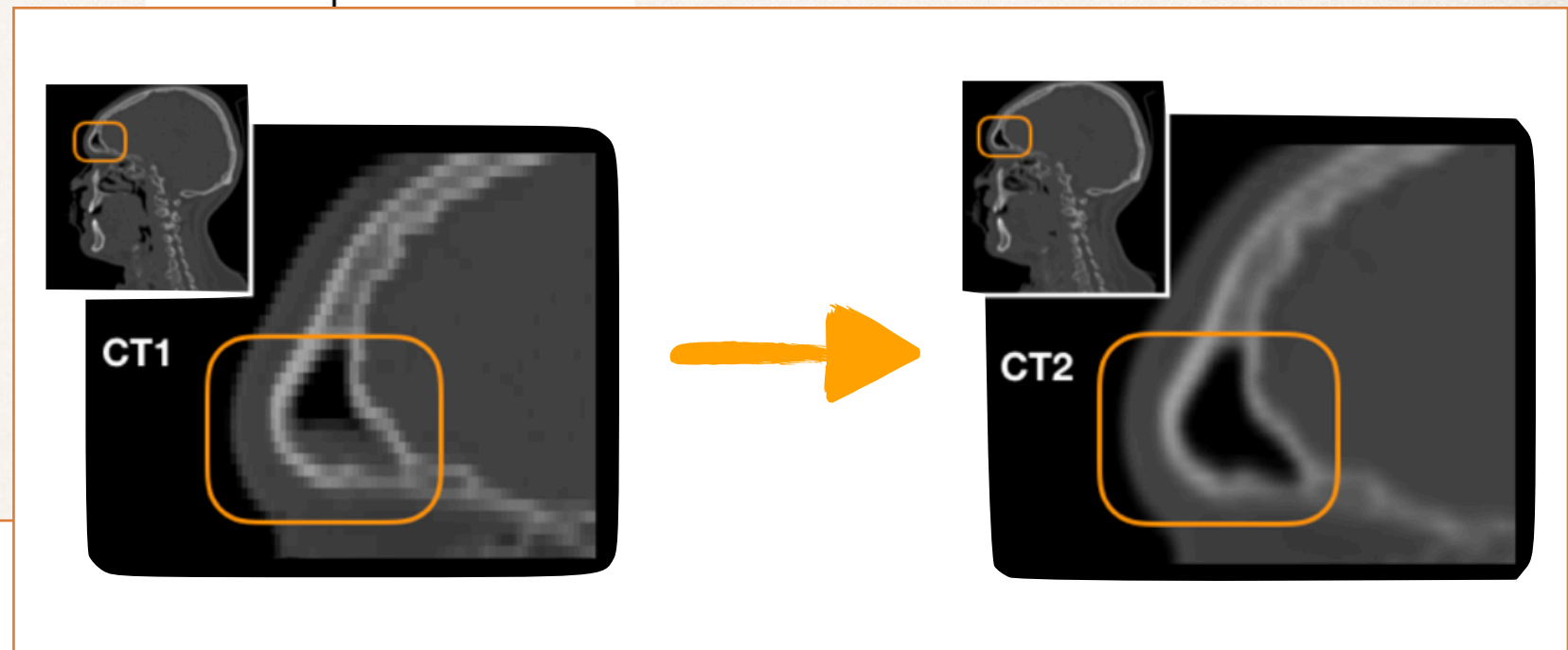
A little density mismatch => sensible change in dose release



Range Monitoring

**Why it is so crucial to monitor the beam range in PT?
It is like firing with a precision rifle!**

- TPS dose calculation errors
 - Inhomogeneities, metallic implants
 - Conversion HU ion range
 - CT artifacts
- Difference TP / delivery
 - Daily setup variation
 - Internal organ motion
 - Anatomical / physiological changes



**INTER-FRACTIONAL
MONITORING**

How to monitor the released dose

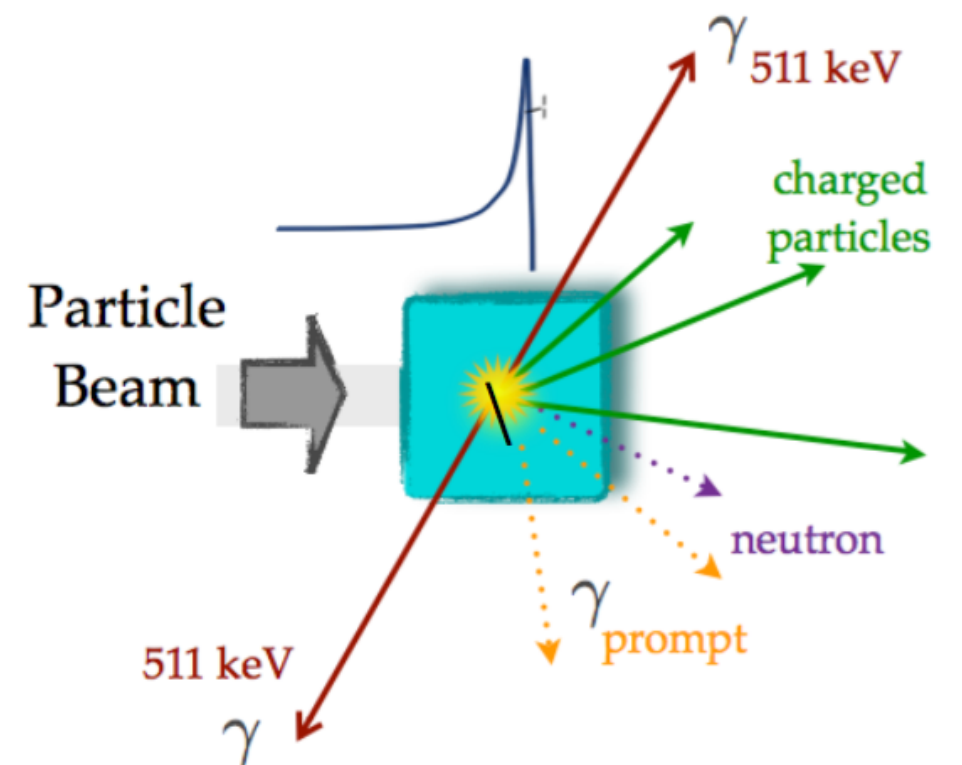
In conventional RT (photons) the beam crosses the patient body while in PT the beam is absorbed inside the patient!

An ideal PT monitor device:

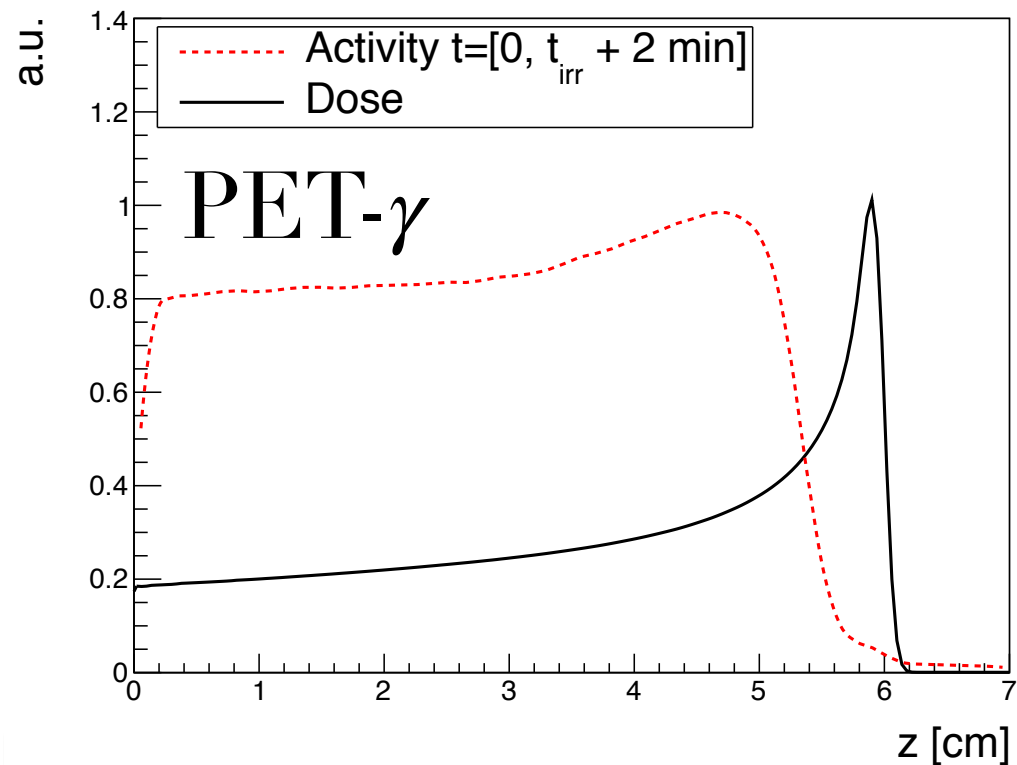
- ❖ Must rely on secondary products generated by the beam that come out from the patient to spot the dose release position
- ❖ Should measure the **dose shape and absolute value** to check the agreement between the planned target volume and the actually irradiated volume
- ❖ The **measurement** should be done during the treatment (*on-line*)
- ❖ Must be able to **deal with** other secondaries that act like **background**

Different secondary particles are produced.

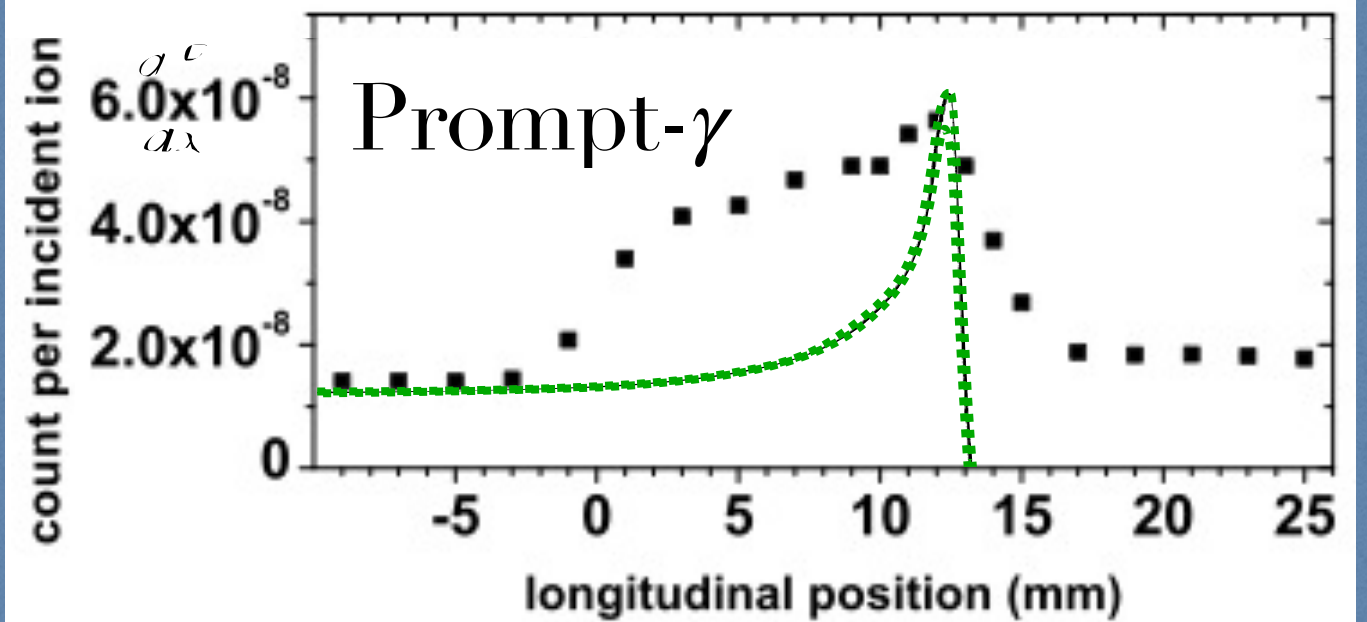
Which ones to choose for monitoring?



Secondary Products: PET- γ , Prompt- γ , Charged fragments

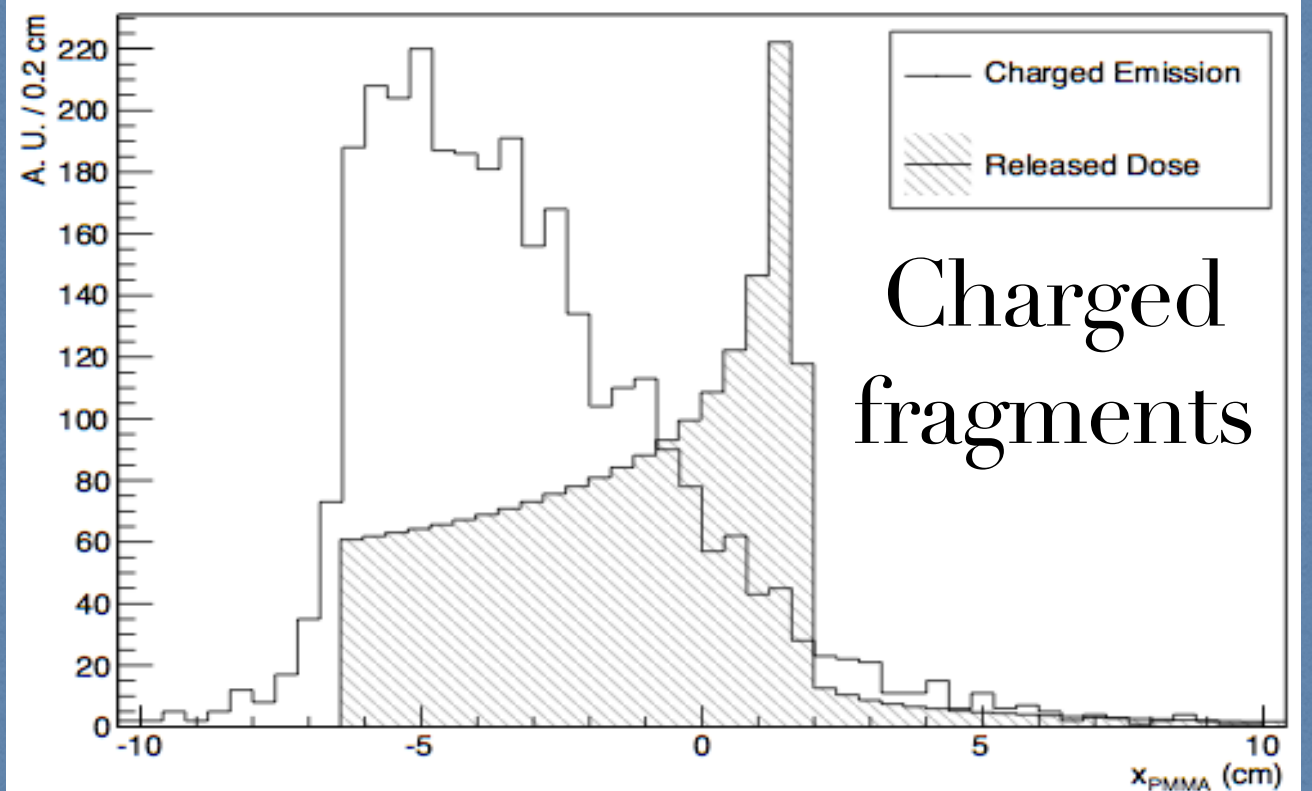


95 MeV proton beam (FLUKA)



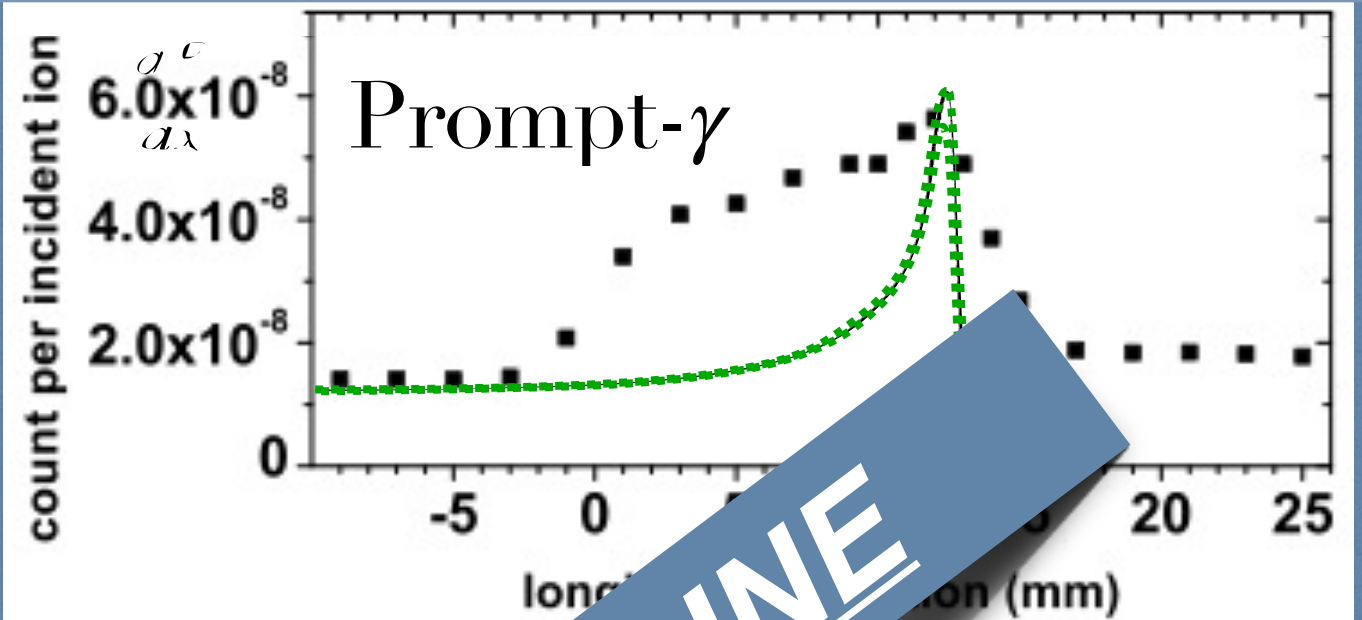
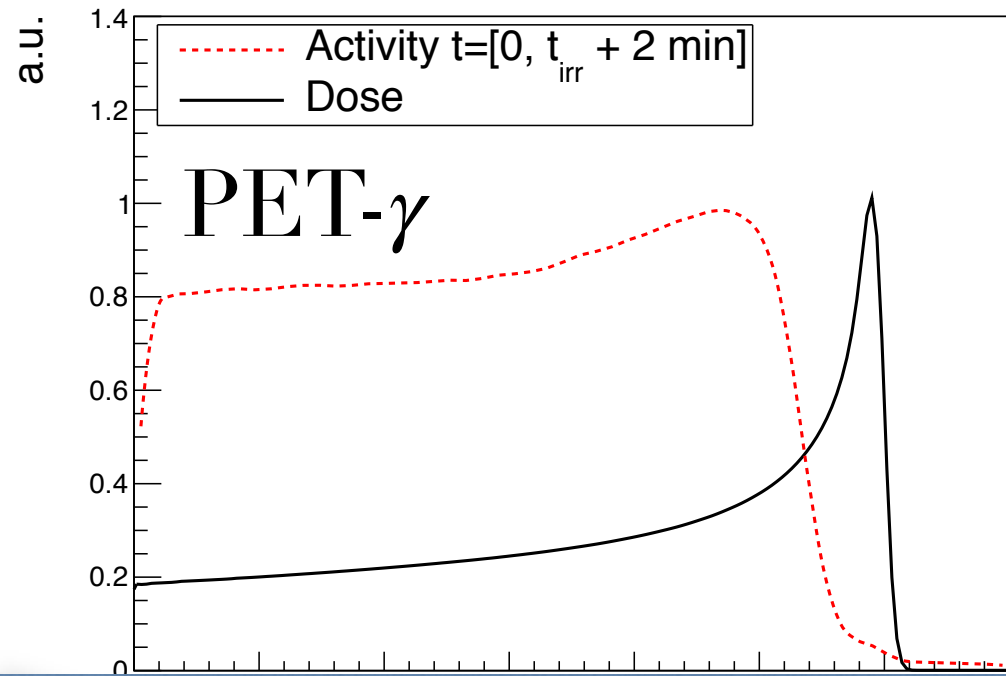
73 MeV/u ^{12}C ion beam (*Testa et al.*)

220 MeV/u ^{12}C ion beam
(*Piersanti, Mattei et al.*)



Charged
fragments

Secondary Products: PET- γ , Prompt- γ , Charged fragments

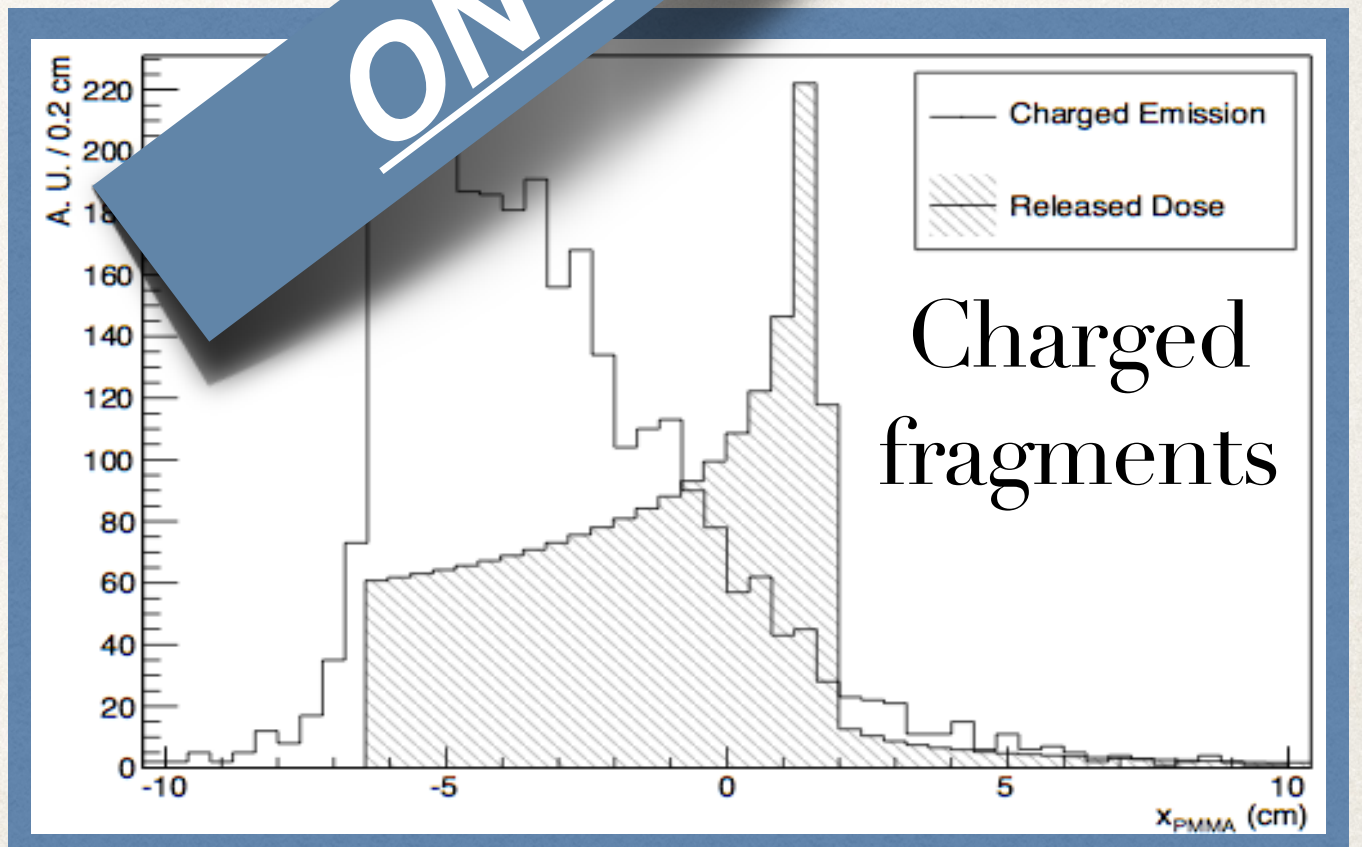


73 MeV/u beam (Testa et al.)

OFF - LINE

- β^+ isotopes of short lifetime ^{11}C (~20min), ^{15}O (~2min), ^{10}C (~20s)
- Low β^+ activity, long acquisition time
- Patient metabolic washout

beam
al.)



The Dose Profiler

For the inter-fractional beam range monitoring purpose, a new device has been developed: the *Dose Profiler*.
Clinical trial on patients @ CNAO started in 2019

PRIN MIUR
2010

INFN RDH
project

Centro Fermi
project

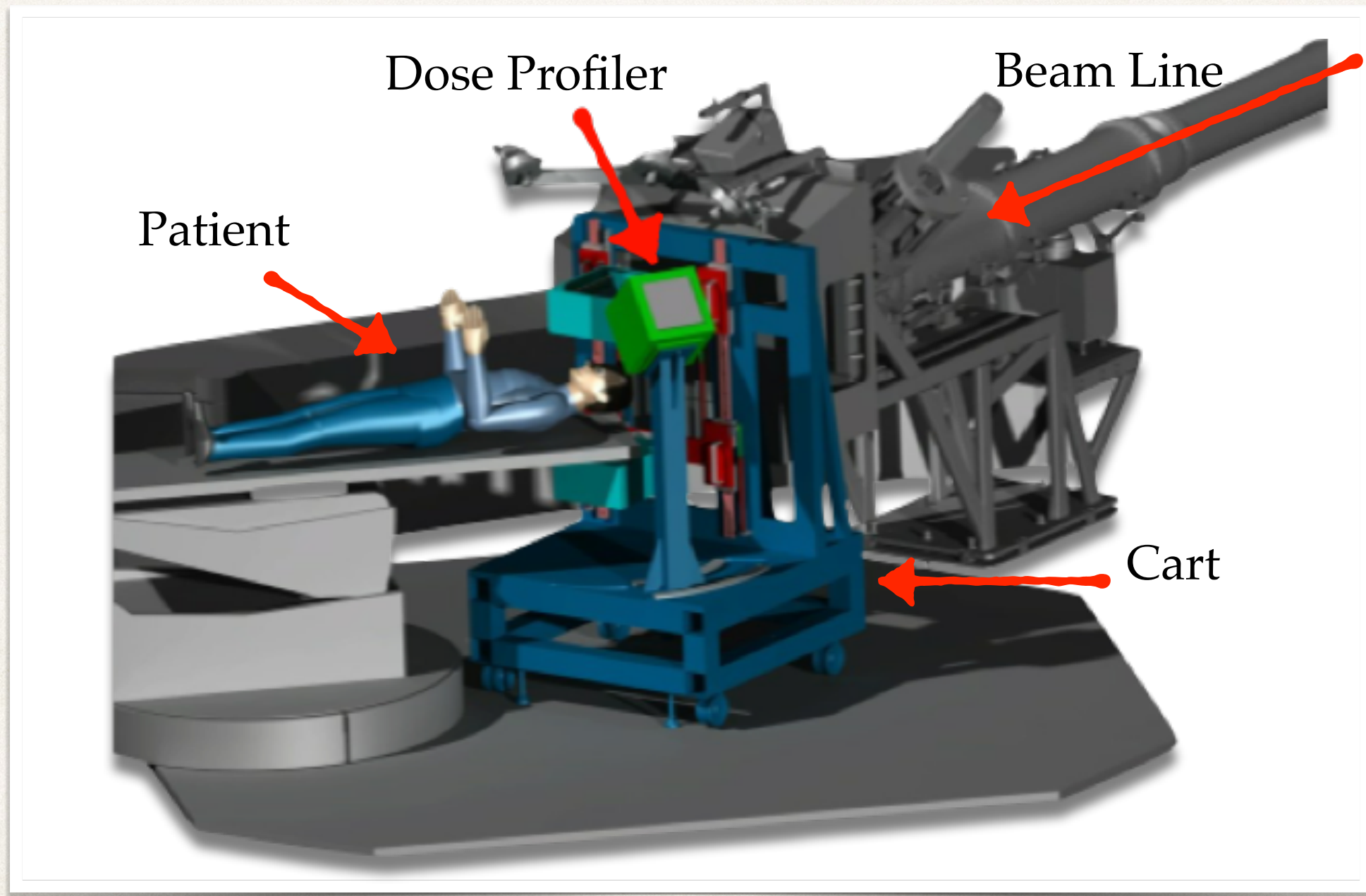


INnovative **S**olutions for **I**n-beam
Dosim**E**try in Hadrontherapy



The Dose Profiler project

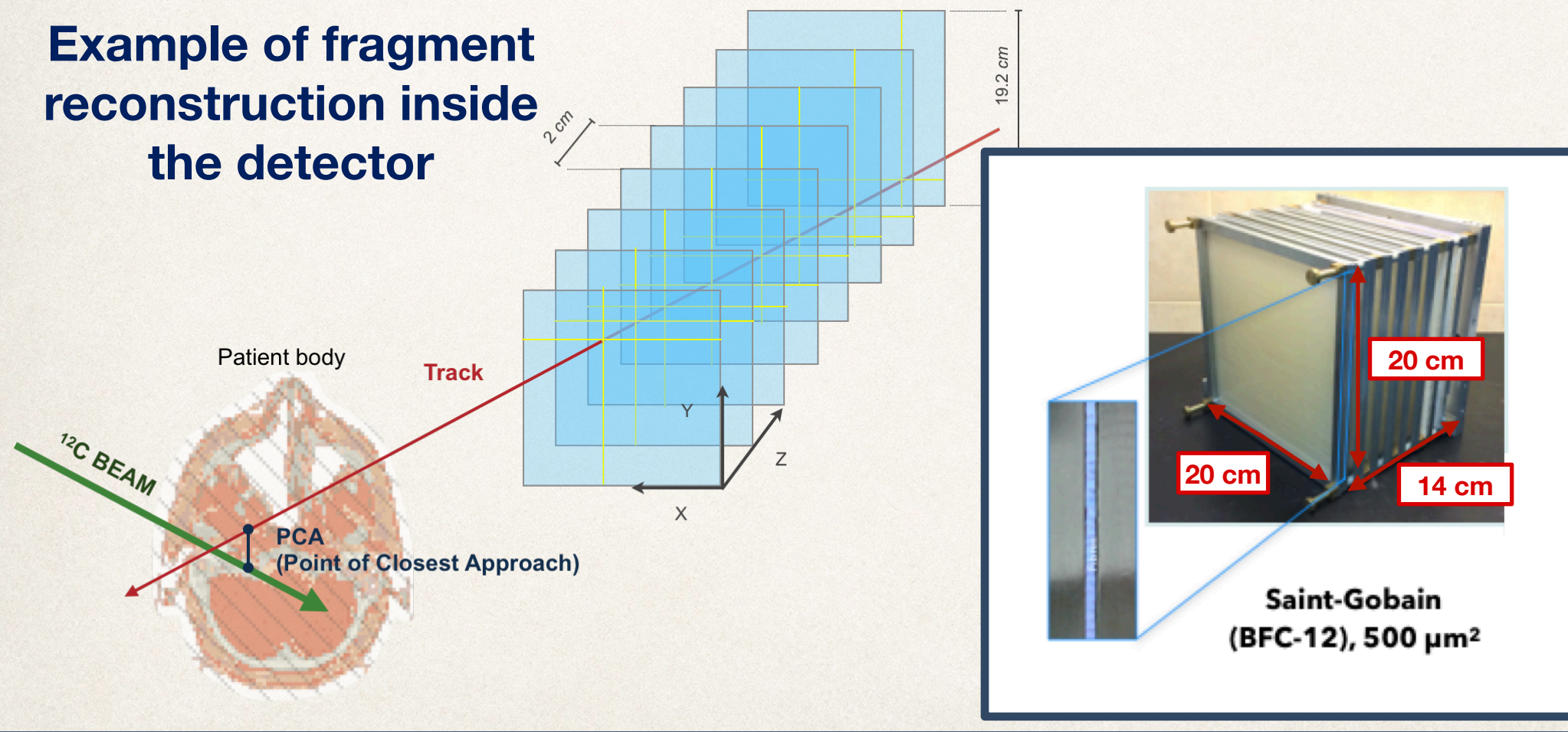
The Dose Profiler is a tracker of secondary charged particles



Detector Overview

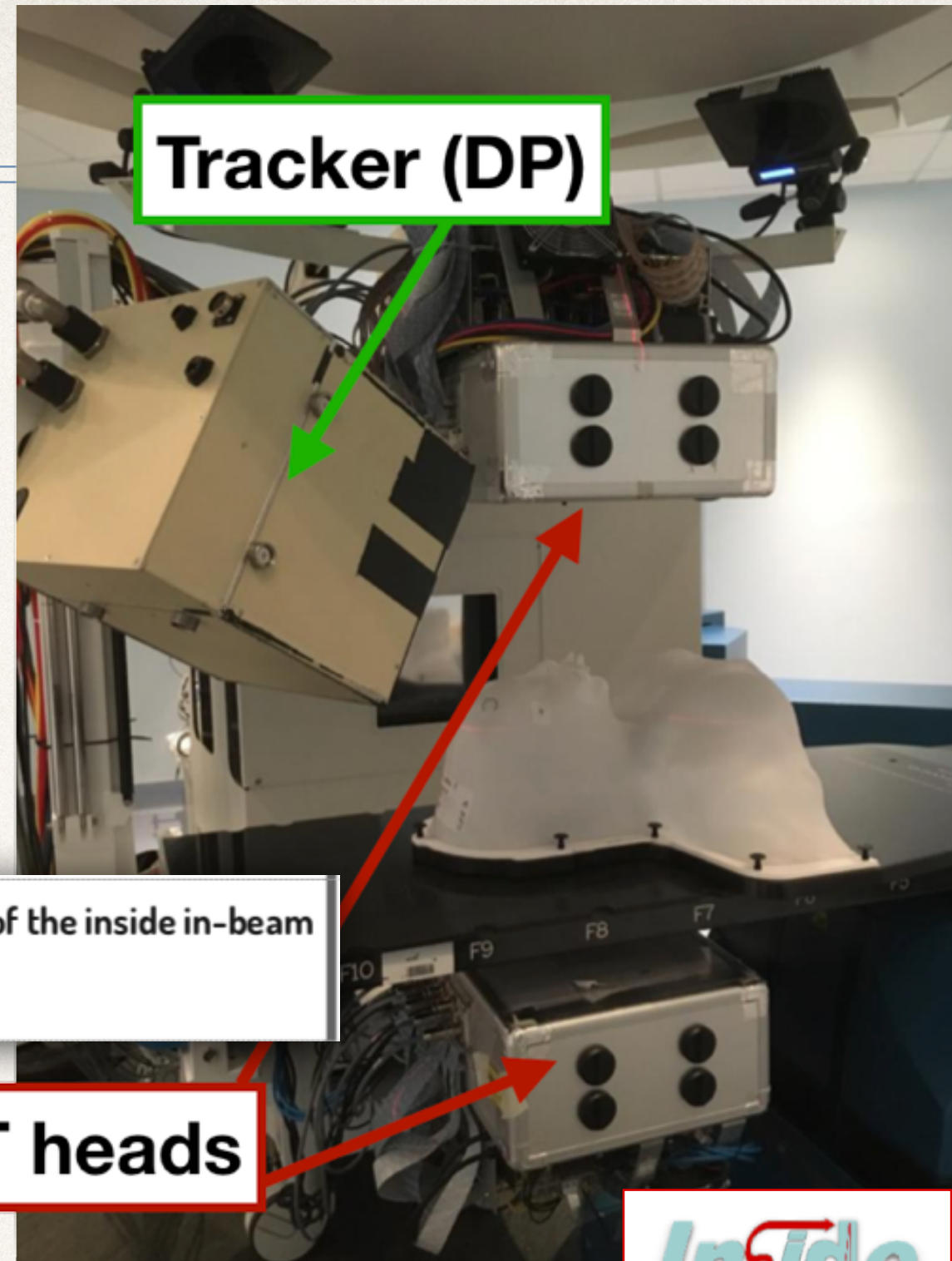
- ❑ 8 planes each one composed of 2 orthogonally oriented layers of **plastic scintillating fibres** (squared $500\ \mu\text{m}$, double cladding) are used to track the incoming particles
- ❑ 3072 SiPMs readout ($1\ \text{mm}^2$)
- ❑ Interface with the **Dose Delivery system** of CNAO

Example of fragment reconstruction inside the detector



Detector Overview

The DP is integrated within the **INSIDE** system @ CNAO with a PET device using a bi-modal approach: **charged fragments** detection and β^+ activity map measurement for **carbon ion** and **proton** treatments monitoring, respectively.



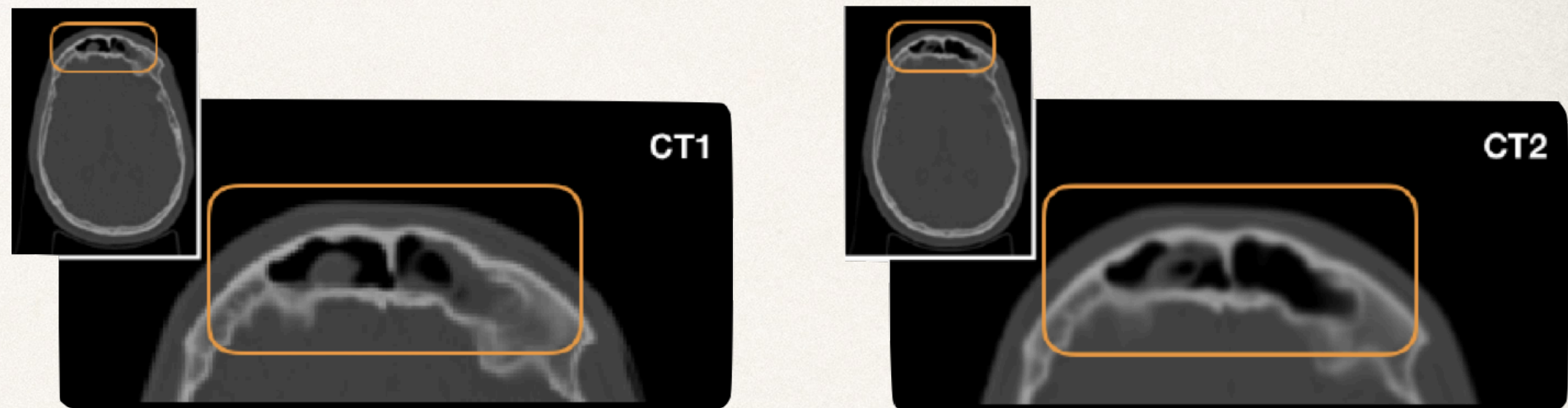
Clinical results of in-vivo inter-fractional monitoring in particle therapy by means of the inside in-beam PET
Elisa Fiorina - **ON-LINE** doi: 10.3389/fphy.2020.578388

DP is placed at **50 cm** from the treatment room isocenter and at **60°** wrt the beam direction.

Inter-fractional Monitoring

- ❖ Carbon ion treatments at CNAO typically lasts ~ 4 weeks
- ❖ A CT scan is performed and used as input for the treatment planning
- ❖ The ^{12}C beam is delivered in 20-30 fractions
- ❖ The decision to perform a mid-treatment CT and eventually to re-plan the treatment is taken only accordingly to the pathology under treatment and on the basis of the collected statistics of patients with similar pathologies

Example of morphological changing occurred during the treatment



Monitoring strategy: As the fragments production yield along the beam path depends on the **density** and the **atomic mass** of the crossed tissues, the dis-homogeneities onset can be monitored comparing the reconstructed emission map of the fragments in different fractions of the treatment to help the decision on when a replanning CT is needed.

Clinical Trial: 8-12/2019@CNAO

- ❖ A clinical trial ([ClinicalTrials.gov Identifier: NCT03662373](https://clinicaltrials.gov/ct2/show/study/NCT03662373)) is started at CNAO in August 2019 to evaluate the Dose Profiler capability and sensitivity in detecting morphological changes arising in pathologies of the **neck-head district**. At present, data on 10 patients have been collected.



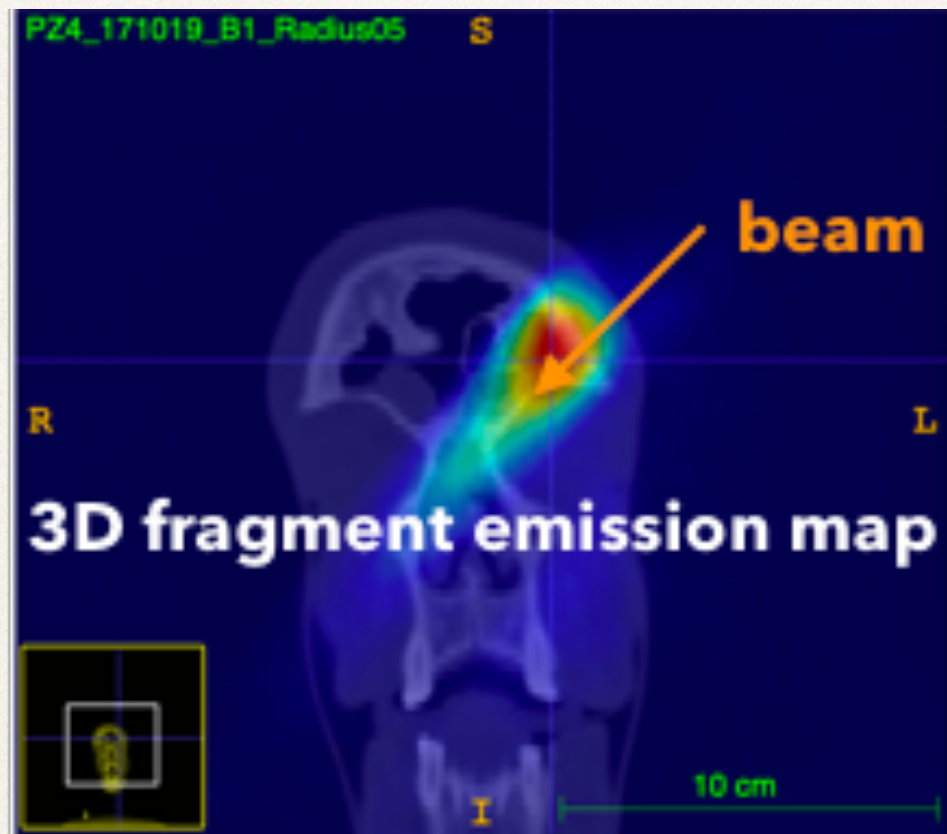
Patient ID	Pathology	Re-evaluation CT	Re-planning
PZ1	ACC	7° fraction	no
PZ2	ACC	5° and 10° fraction	no
PZ3	ACC	no	no
PZ4	ACC	8° fraction	no
PZ5	clival chordoma	no	no
PZ6	ITAC	7° fraction	yes
PZ7	clival chordoma	no	no
PZ8	ACC	7° fraction	no
PZ9	clival chordoma	no	no
PZ10	ITAC	8° fraction	yes

The **1D inter-fractional monitoring results** have been published
 Fischetti, M. *et al.*, *Sci Rep* 10, 20735 (2020)
<https://doi.org/10.1038/s41598-020-77843-z>

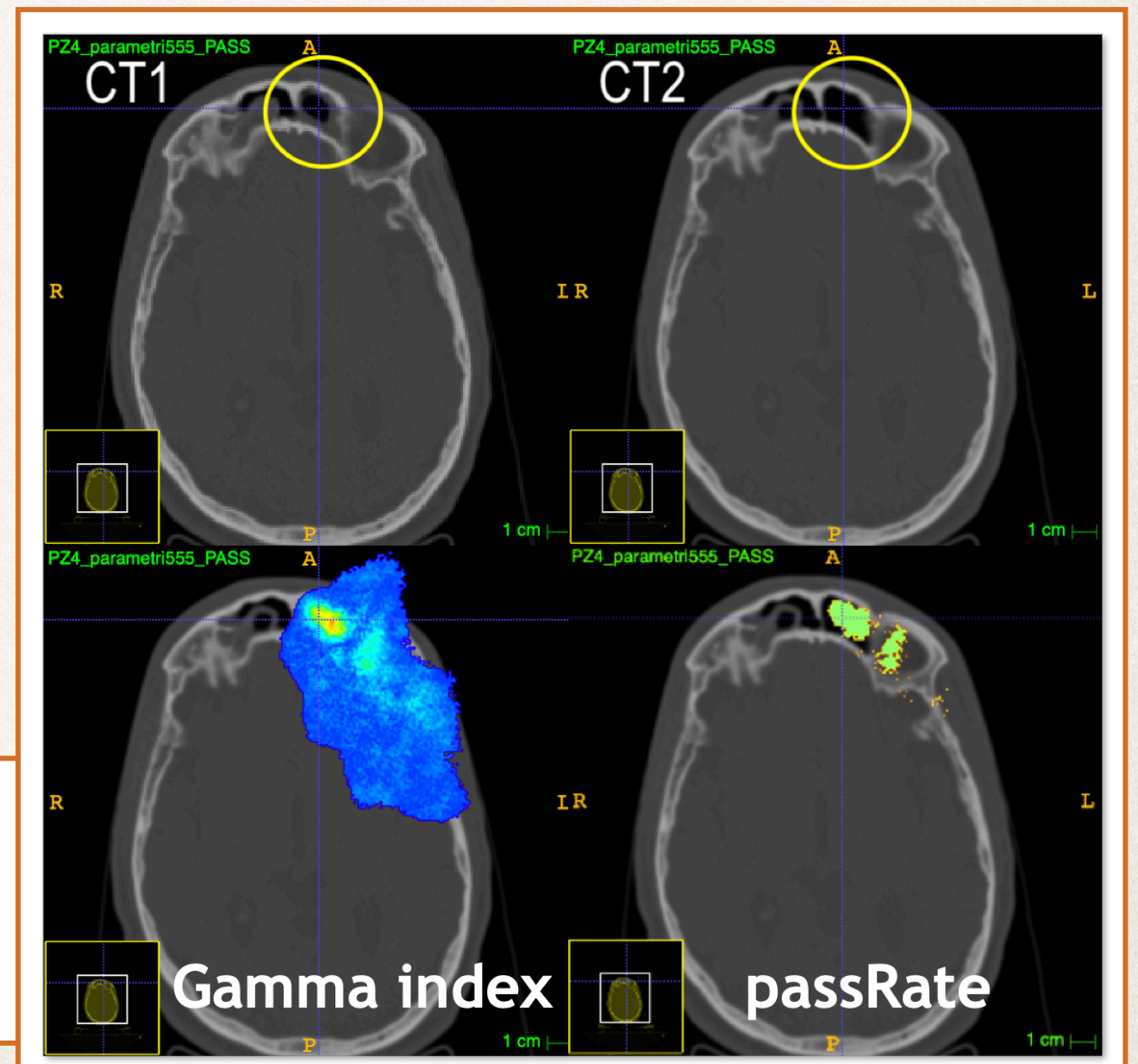


3D Inter-fractional Monitoring

- ❖ Data on PZ4 are here shown: **CT1 before 16 October; CT2 the 29 October**
- ❖ The 3D map of emission points of detected fragments are reconstructed in each fraction
- ❖ The difference of maps taken at the first fraction and at the replanning-CT fraction is evaluated in terms of gamma-index (pass rate) map

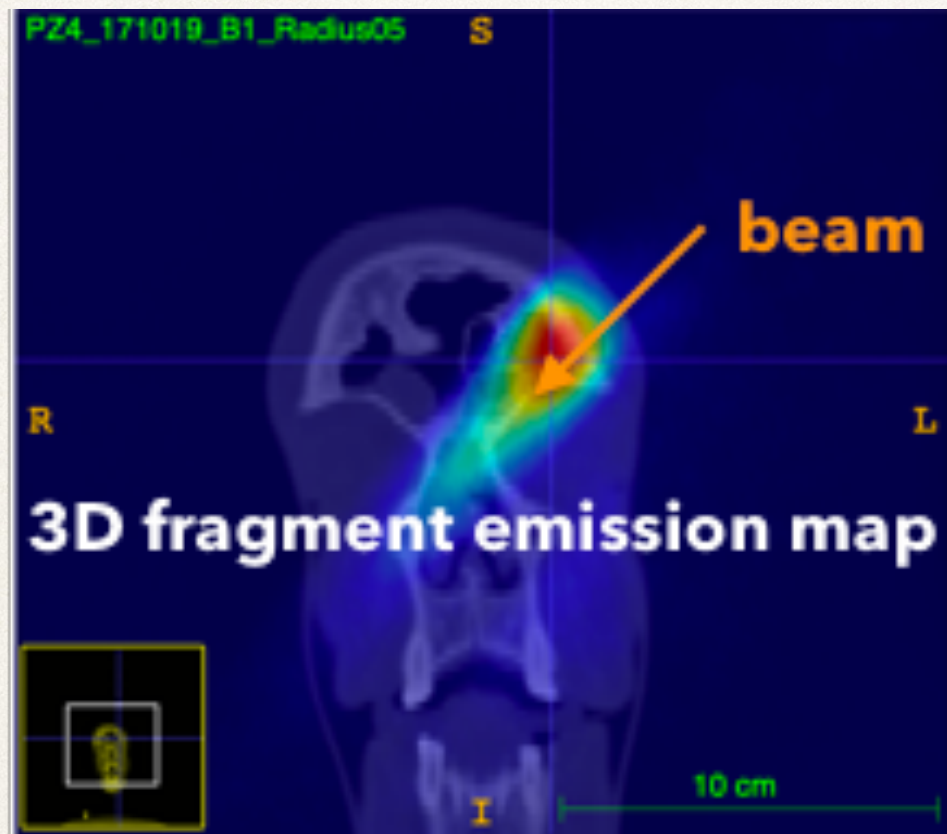


PZ4 underwent the emptying of the frontal sinuses, as noticed by a mid-term CT (CT2).
Such modification has been clearly identified by the gamma-index map.

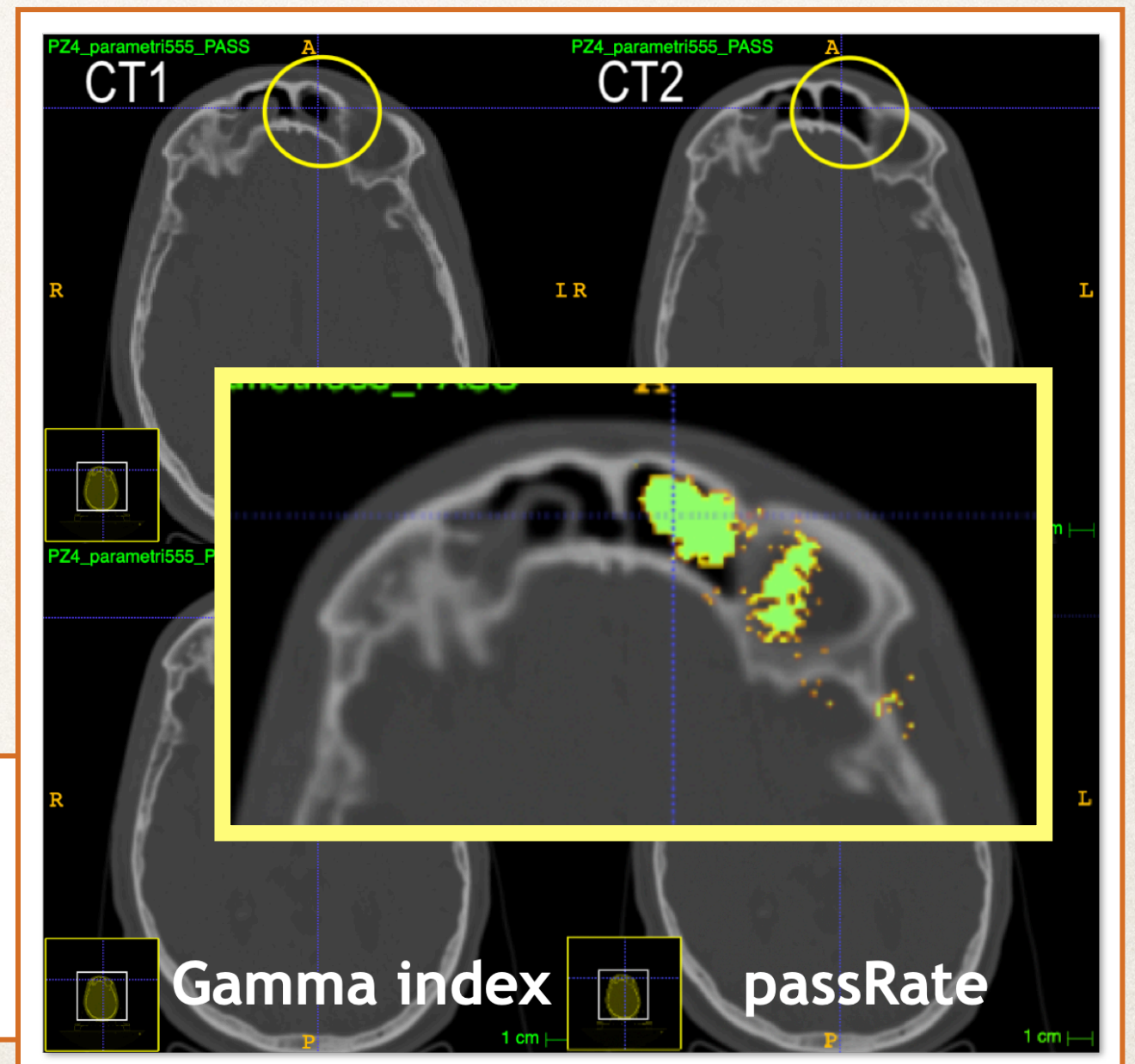


3D Inter-fractional Monitoring

- ❖ Data on PZ4 are here shown: **CT1 before 16 October; CT2 the 29 October**
- ❖ The 3D map of emission points of detected fragments are reconstructed in each fraction
- ❖ The difference of maps taken at the first fraction and at the replanning-CT fraction is evaluated in terms of gamma-index (pass rate) map



PZ4 underwent the emptying of the frontal sinuses, as noticed by a mid-term CT (CT2).
Such modification has been clearly identified by the gamma-index map.



3D Inter-fractional Monitoring

- ❖ Data on PZ4 are here shown: CT1 before 16 October; CT2 the 29 October
- ❖ The 3D map of emission points of detected fragments are reconstructed in each fraction
- ❖ The difference of maps taken at the first fraction and at the replanning-CT fraction is evaluated in terms of gamma-index (pass rate) map

For the first time ever, patients treated with 12C have been monitored and morphological changes occurred during the treatment have been identified.

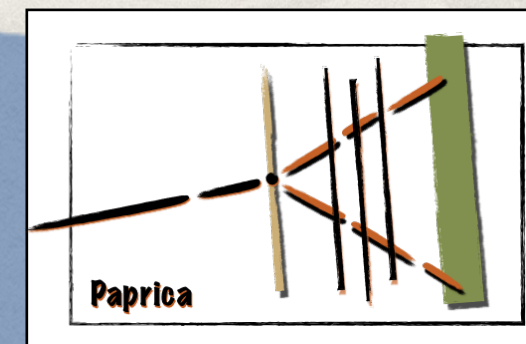
Another clinical trial campaign is going to start in 2022.



PZ4 underwent the emptying of the frontal sinuses, as noticed by a mid-term CT (CT2). Such modification has been clearly identified by the gamma-index map.



The PAPERICA project



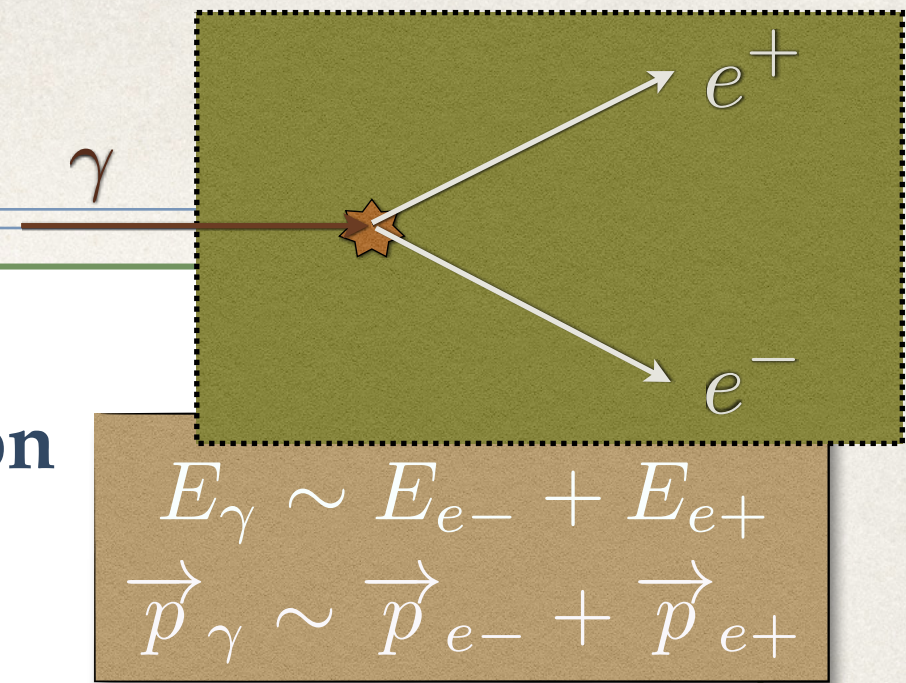
For the beam range monitoring purpose, a new technique has been proposed within a young researcher grant: the **PAPERICA (PAir PROduction Imaging ChAMber) project**.

The detector is under construction and will be tested in-beam in 2022.

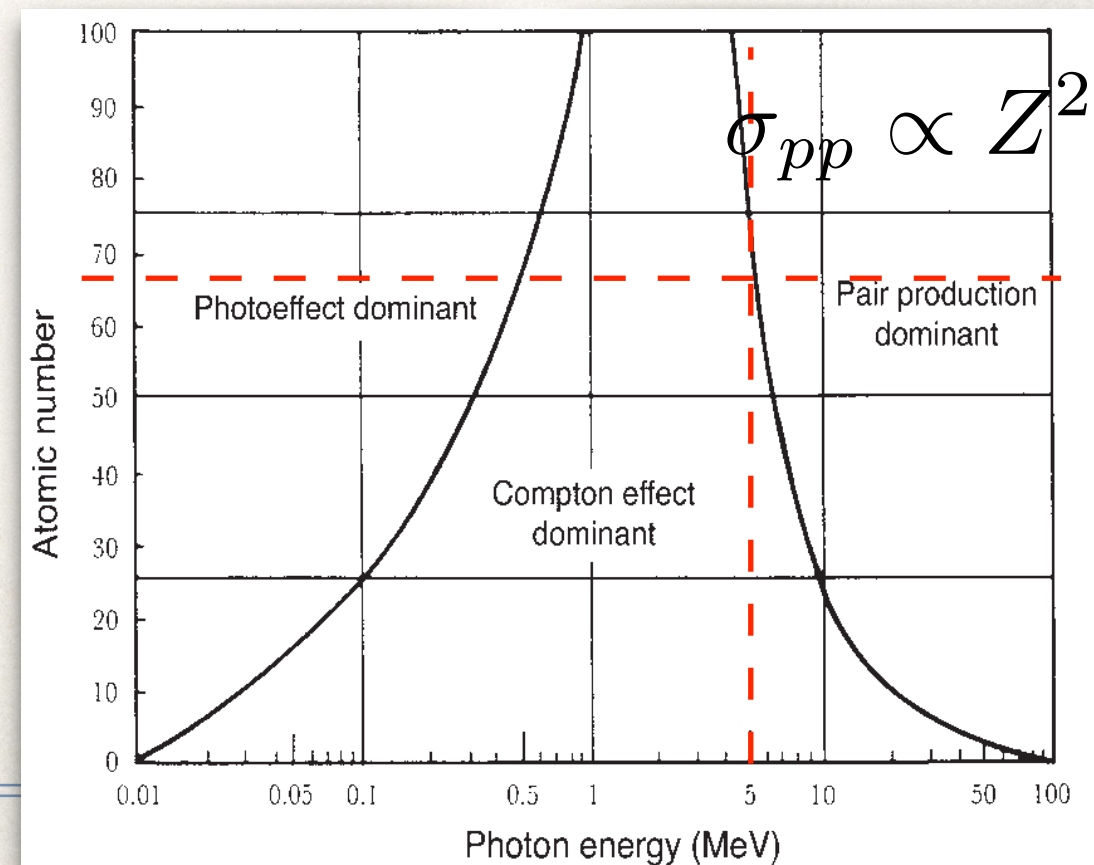


The PAPRICA project

PAPRICA proposes a **novel 3D prompt gamma imaging strategy**, exploiting the **pair production** mechanism of prompt photons for range monitoring purpose.

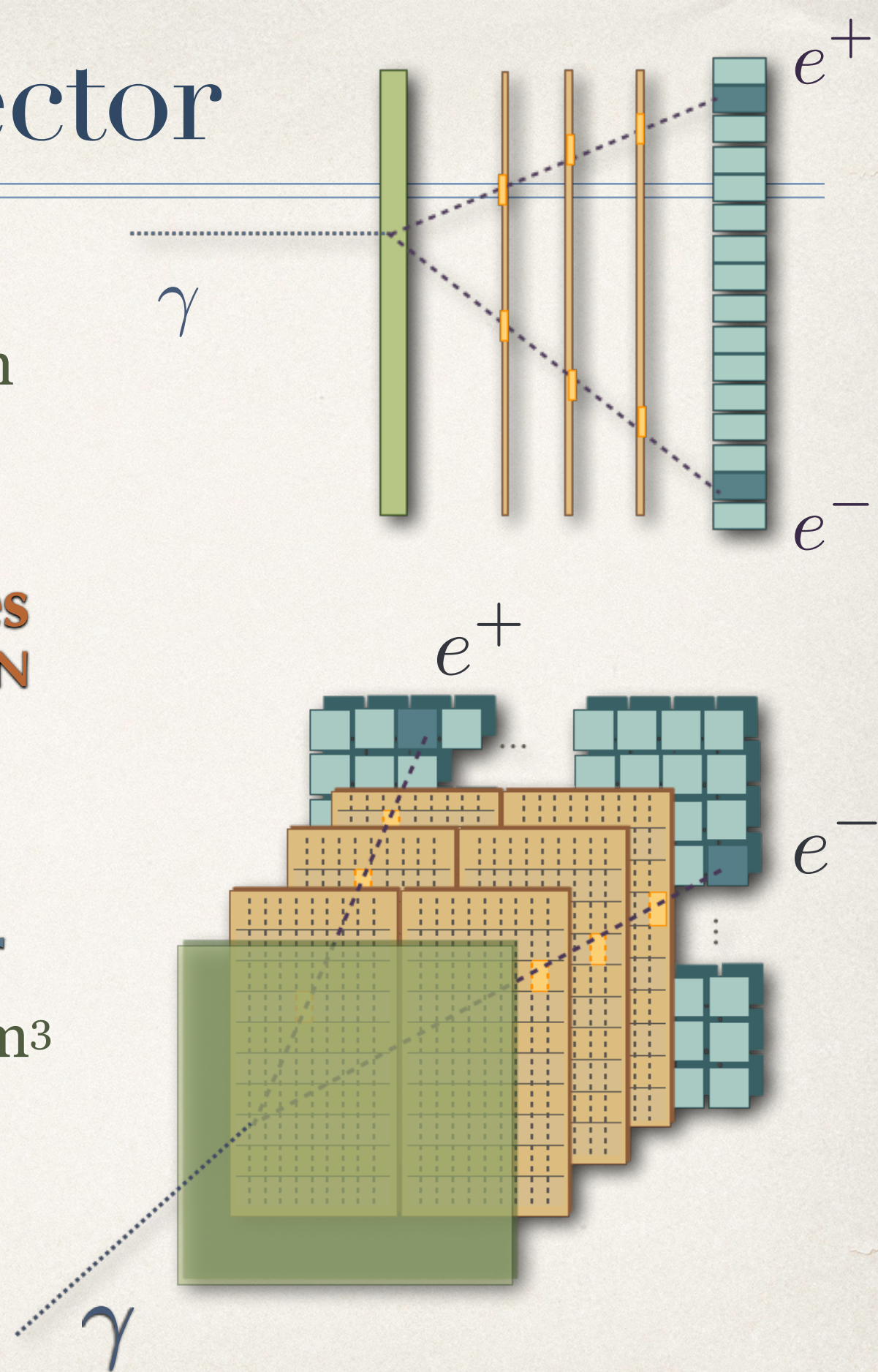


- ❖ Technique used by pair telescopes in astrophysics applications for cosmic photons imaging $E > 30$ MeV
- ❖ Never explored in the lower PG energy range $E \sim 2-10$ MeV
- ❖ Topological event signature: no n bkg
- ❖ No collimation
- ❖ Easy to 3D reconstruct the PG emission point
- ❖ Potentially to be used both in proton and ^{12}C PT



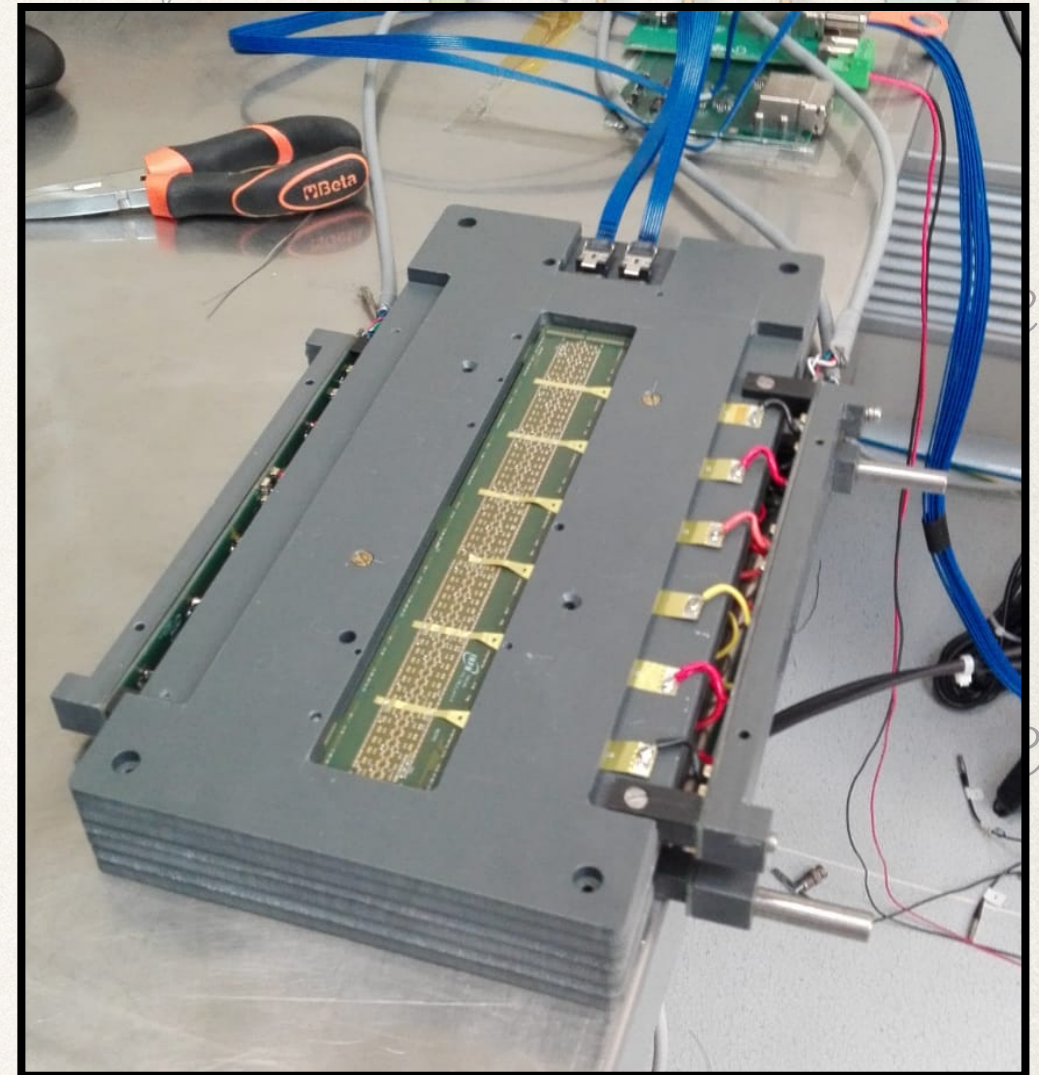
The PAPRICA detector

- ▶ **CONVERTER plane: LYSO fibers**
high Z_{eff} (66), fiber thickness 1.5 mm
active medium (trigger and reco)
- ▶ **TRACKER: MAPS ALPIDE* modules**
low budget material
*ALICE@CERN
intrinsic resolution < 10 μm
- ▶ **CALORIMETER: plastic scintillator**
2 matrices 8 x 8 pixels, 6 x 6 x 50 mm³
low leptons backscattering
same converter readout
energy resolution < 3%

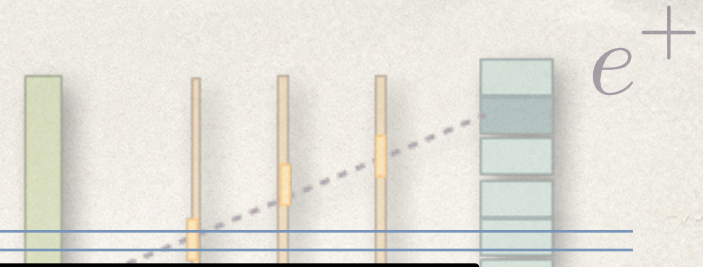


The PAPRICA detector

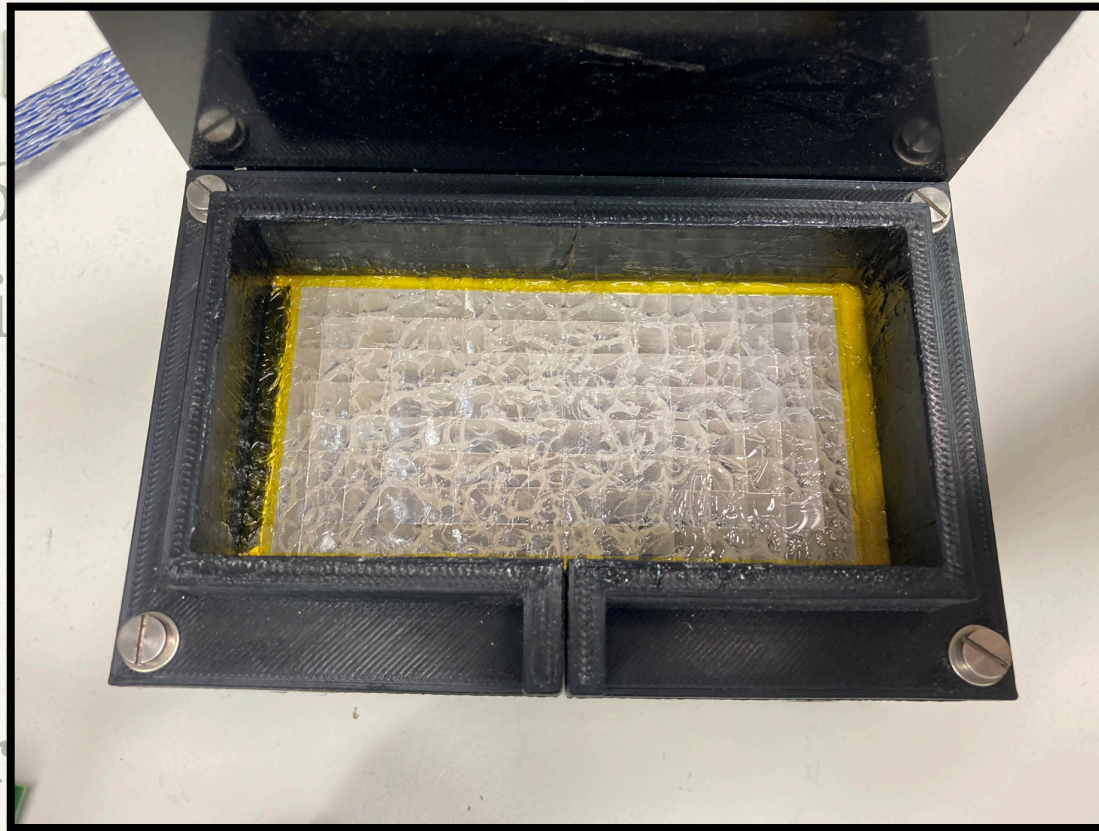
- ▶ **CONVERTER plane: LYSO fibers**
high Z_{eff} (66), fiber thickness 1.5 mm
active medium (trigger and reco)
- ▶ **TRACKER: MAPS ALPIDE* modules**
low budget material
intrinsic resolution $< 10 \mu\text{m}$
*ALICE@CERN
- ▶ **CALORIMETER: plastic scintillator**
2 matrices 8×8 pixels, $6 \times 6 \times 50 \text{ mm}^3$
low leptons backscattering
same converter readout
energy resolution $< 3\%$



The PAPRICA detector

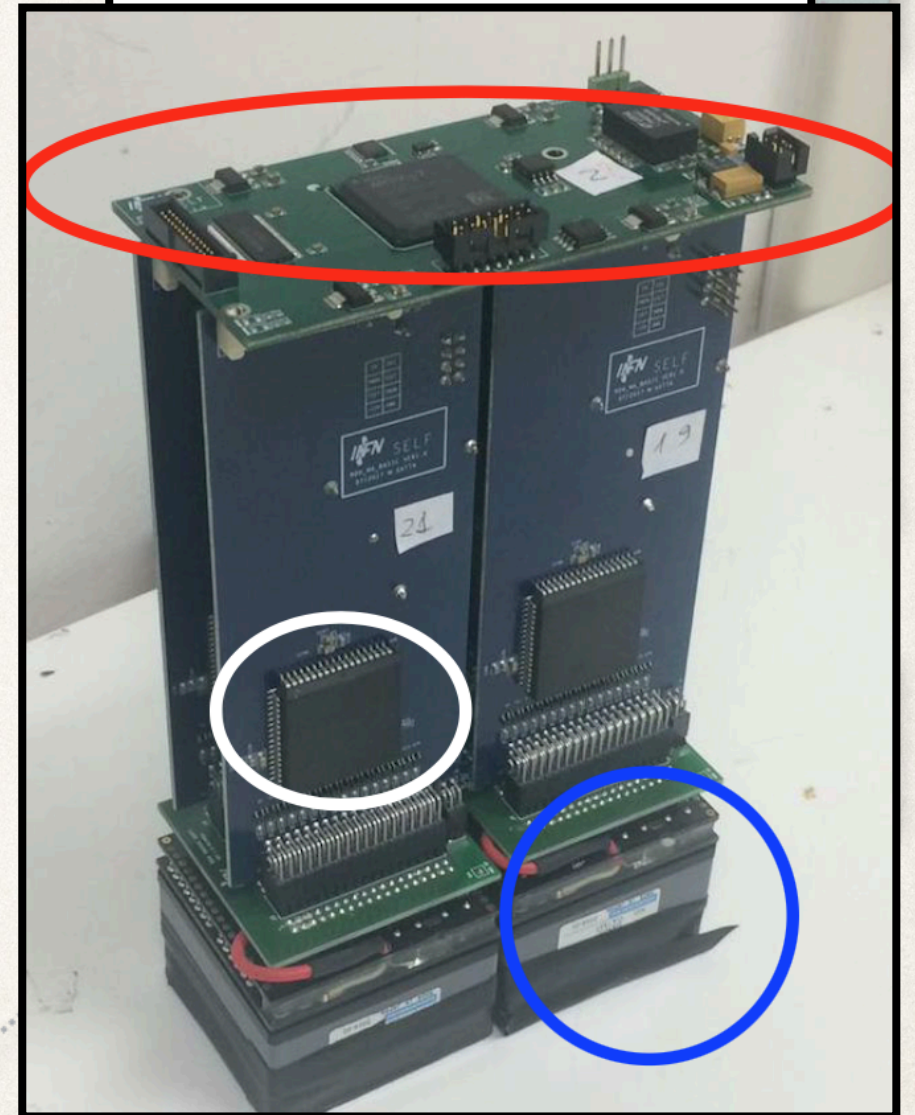


- ▶ **CONVERTER:**
high Z_{eff} (6)
active medium
- ▶ **TRACKER:**
low budget
intrinsic resolution



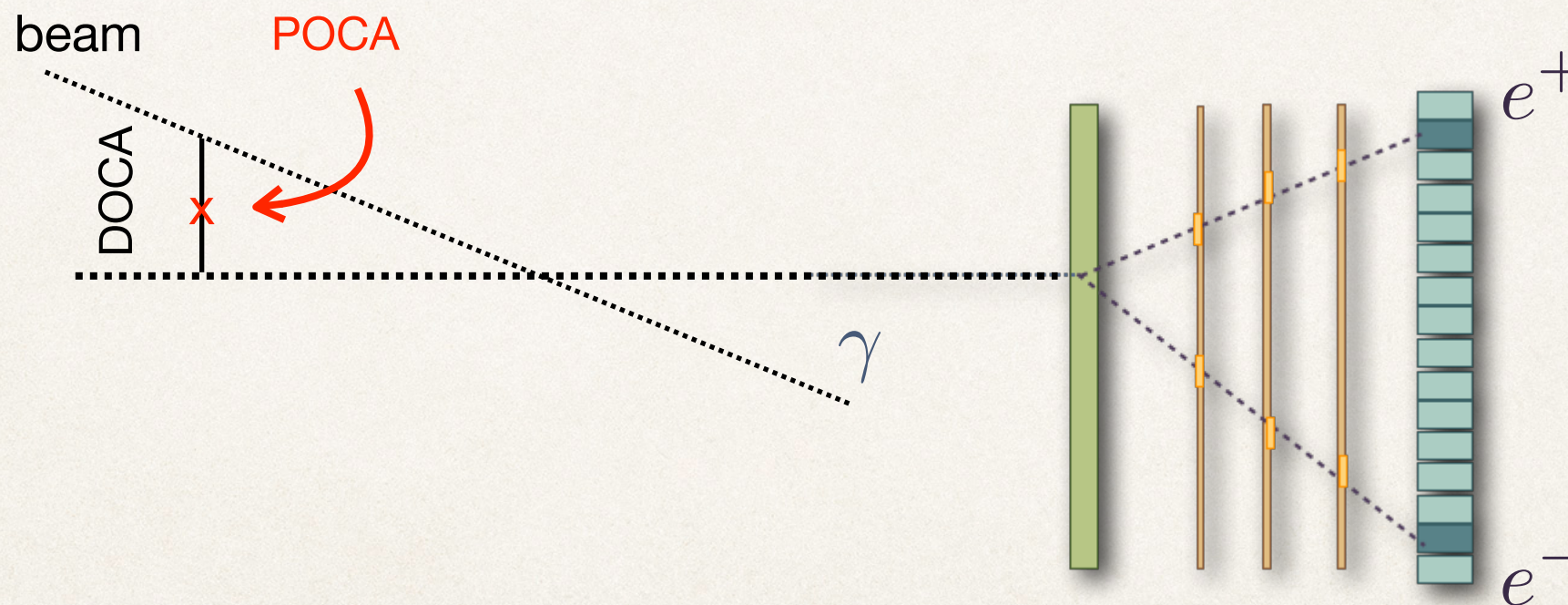
MAPM
ASIC 32 channels
FPGA

- ▶ **CALORIMETER: plastic scintillator**
4 matrices 8×8 pixels, $6 \times 6 \times 50 \text{ mm}^3$
low leptons backscattering
same converter readout
energy resolution $< 3\%$



Resolution Study (MC)

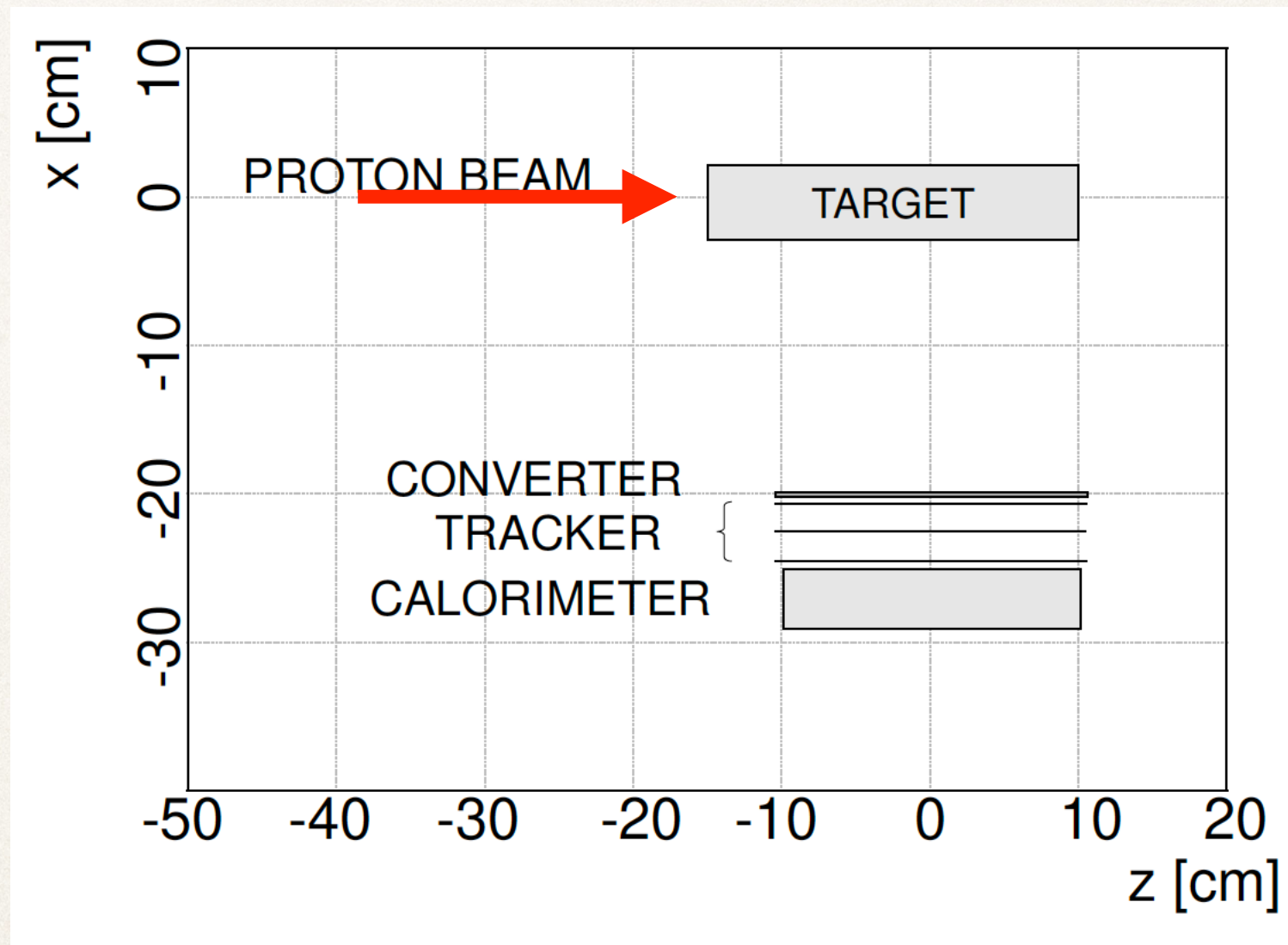
- ❖ The **detector geometry has been optimised** by exploiting MC (FLUKA) simulations
- ❖ In **MC**, lepton pairs are reconstructed as in a **real signal event** (energy loss, resolutions)
- ❖ Prompt photons **directions are reconstructed** exploiting the pair production kinematics and the emission points are obtained as the point of closest approach (POCA) between the photon and beam directions*



*Toppi, M. *et al.*, *Front. Phys.* 9:568139 (2021) <https://doi.org/10.3389/fphy.2021.568139>

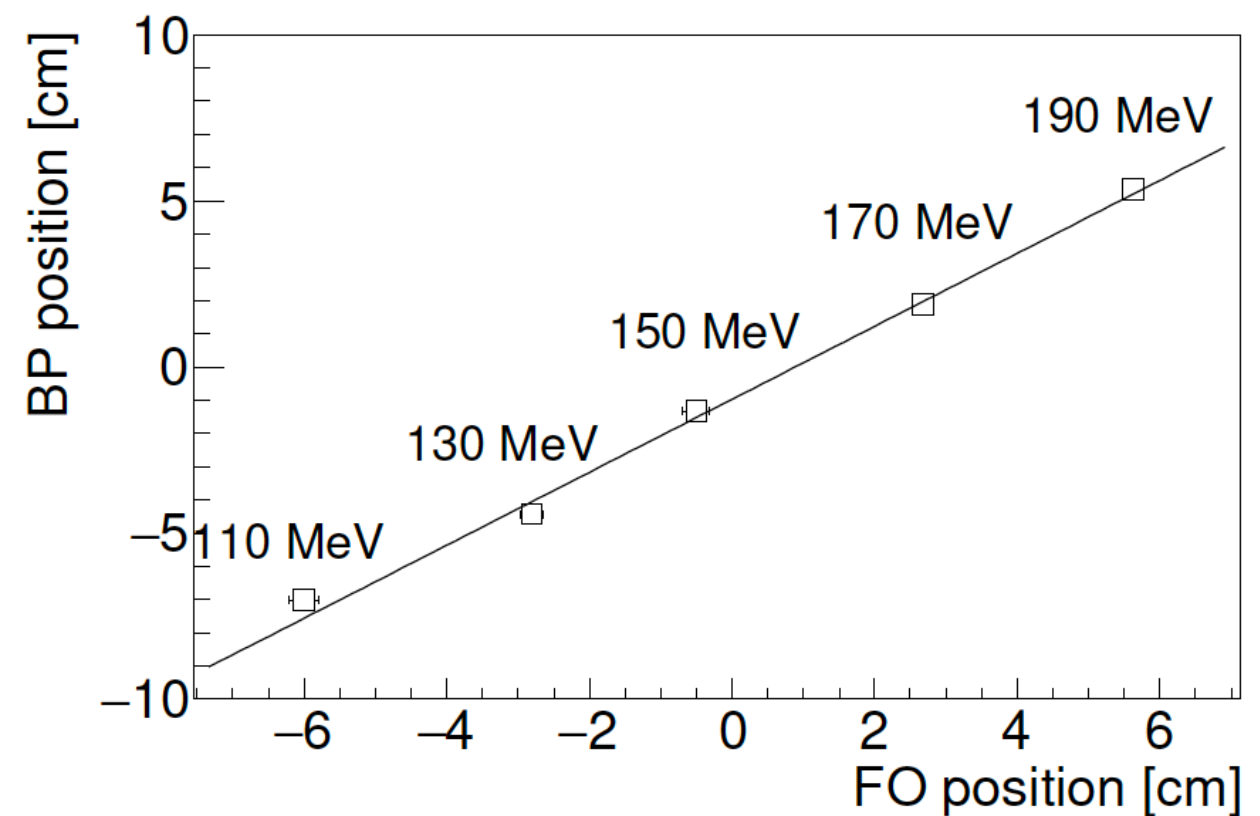
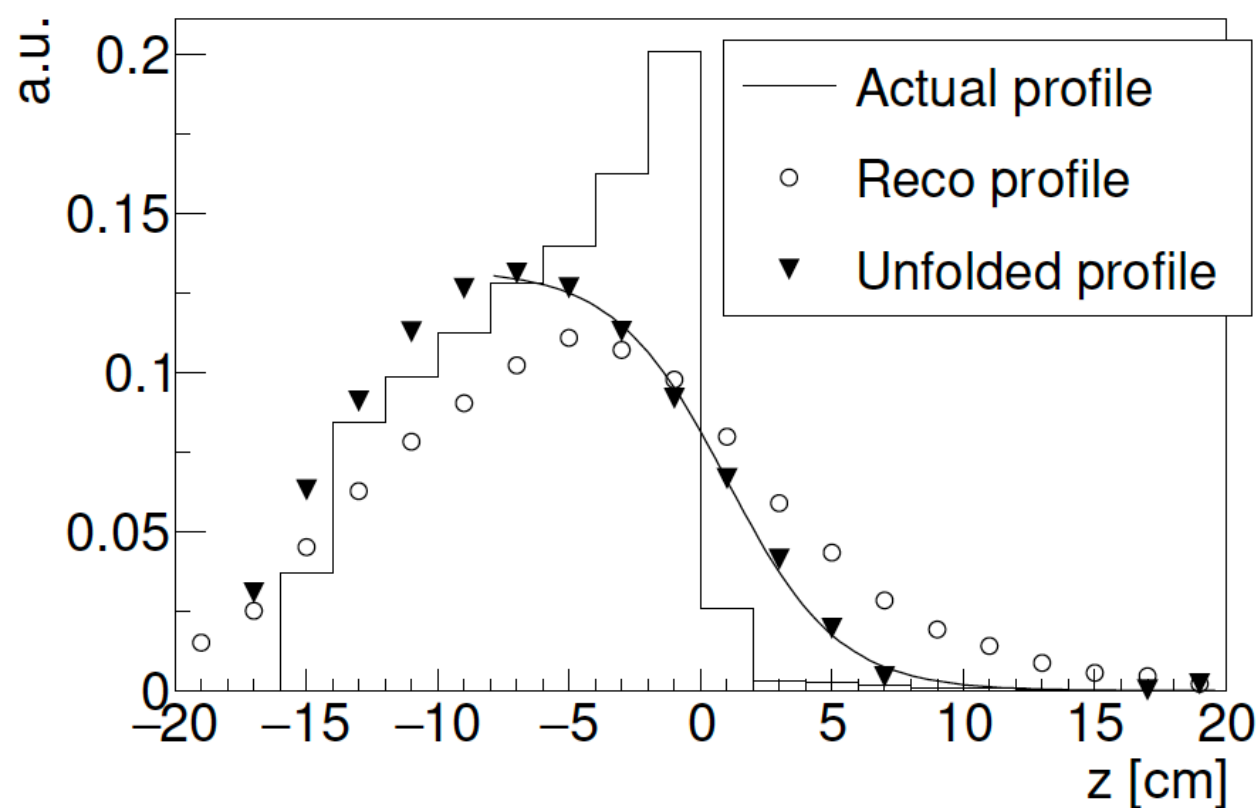
Resolution Study (MC)

- ❖ A simulation of a 160 MeV proton beam impinging on a PMMA ($C_5O_2H_8$) target has been performed



Resolution Study (MC)

- ❖ A simulation of a 160 MeV proton beam impinging on a PMMA ($C_5O_2H_8$) target has been performed
- ❖ An **unfolding procedure** to retrieve the true emission position was needed due to a bias in the 1D reconstruction and a **calibration** to evaluate the Bragg peak position (i.e. the beam range) was applied to reconstructed data*



*Calvi, G. *et al.*, *IL NUOVO CIMENTO* 44 C (2021) 147 <https://doi.org/10.1393/ncc/i2021-21147-9>

Resolution Study (MC)

- ❖ A simulation of a 160 MeV proton beam impinging on a PMMA ($C_5O_2H_8$) target has been performed
- ❖ An **unfolding procedure** to retrieve the true emission position was needed due to a bias in the 1D reconstruction and a **calibration** to evaluate the Bragg peak position (i.e. the beam range) was applied to reconstructed data
- ❖ The **accuracy** achieved in the measurement of the 160 MeV proton Bragg peak position is approximately **4 mm***

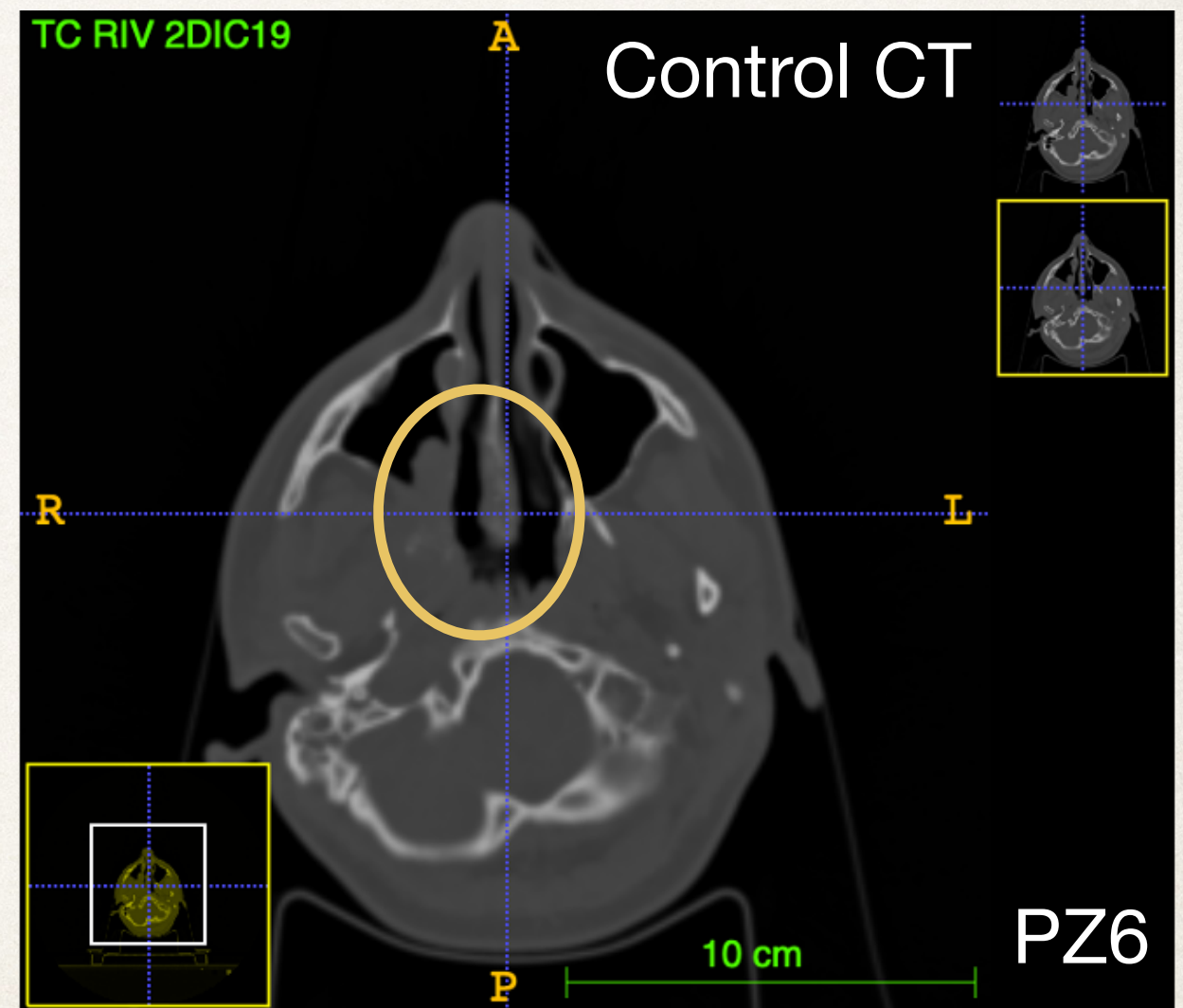
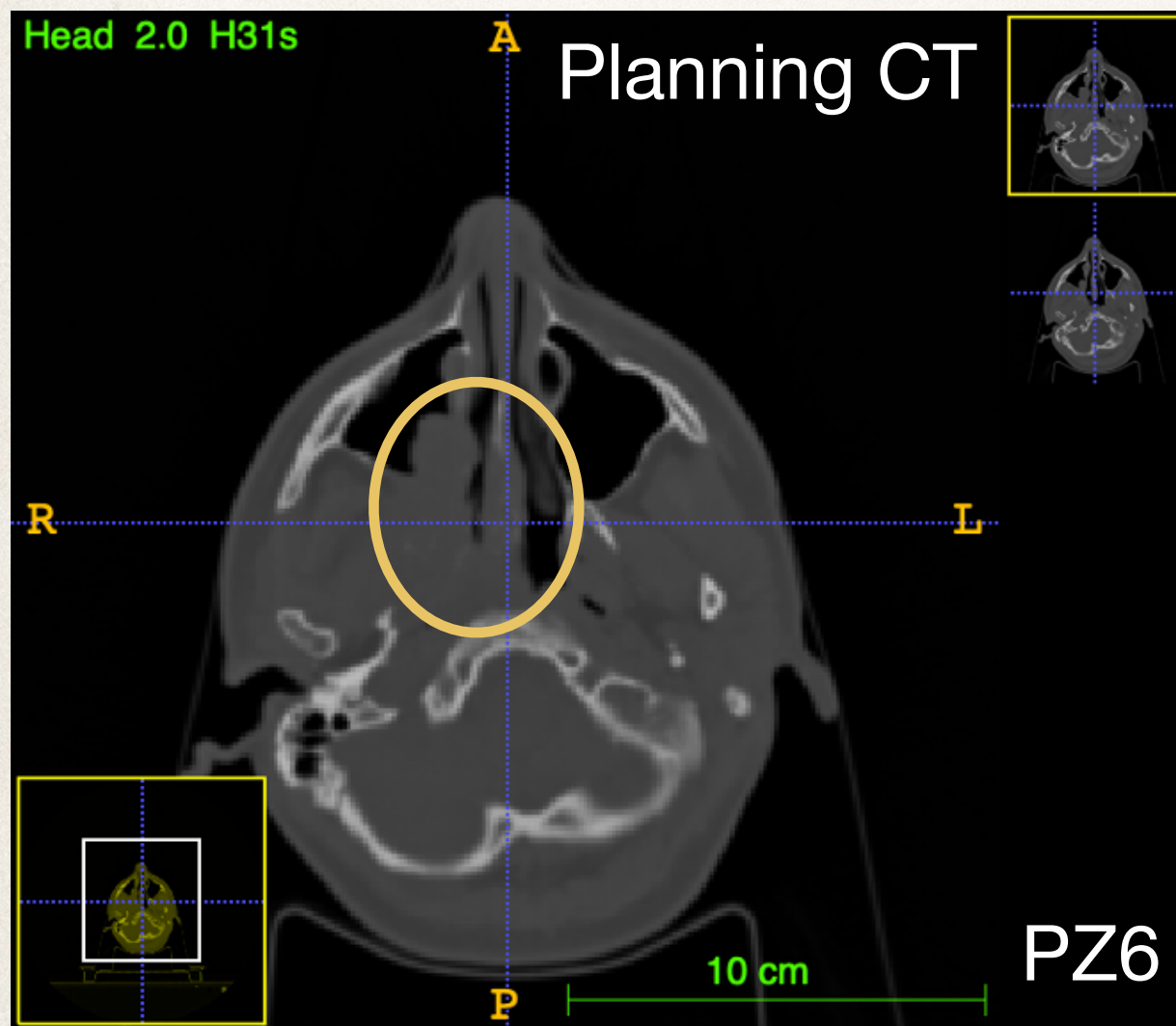


Promising result!

*Calvi, G. *et al.*, *IL NUOVO CIMENTO* 44 C (2021) 147 <https://doi.org/10.1393/ncc/i2021-21147-9>

3D Inter-fractional Monitoring (MC)

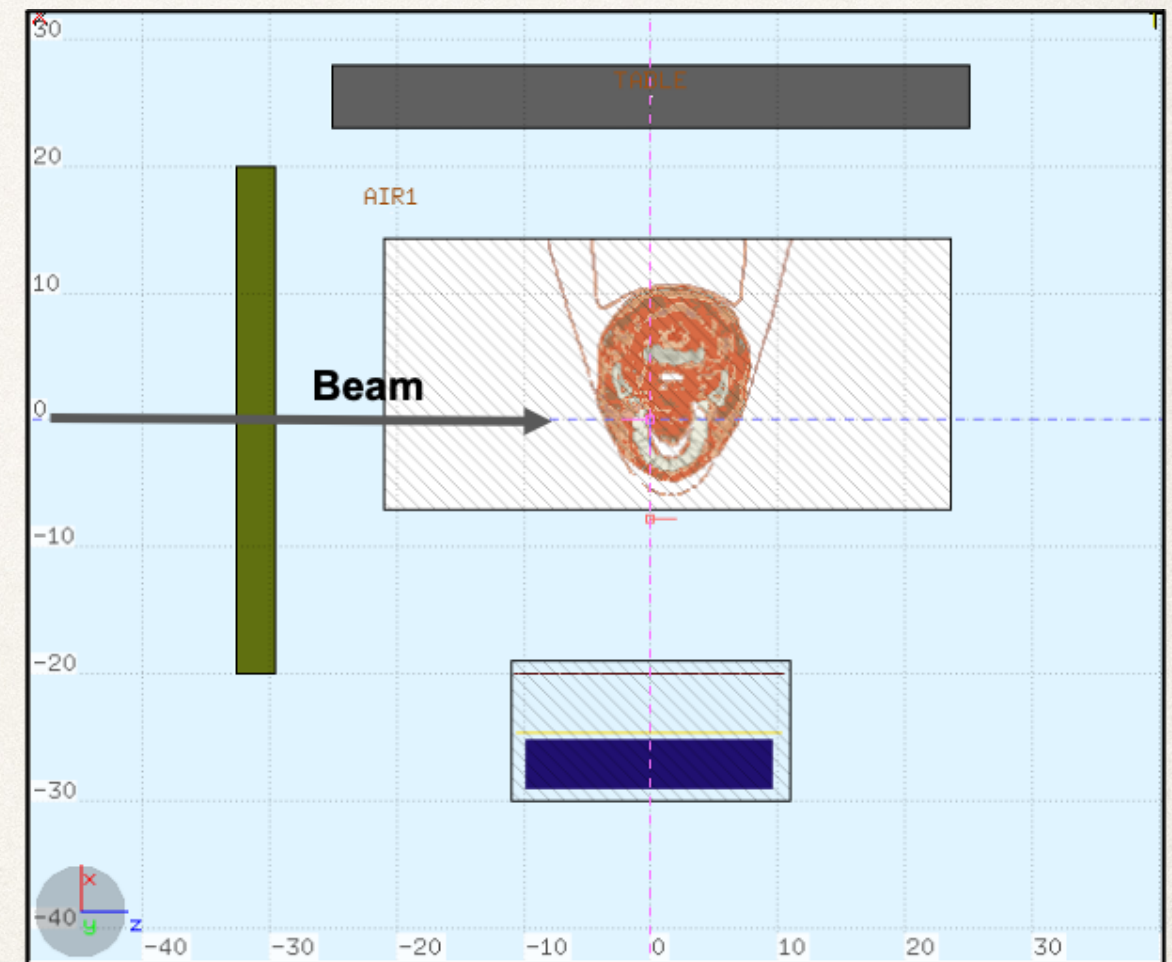
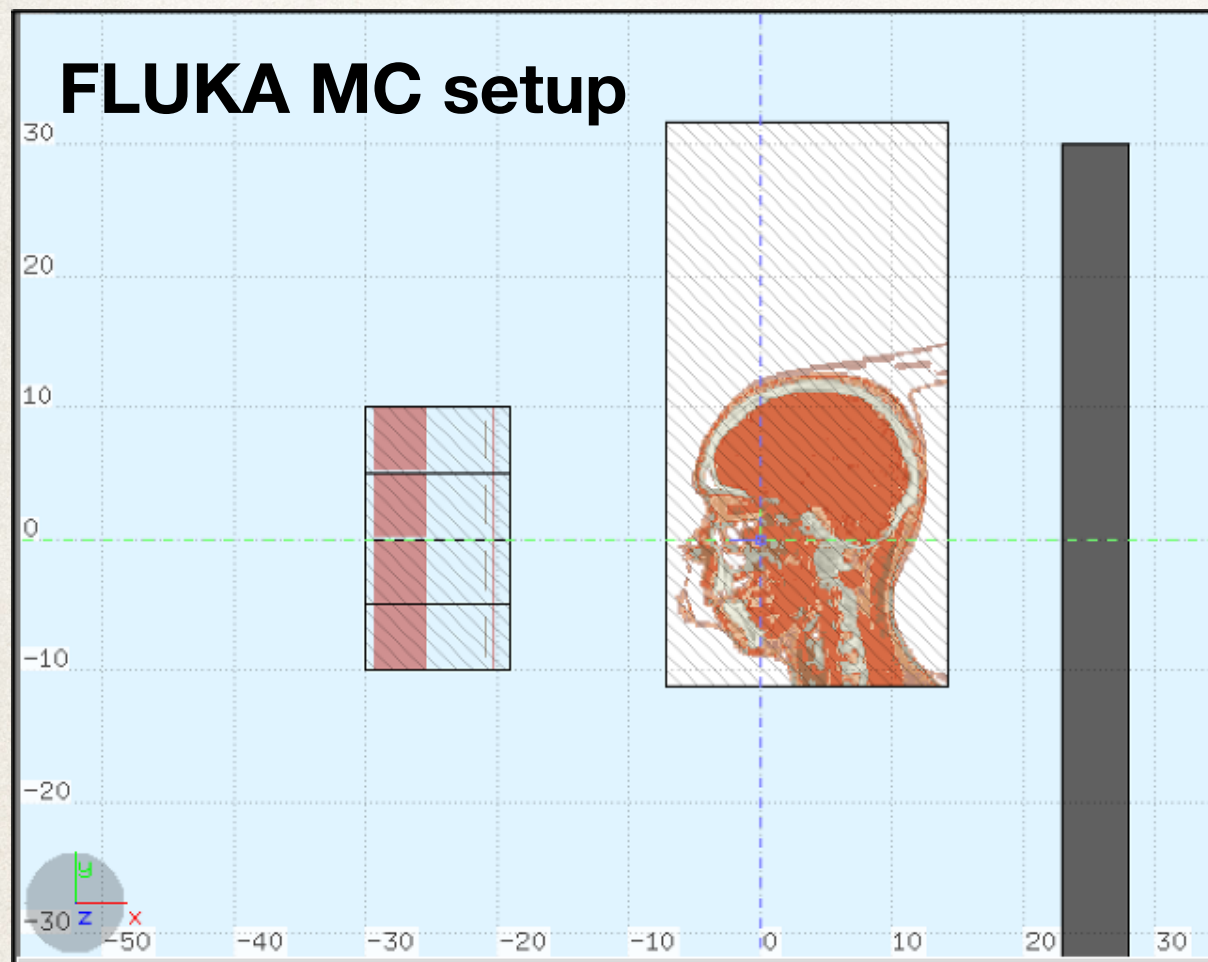
- ❖ A Monte Carlo study has been performed on a patient of the clinical trial at CNAO, treated with protons and monitored with the INSIDE-PET system*. The patient had an Adenoid Cystic Carcinoma, where morphological changes occurred, spotted by the PET system and confirmed by the control CT.



*Fiorina, E. *et al.*, *Frontiers in Physics* 8 (2021) 578388 <https://doi.org/10.3389/fphy.2020.578388>

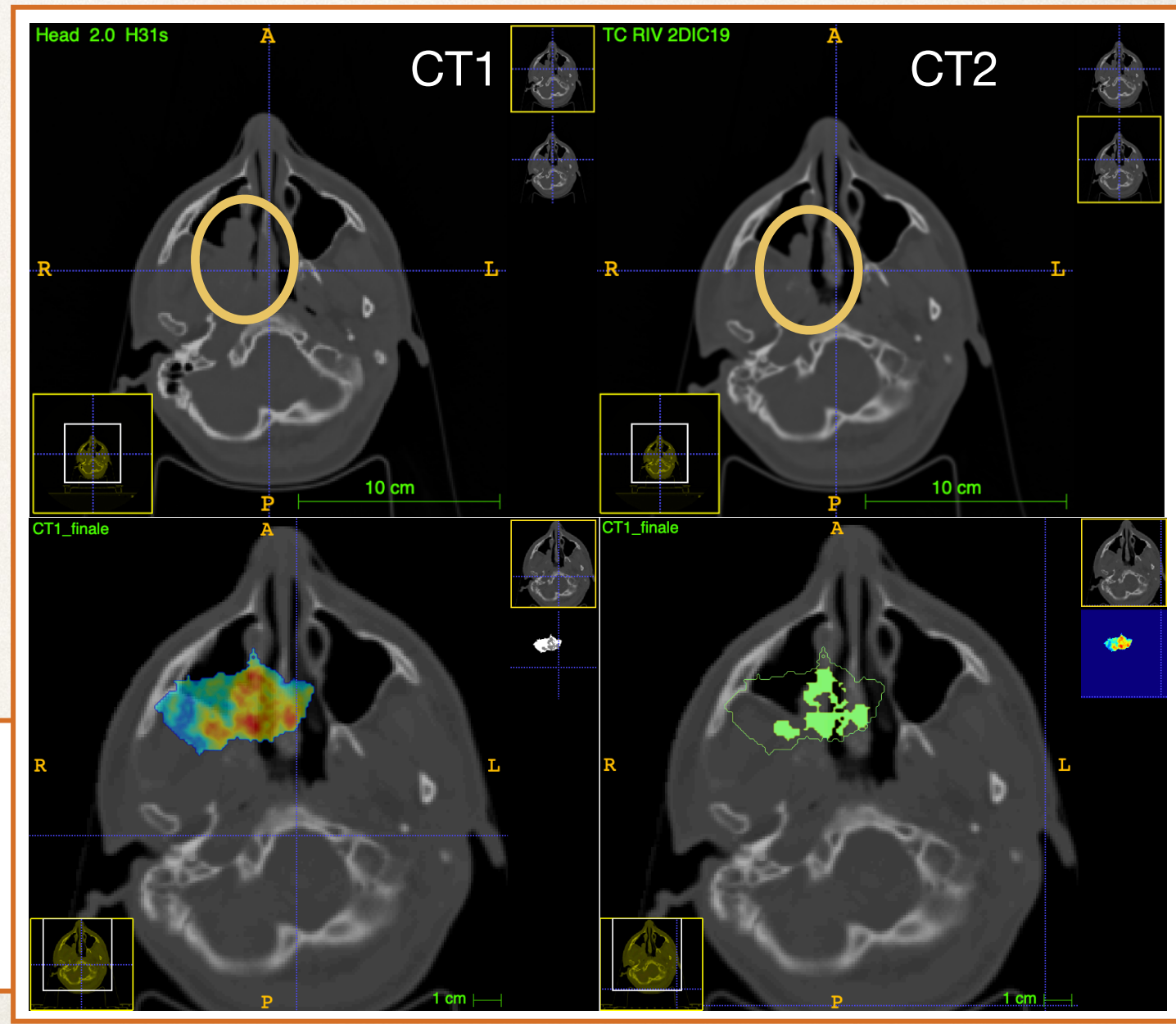
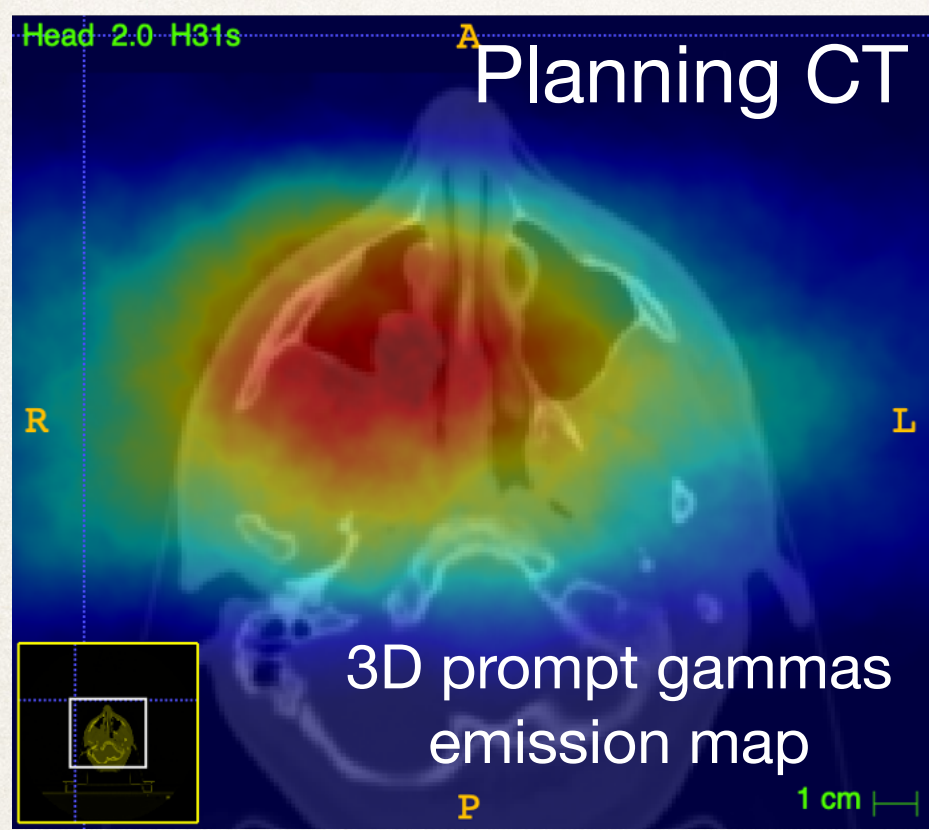
3D Inter-fractional Monitoring (MC)

- ❖ PAPERICA has been simulated as 4 modules, to have a 1 sr detector
- ❖ 2 simulations (FLUKA) of the **full treatment delivered on the planning and control CT**



3D Inter-fractional Monitoring (MC)

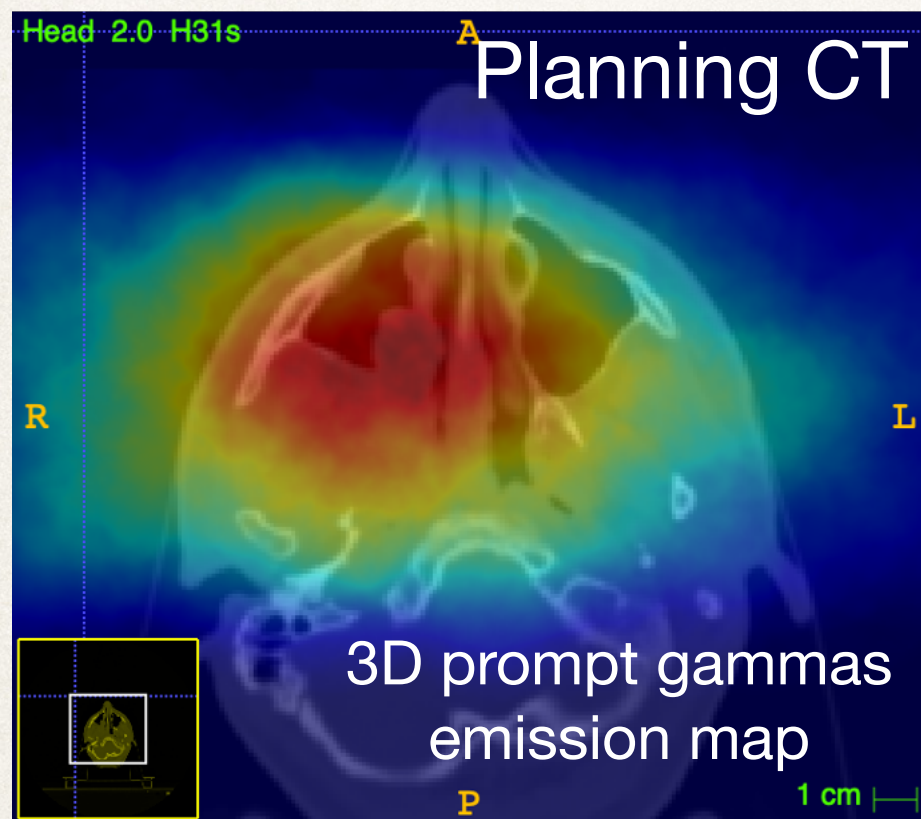
- ❖ PAPERICA has been simulated as 4 modules, to have a 1 sr detector
- ❖ 2 simulations (FLUKA) of the full treatment delivered on the planning and control CT
- ❖ 2 maps of the emission points of prompt photons reconstructed by the PAPERICA detectors have been obtained and the gamma-index map has been calculated



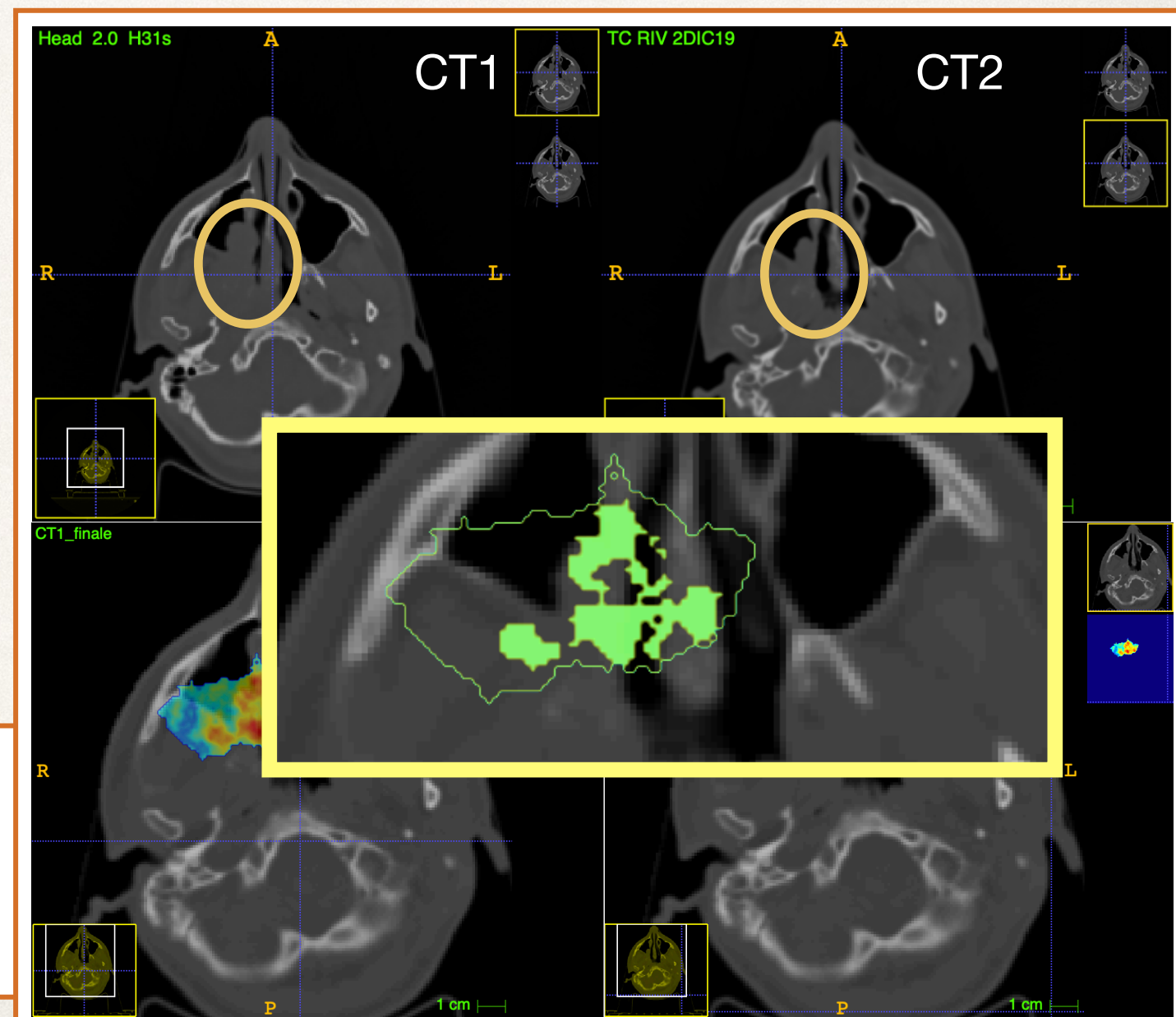
PZ6 underwent the emptying of the nasal cavity, as noticed by a mid-term CT (CT2).
Such modification has been clearly identified by the gamma-index map.

3D Inter-fractional Monitoring (MC)

- ❖ PAPERICA has been simulated as 4 modules, to have a 1 sr detector.
- ❖ 2 simulations (FLUKA) of the full treatment delivered on the planning and control CT
- ❖ 2 maps of the emission points of prompt photons reconstructed by the PAPERICA detectors have been obtained and the gamma-index map has been calculated



PZ6 underwent the emptying of the nasal cavity, as noticed by a mid-term CT (CT2).
Such modification has been clearly identified by the gamma-index map.

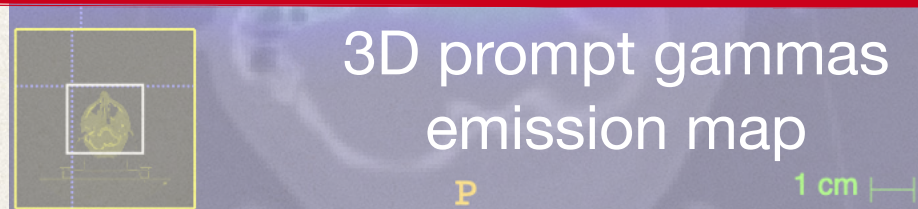


3D Inter-fractional Monitoring (MC)

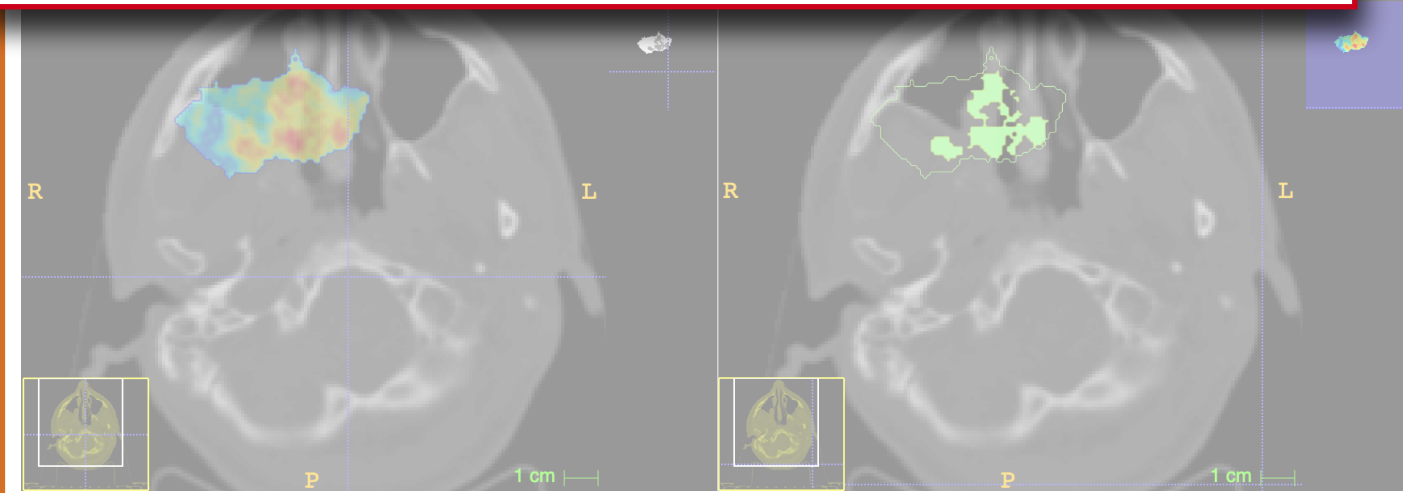
- ❖ PAPERICA has been simulated as 4 modules, to have a 1 sr detector
- ❖ 2 simulations (FLUKA) of the full treatment delivered on the planning and control CT
- ❖ 2 maps of the emission points of prompt photons reconstructed by the PAPERICA detectors have been obtained and the gamma-index map has been calculated

A study on the parameter of the gamma index test is going, to optimise the PAPERICA sensitivity to spot 3D morphological changes.

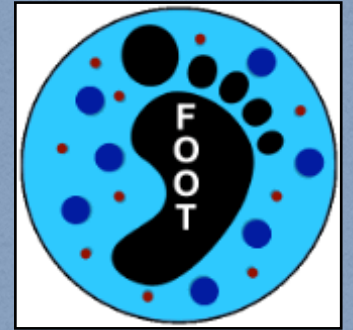
The detector is under construction and will be tested on beam in 2022.



PZ6 underwent the emptying of the nasal cavity, as noticed by a mid-term CT (CT2). Such modification has been clearly identified by the gamma-index map.



The FOOT experiment



The aim of the FOOT
(FragmentatiOn Of Target)
experiment* is to measure
the nuclear fragmentation
cross sections of interest in
Particle Therapy and
radioprotection in space.

The Collaboration

Aachen: Hetzel Ronja³, Stahl Achim³,
Bari: Galati Giuliana²⁹, Pastore Alessandra²⁹,
Bologna: Biondi Silvia^{4,20}, Bruni Graziano⁴, Colombi Sofia⁴, Franchini Matteo^{4,20}, Massimi Cristian^{4,20}, Mengarelli Alberto⁴, Ridolfi Riccardo^{4,20}, Sartorelli Gabriella^{4,20}, Selvi Marco⁴, Spighi Roberto⁴, Villa Mauro^{4,20}, Zarrella Roberto^{4,20}, Zoccoli Antonio^{4,20},
CEADEN: Arteché Diaz Raul³⁰, Lopez Torres Ernesto^{30,17},
CNAO: Meneghetti Alessio⁵, Pullia Marco⁵, Savazzi Simone⁵,
Frascati: Clozza Alberto⁷, Iarocci Enzo⁷, Laurenza Martina⁷, Sanelli Claudio⁷, Sciubba Adalberto^{7,22}, Spiriti Eleuterio⁷, Tomassini Sandro⁷, Toppi Marco^{7,22},
GSI: Durante Marco^{6,32}, Reidel Claire-Anne⁶, Schuy Christoph⁶, Weber Ulrich⁶,
GSSI: Gentile Valerio³¹,
Milano: Battistoni Giuseppe⁸, Dong Yunsheng^{8,23}, Mattei Ilaria⁸, Muraro Silvia⁸, Valle Serena Marta⁸,
Nagoia: Sato Osamu⁹,
Napoli: Alexandrov Andrey^{10,19,33,34}, De Lellis Giovanni^{10,19}, Di Crescenzo Antonia^{10,19}, Lauria Adele^{10,19}, Montesi Maria Cristina^{10,19}, Valeri Tioukov¹⁰,
Perugia: Alpat Behcet¹¹, Ambrosi Giovanni¹¹, Barbanera Mattia¹¹, Fiandrini Emanuele^{11,24}, Ionica Maria¹¹, Kanxheri Keida¹¹, Placidi Pisana^{11,25}, Servoli Leonello¹¹, Silvestre Gianluigi^{11,24},
Pisa: Belcarì Nicola^{2,1}, Bisogni Maria Giuseppina^{2,1}, Carra Pietro^{2,1}, Ciarrocchi Esther^{2,1}, Del Guerra Alberto^{2,1}, Francesconi Marco^{2,1}, Galli Luca¹, Kraan Aafke Christine¹, Massa Maurizio¹, Moggi Andrea¹, Morrocchi Matteo^{1,2}, Rosso Valeria^{2,1}, Sportelli Giancarlo^{2,1},
Roma: De Simoni Micol^{12,26}, Fischetti Marta^{12,22}, Franciosini Gaia^{12,26}, Marafini Michela^{12,21}, Patera Vincenzo^{12,22}, Sarti Alessio^{12,22}, Schiavi Angelo^{12,22}, Traini Giacomo^{12,26},
Roma Tor V.: Morone Maria Cristina^{13,27},
Strasbourg: Finck Christian¹⁴, Sécher Alexandre¹⁴, Vanstalle Marie¹⁴,
Trento: Bellinzona Elettra¹⁵, Di Ruzza Benedetto¹⁵, La Tessa Chiara^{15,16}, Scifoni Emanuele¹⁵, Tommasino Francesco^{15,16},
Torino: Argirò Stefano^{28,17}, Bartosik Nazar¹⁷, Cavanna Francesca¹⁷, Cerello Piergiorgio¹⁷, Donetti Marco^{17,5}, Ferrero Veronica¹⁷, Fiorina Elisa¹⁷, Giraudo Giuseppe¹⁷, Pastrone Nadia¹⁷, Pennazio Francesco¹⁷, Ramello Luciano^{18,17}, Scavarda Lorenzo^{28,17}, Sitta Mario^{18,17},

*Battistoni, G. et al., *Frontiers in Physics* 8 (2021) 568242 <https://doi.org/10.3389/fphy.2020.568242>

FOOT in Particle Therapy

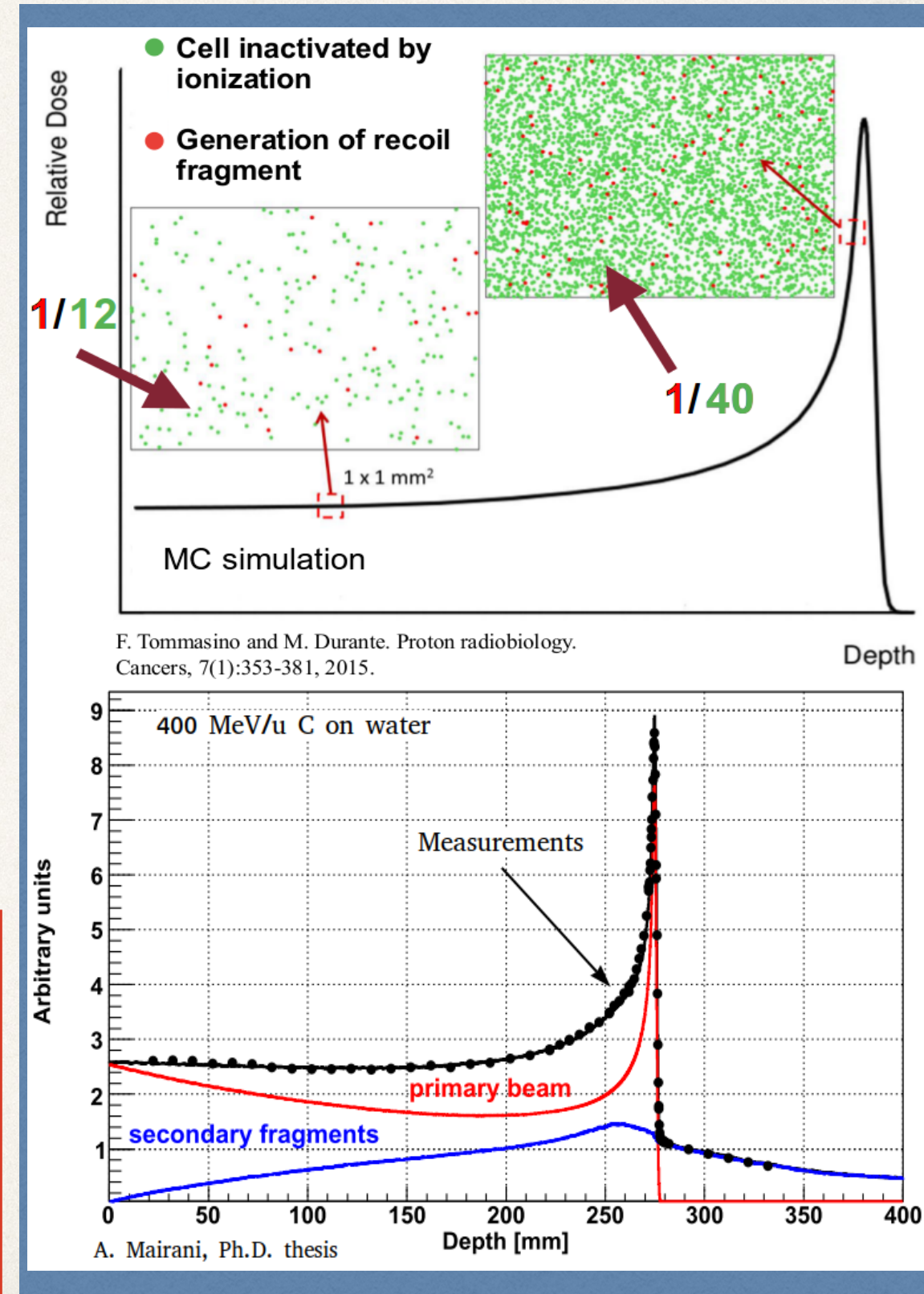
Target Fragmentation in proton therapy:

- ❖ Fragments with low ranges ($\sim\mu\text{m}$)
- ❖ Dose deposition in beam entrance channel

Projectile fragmentation in heavy ion therapy:

- ❖ Fragments with similar direction and velocity of primaries, but with lower mass
- ❖ Dose deposition beyond the Bragg peak

Need of fragmentation cross sections to benchmark MC tools and to improve the nuclear interaction models adopted in the current treatment planning systems (TPS)



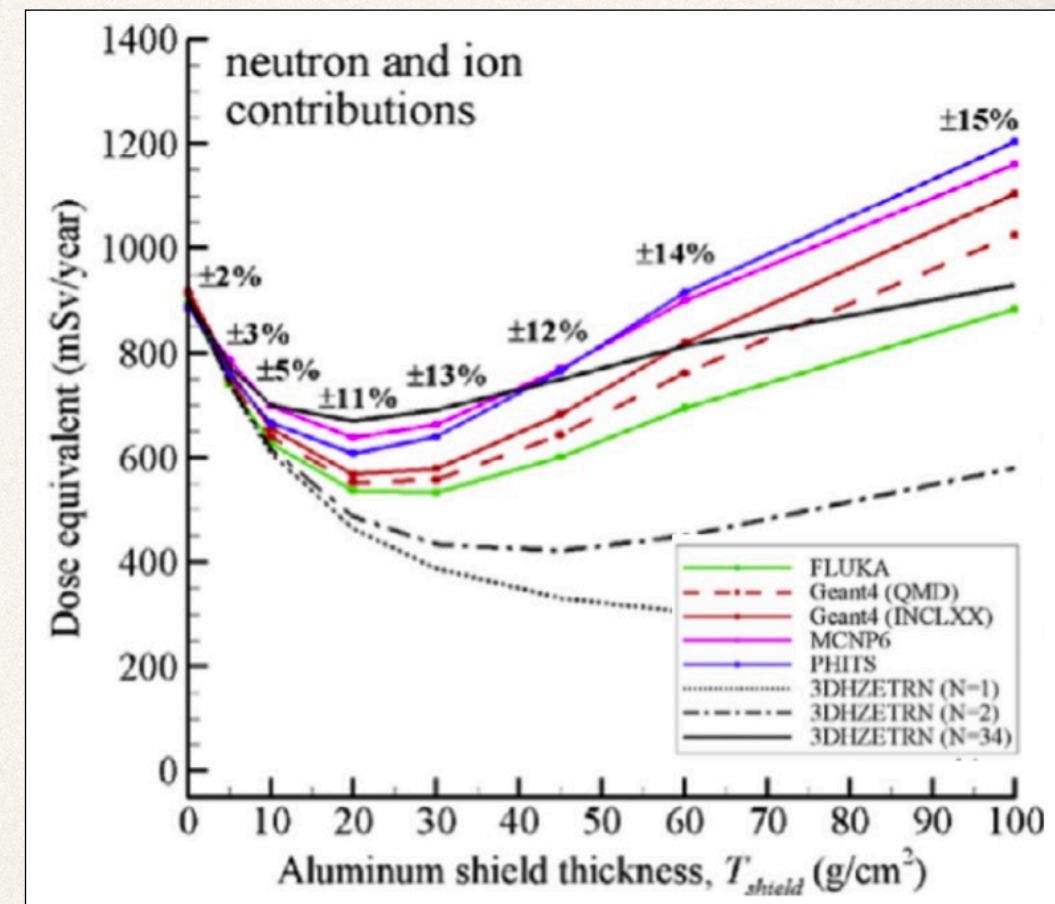
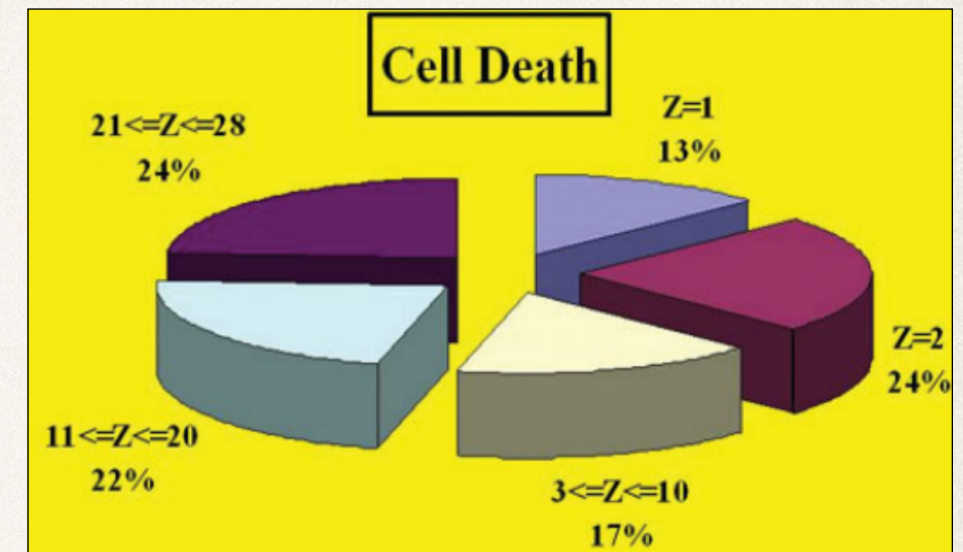
FOOT in Radioprotection in Space

Main radiation hazards in future long term and far from Earth space missions to Moon and Mars:

- ❖ Galactic cosmic radiations ($E < 10^{20}$ eV) and Solar particles events ($E < 10^5$ eV)
- ❖ Particle species: H~85-90%, He~10-14%, $Z > 2$ ~1%

High contribution to the equivalent dose from:

- ❖ Primary light ions (mainly He) and fragments produced by primary high Z and Energy particles
- ❖ Secondary neutrons that can penetrate deeply



Large discrepancies between transport codes, mainly for light fragments and neutrons

Slaba T. C. et al, Life Sciences in Space Research 12 (2017) 1–15
doi:10.1016/j.lssr.2016.12.003

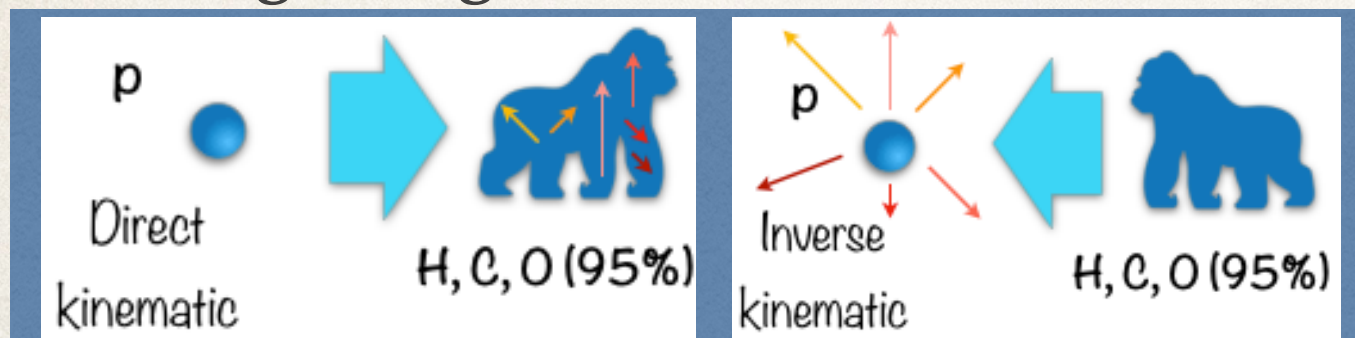
Measurement Strategy

Target material

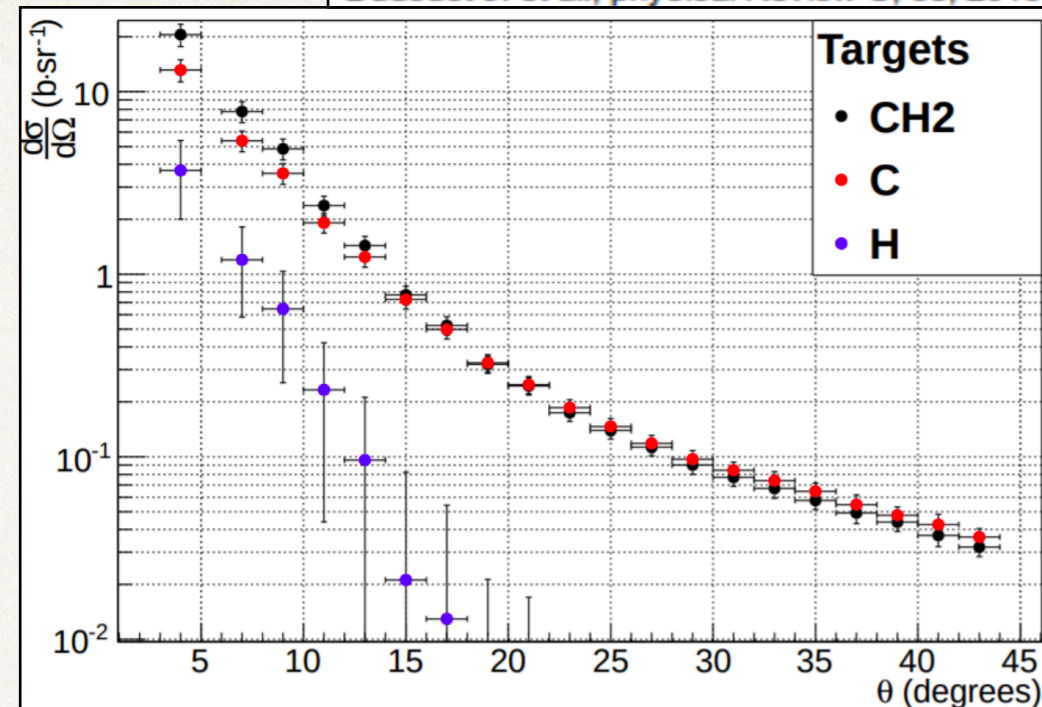
- ❖ Body composition: ^{16}O (61%), ^{12}C (23%), H (10%)
- ❖ Difficulties with gaseous target of ^{16}O and H
- ❖ **Use of C, CH_2 and PMMA targets**

Target fragmentation measurements

- ❖ Target fragments produced in proton therapy have ranges of $\sim \mu\text{m}$
- ❖ Technical difficulties for a direct detection
- ❖ **Use of an inverse kinematic approach for the target fragmentation measurements**



Dudouet J. et al., physical Review C, 88, 2013



Expected average physical parameters for target fragments produced in water by a 180 MeV proton beam

Fragment	E (MeV)	LET (keV/ μm)	Range (μm)
^{15}O	1.0	983	2.3
^{15}N	1.0	925	2.5
^{14}N	2.0	1137	3.6
^{13}C	3.0	951	5.4
^{12}C	3.8	912	6.2
^{11}C	4.6	878	7.0
^{10}B	5.4	643	9.9
^8Be	6.4	400	15.7
^6Li	6.8	215	26.7
^4He	6.0	77	48.5
^3He	4.7	89	38.8
^2H	2.5	14	68.9

GoodHead D.T., Radiation protection dosimetry, 122, 2006

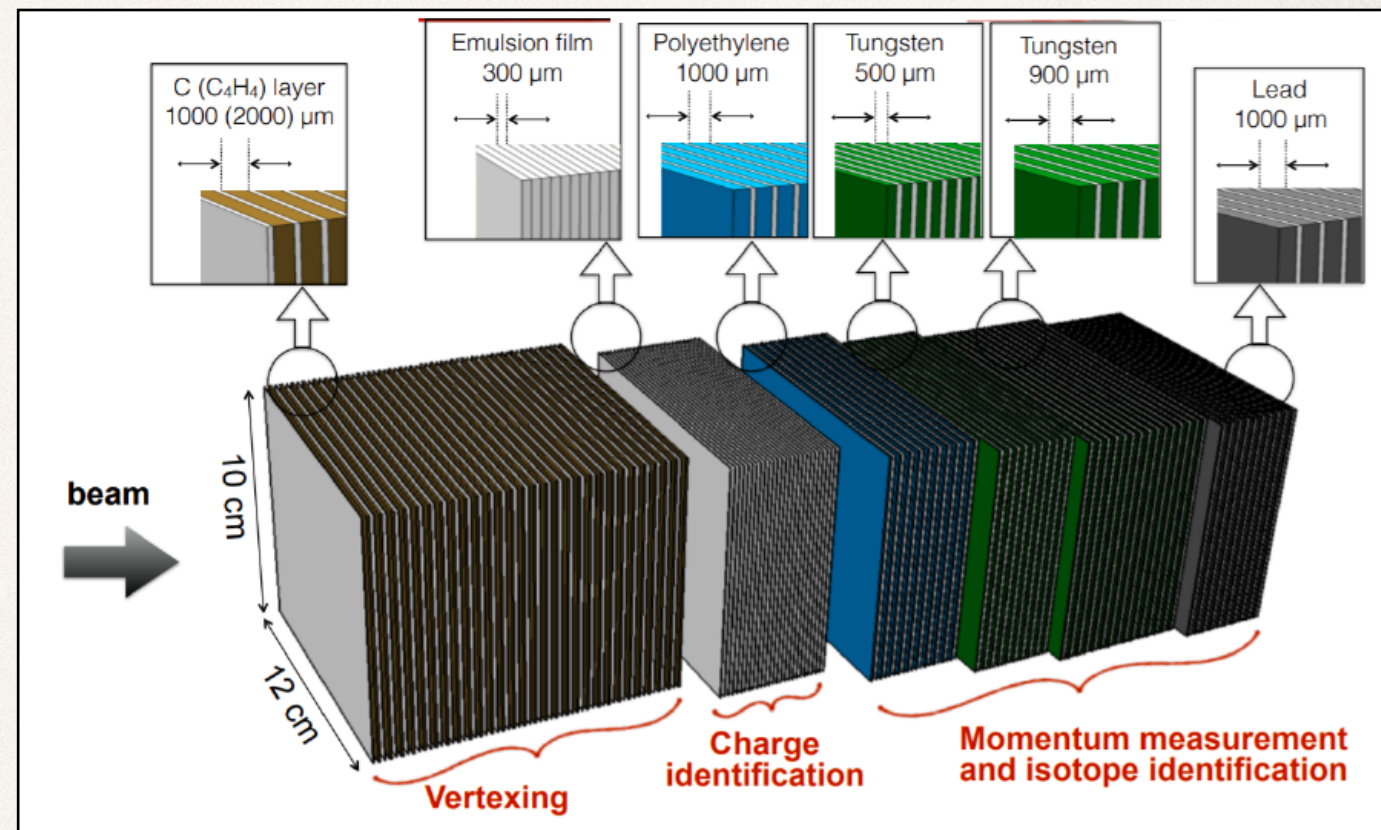
The Emulsion Spectrometer

The emulsion spectrometer is a compact detector realised with the technology adopted in the OPERA experiment.

Emulsion Cloud Chamber adopted to detect the fragments with $\Theta < 70^\circ$ and $Z \leq 3$

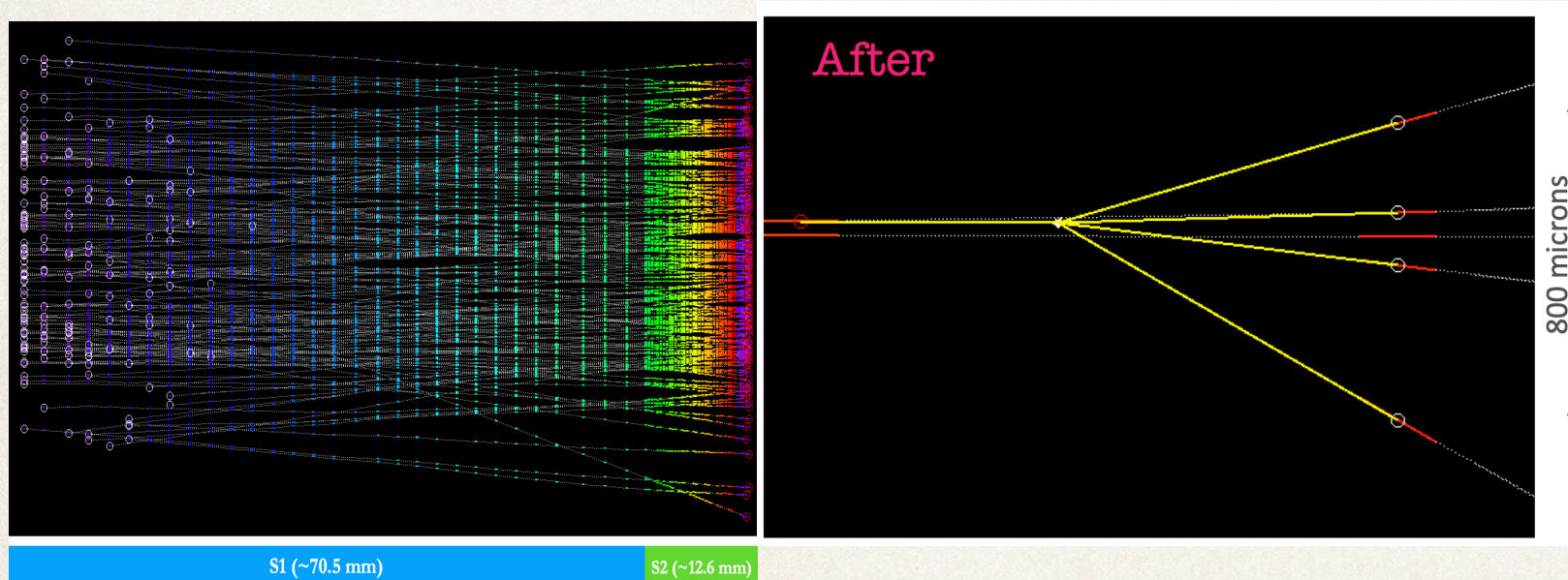
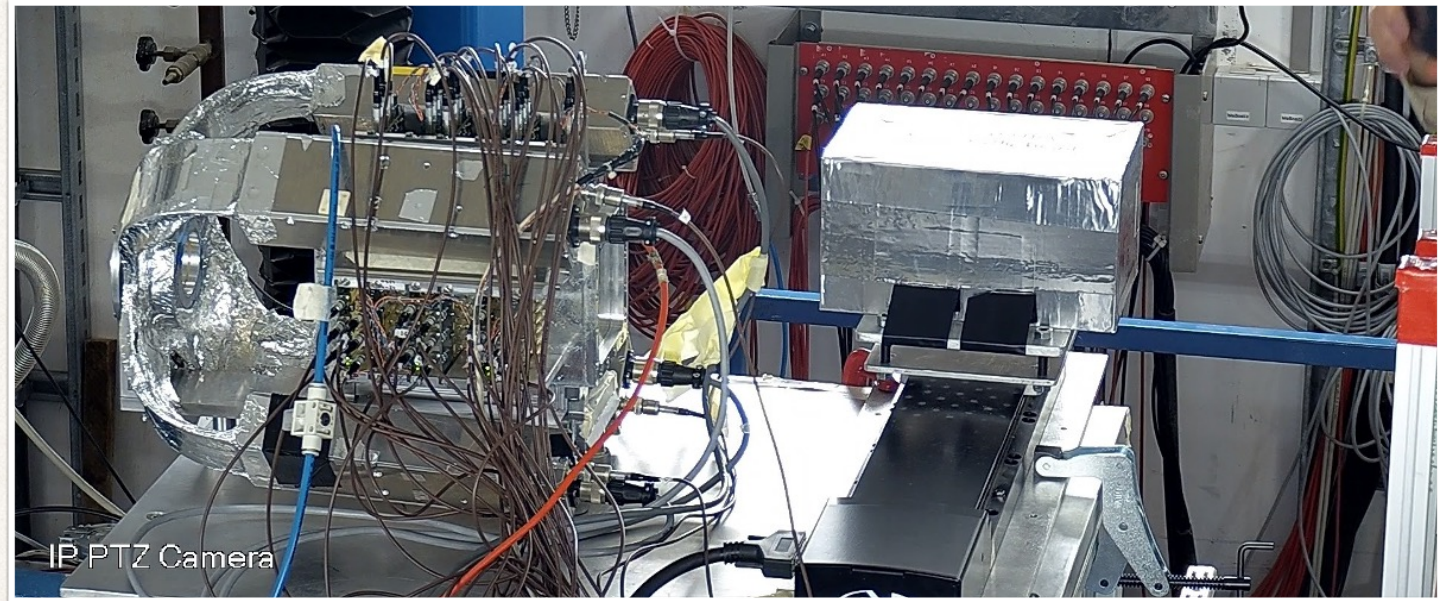
Detector composition:

- ❖ **Vertexing region:** identify the nuclear interaction vertices
- ❖ **Charge id. region**
- ❖ **Absorbing region:** momentum and mass id. exploiting the track length and the Multiple Coulomb Scattering effect



The Emulsion Spectrometer

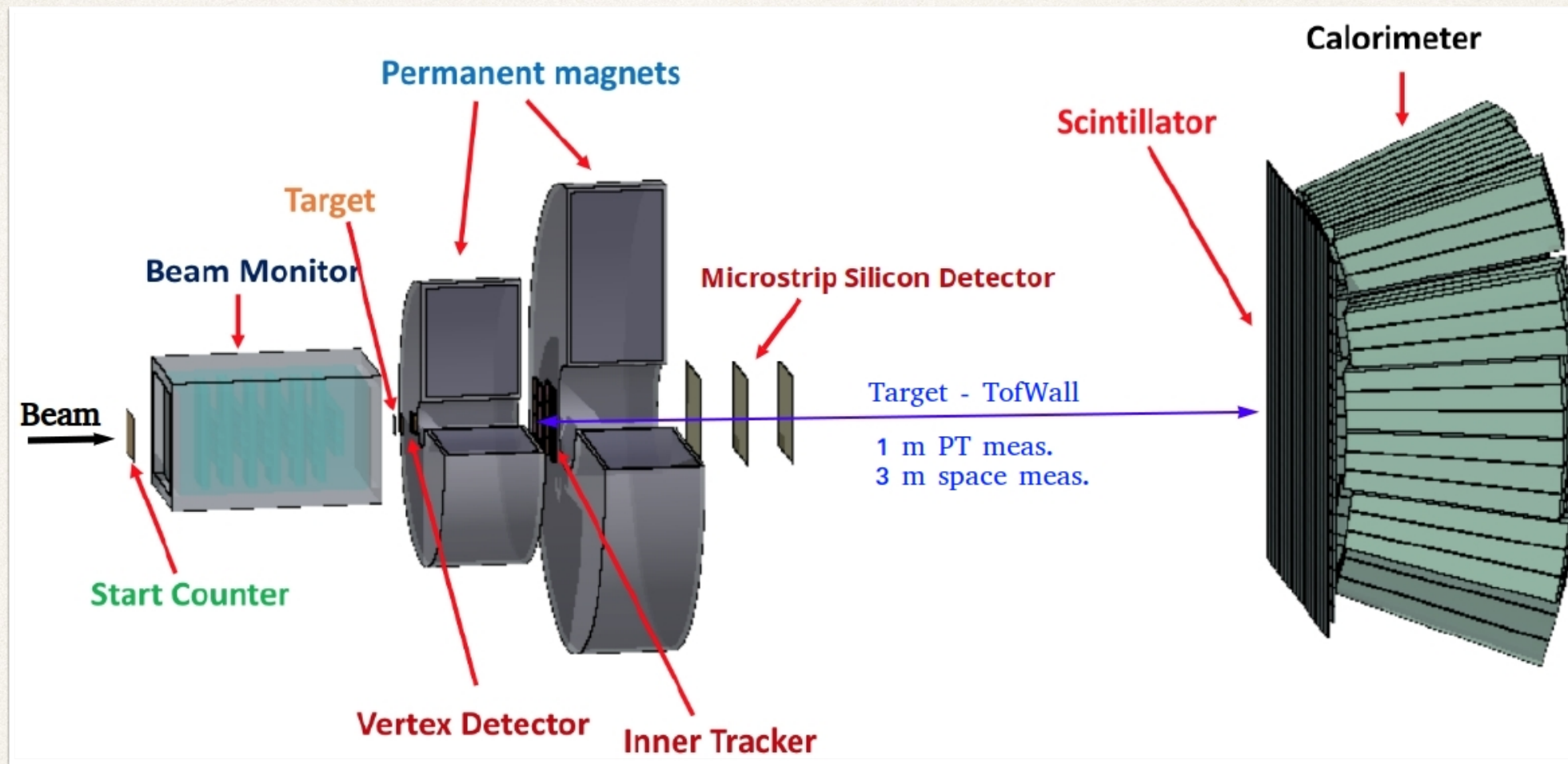
- ❖ Assessment of **detector performances***
- ❖ **Data taking at GSI** with ^{16}O @ 200-400 MeV/u on C and C_2H_4 (cross section evaluation ongoing)**



*Montesi, M.C. *et al.*, *Open physics* 17 (2019) 1 <https://doi.org/10.1515/phys-2019-0024>

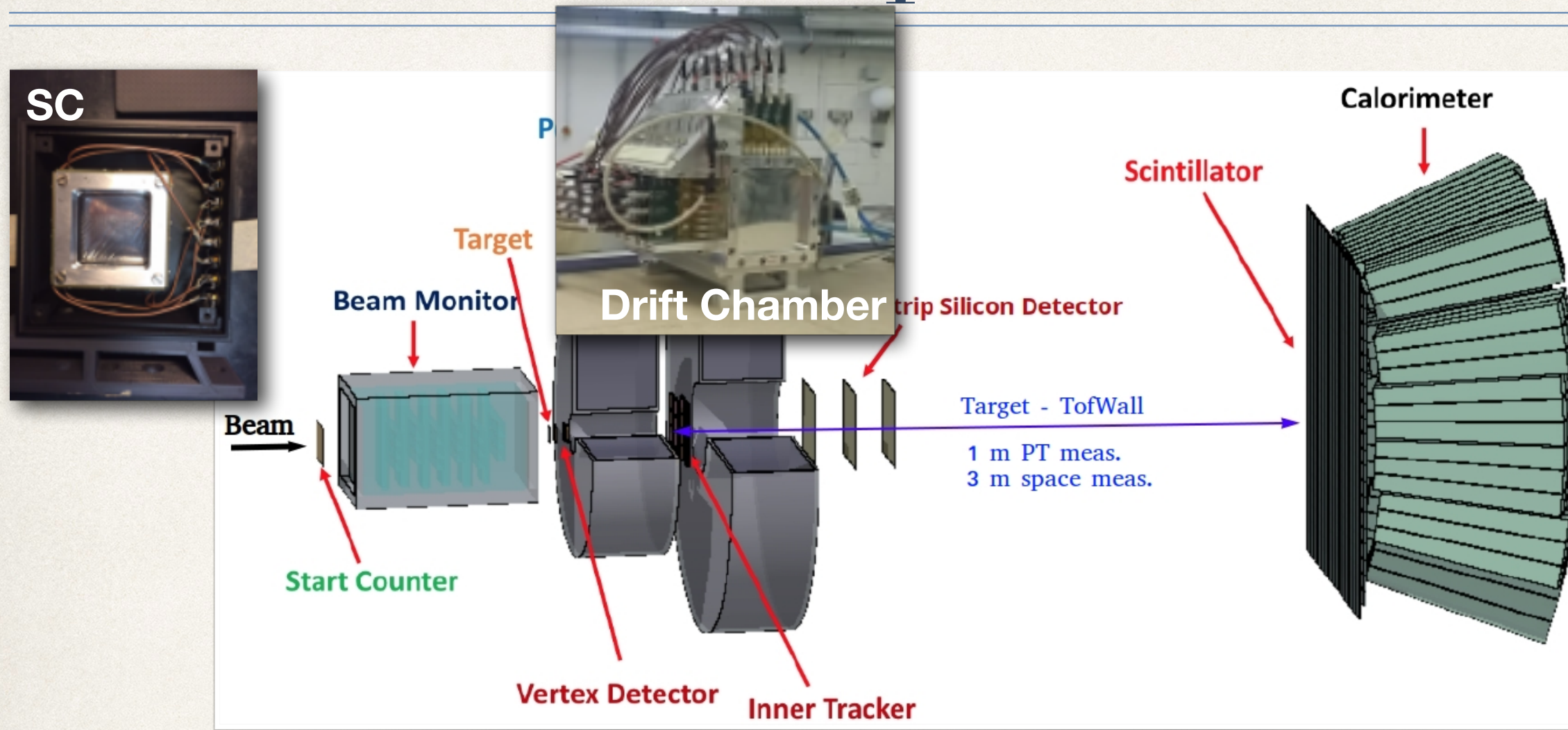
**Galati, G. *et al.*, *Open physics* 19 (2021) 1 <https://doi.org/10.1515/phys-2021-0032>

The Electronic Spectrometer



Different electronic sub detectors adopted to detect the fragments with $\Theta < 10^\circ$ and $Z \geq 3$

The Electronic Spectrometer



Pre target region

- ❖ Plastic scintillator: trigger and Time of Flight (TOF)
- ❖ Drift chamber: beam direction and position*

*Dong, Y. *et al.*, NIM A 986 (2021) 164786 <https://doi.org/10.1016/j.nima.2020.164756>

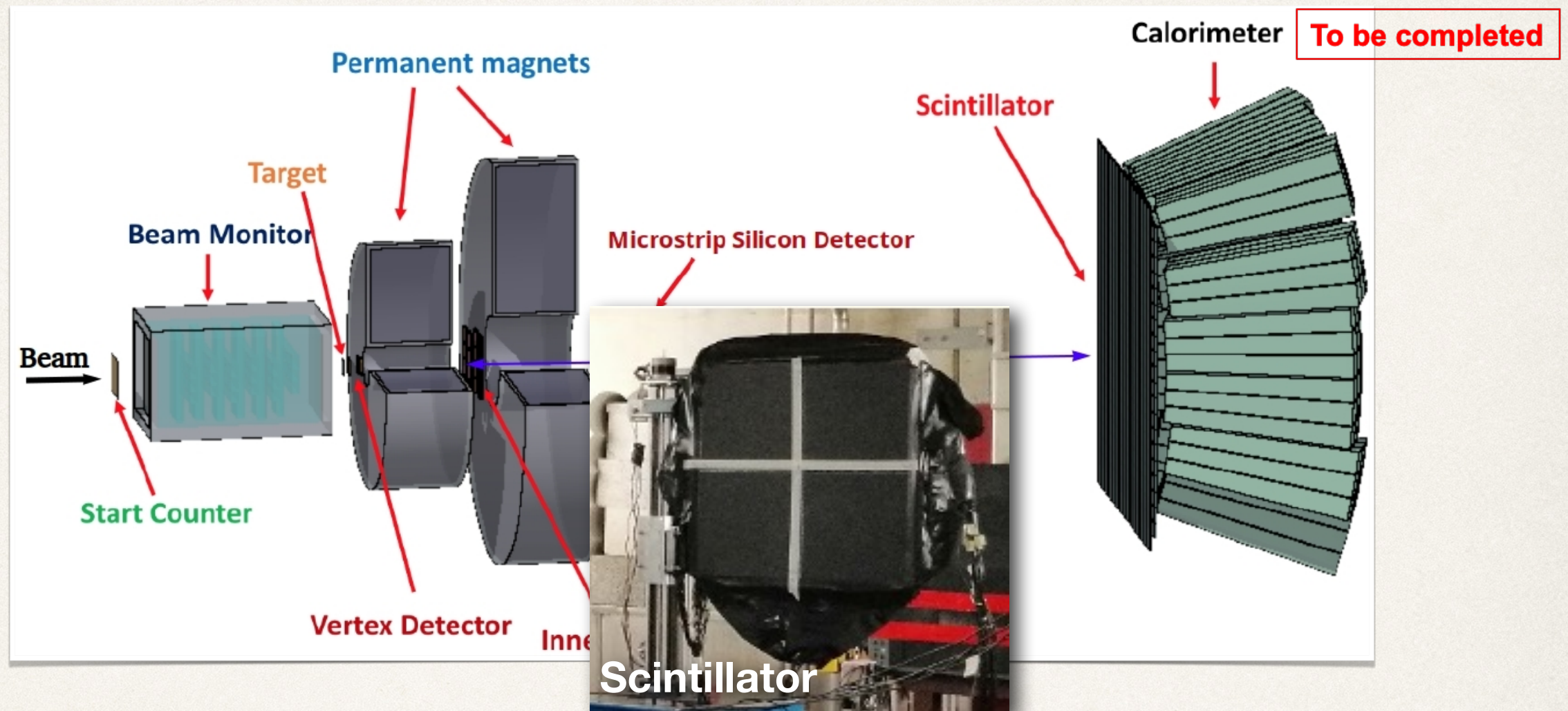
The Electronic Spectrometer



Tracking region

- ❖ Silicon pixel and strip detectors: particle momentum and track reconstruction
- ❖ Two permanent magnets in Halbach configuration: provide up to 1.4 T perpendicular to the beam axis

The Electronic Spectrometer



Downstream region

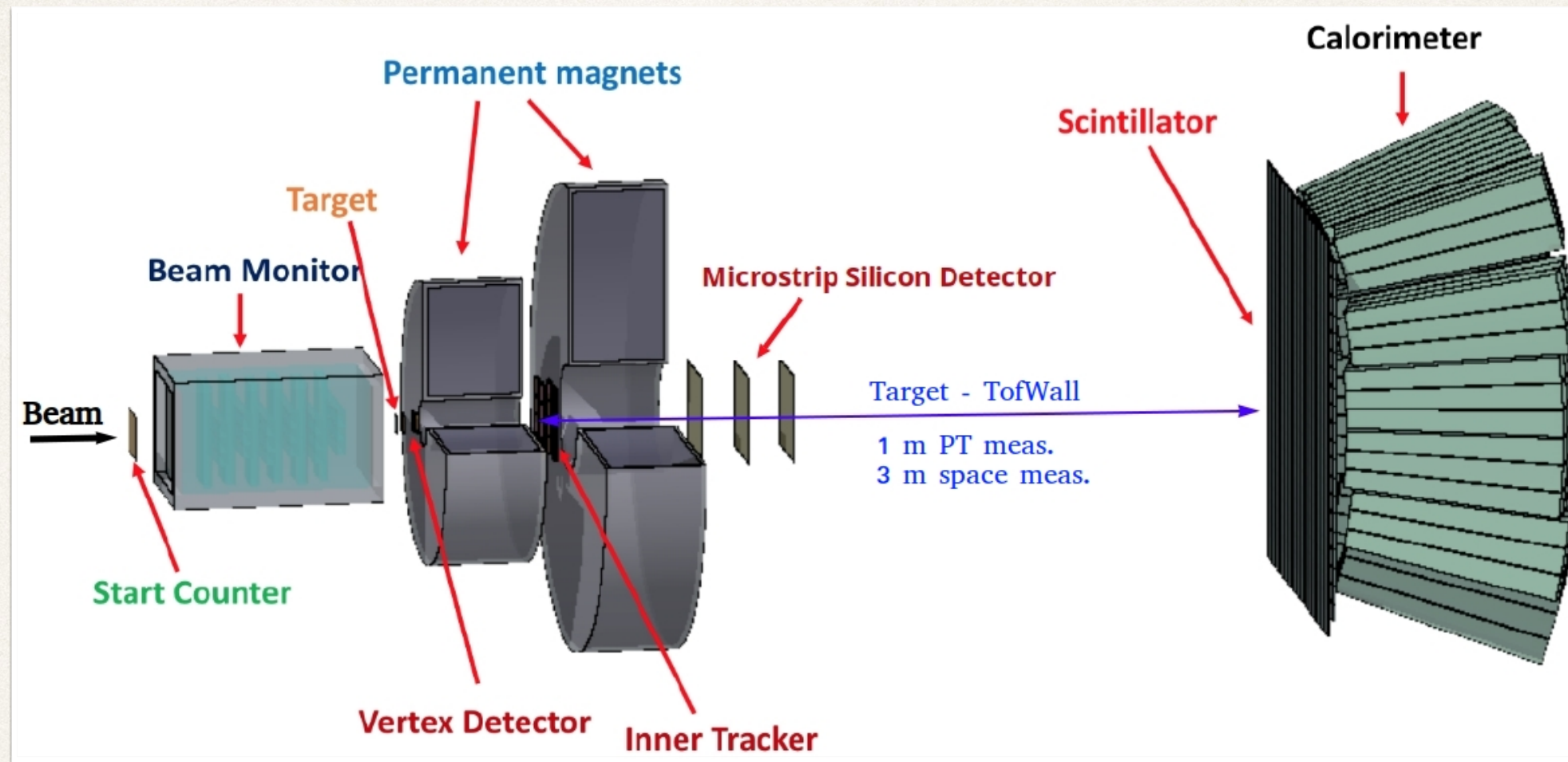
- ❖ Plastic scintillator bars: dE/dx and TOF ^{*,**,***}
- ❖ Calorimeter: kinetic energy

*Galli, L. *et al.*, NIM A 953 (2020) 163146 [https://doi.org/ 10.1016/j.nima.2019.163146](https://doi.org/10.1016/j.nima.2019.163146)

**Morrocchi, M. *et al.*, IEEE Trans. Nucl. Sci. 68 (2020) <https://doi.org/10.1109/TNS.2020.3041433>

***Kraan, A.C. *et al.*, NIM A 1001 (2021) 165206 <https://doi.org/10.1016/j.nima.2021.165206>

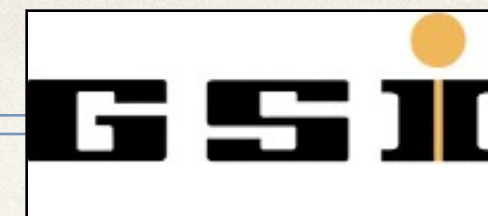
The Electronic Spectrometer



❖ Charge id: $\beta = L/(c \cdot TOF)$; $dE/dx \sim z^2 \cdot f(\beta)$

❖ Mass id: $A_1 = \frac{1}{u} \frac{P\sqrt{1-\beta^2}}{\beta}$; $A_2 = \frac{E_{kin}}{u} \cdot \frac{1 + \sqrt{1 + \gamma^2\beta^2}}{\gamma^2\beta^2}$; $A_3 = \frac{E_{kin}^2 - P^2}{2E_{kin}u}$

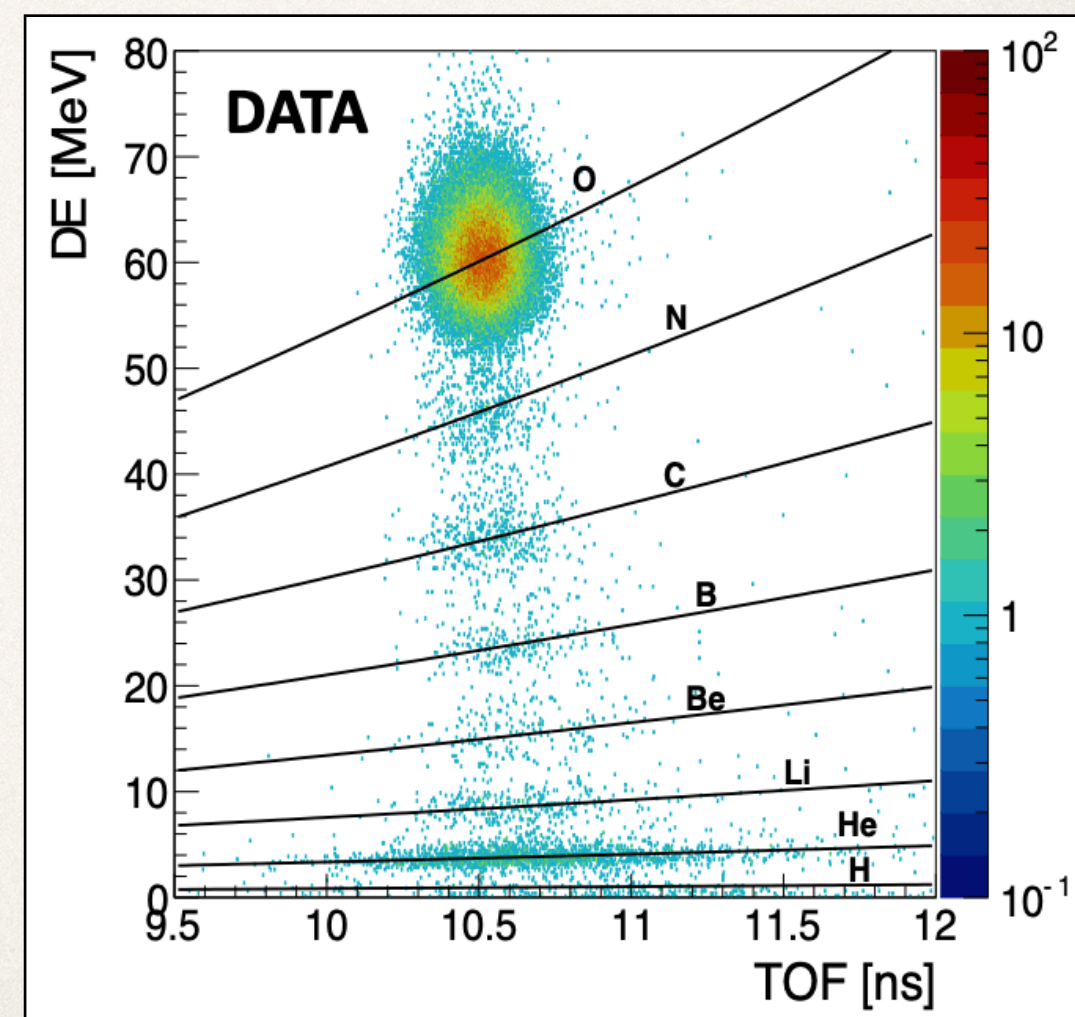
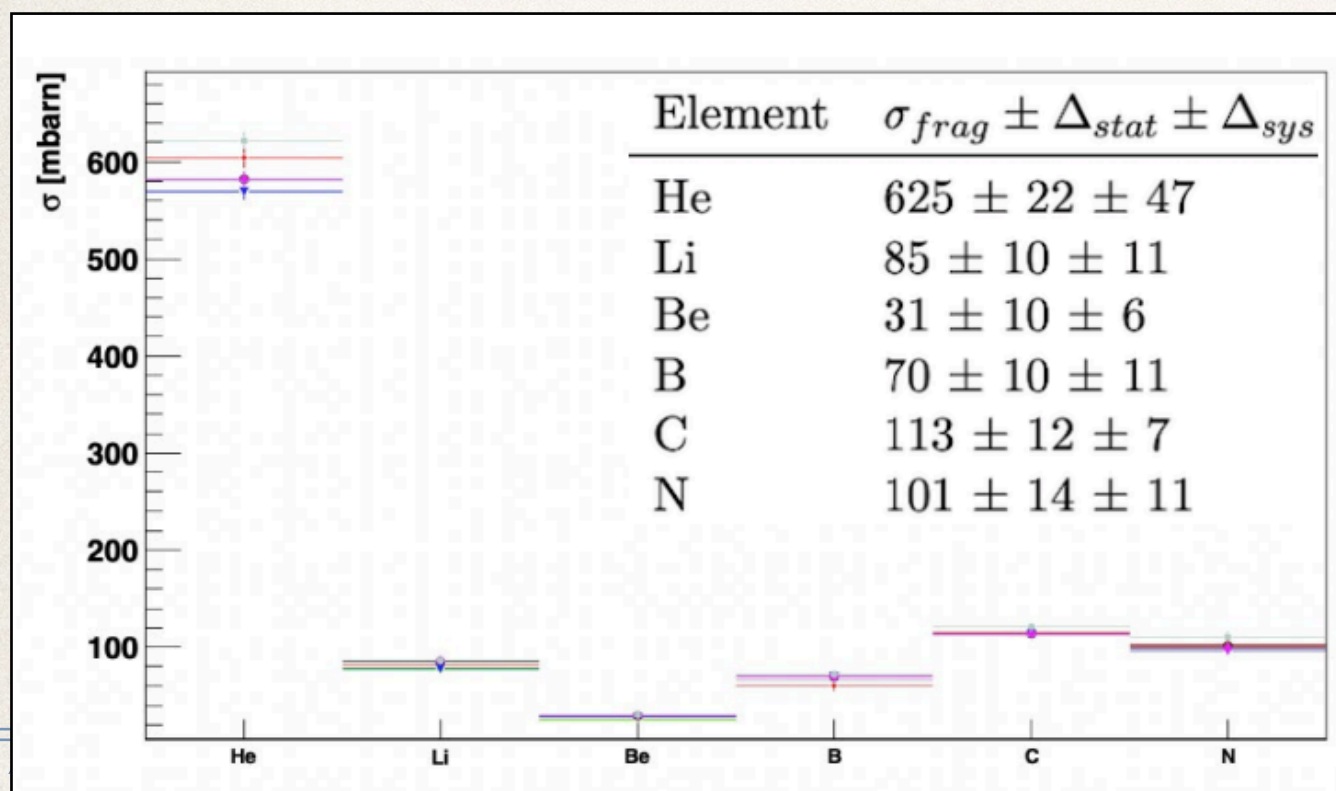
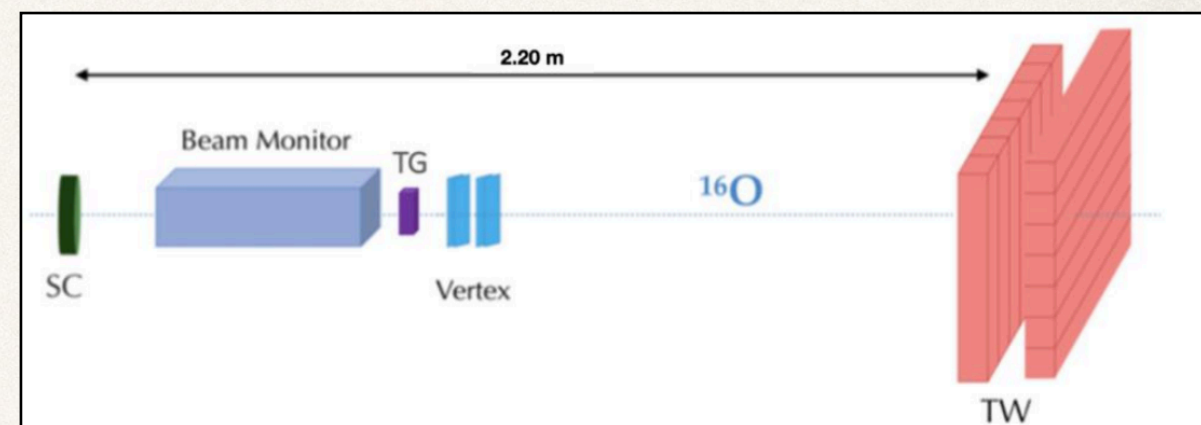
Electronic setup data taking



Characterisation completed for almost all the detectors.

First data taking at GSI with ^{16}O @ 400 MeV/u on C

- ❖ Scintillators, drift chamber and vertex detector
- ❖ TOF and dE/dx \rightarrow Total cross section meas.

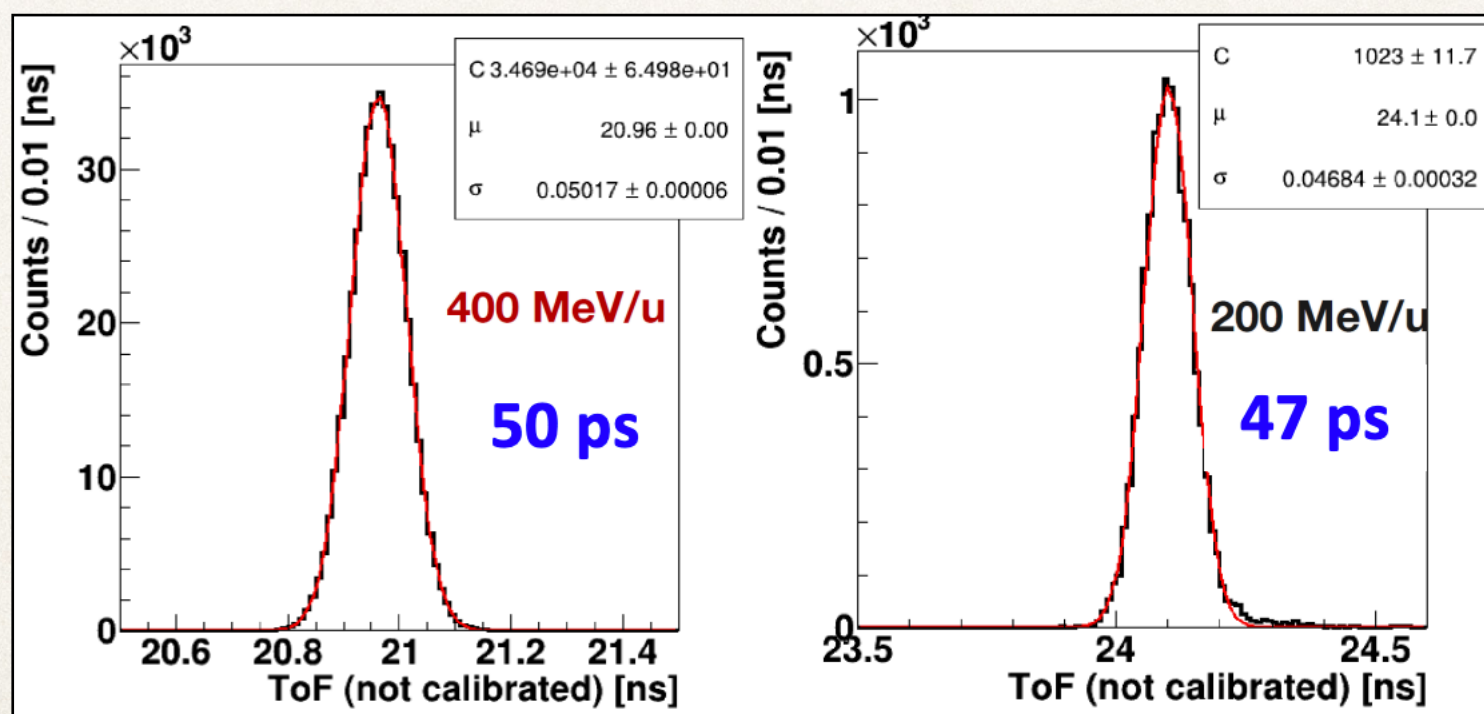
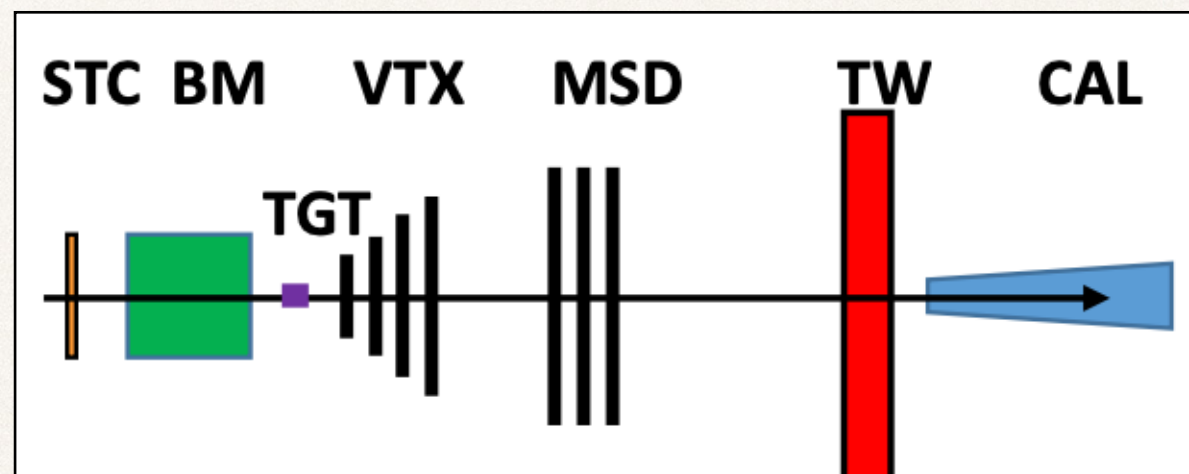


Electronic setup data taking



Data taking at GSI with ^{16}O @ 200-400 MeV/u on C and C_2H_4

- ❖ Scintillators, drift chamber, tracking detectors and a calorimeter module + neutron detectors
- ❖ Data analysis just started



Electronic setup data taking



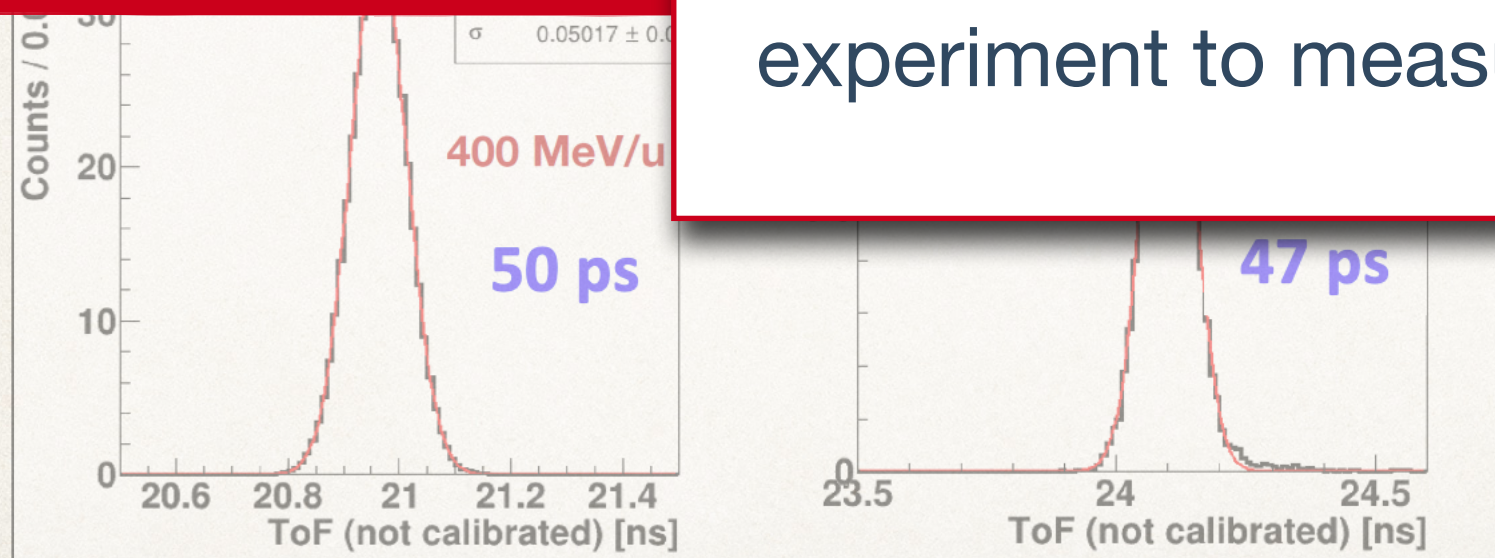
Data taking at GSI with ^{16}O @ 200-400 MeV/u on C and C_2H_4

- ❖ Scintillators, drift chamber, tracking detectors and a calorimeter module + neutron detectors

STC BM VTX MSD TW CAI

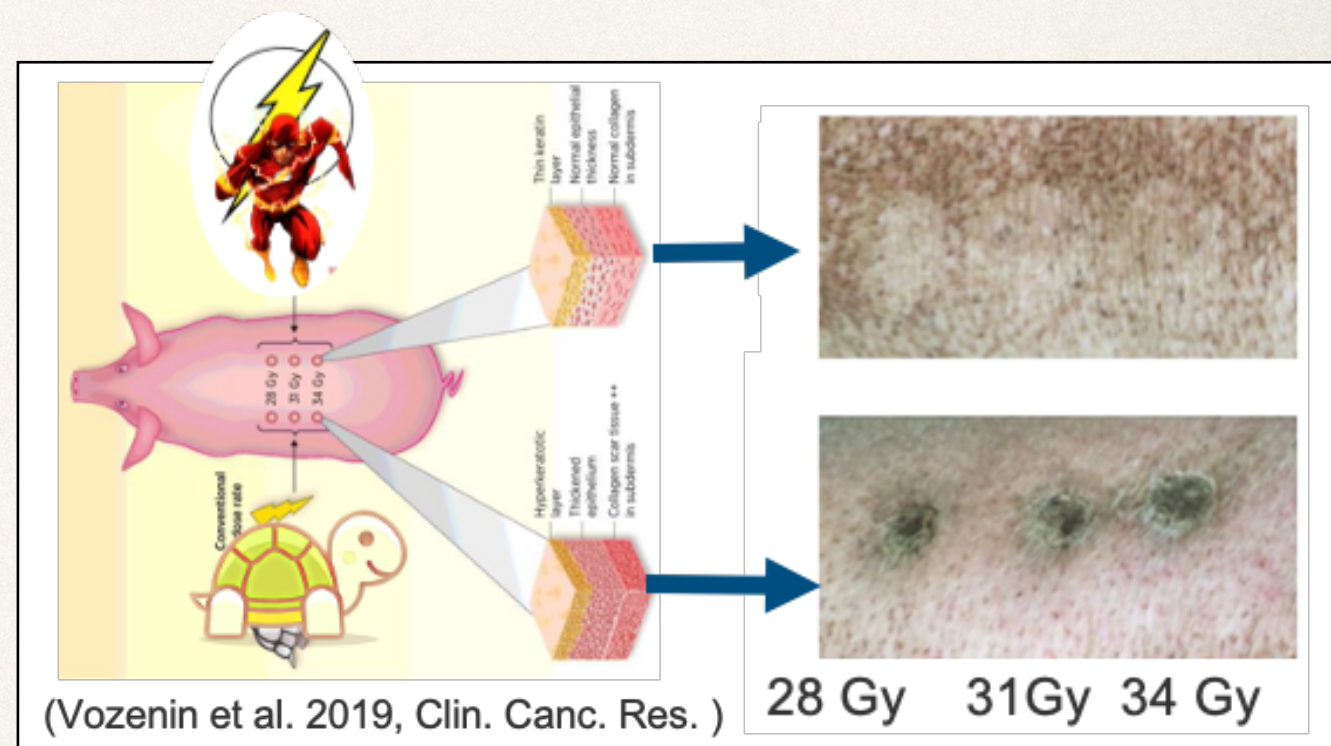
The FOOT full detector will be ready at the beginning of 2022 and new data takings are foreseen at CNAO, GSI, HIT.

An extension of the FOOT experiment to measure neutrons is under study.



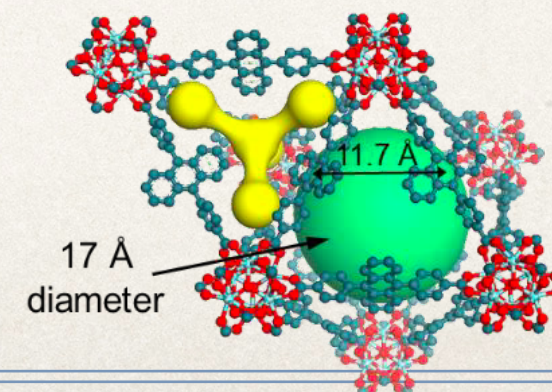
Upcoming Activities

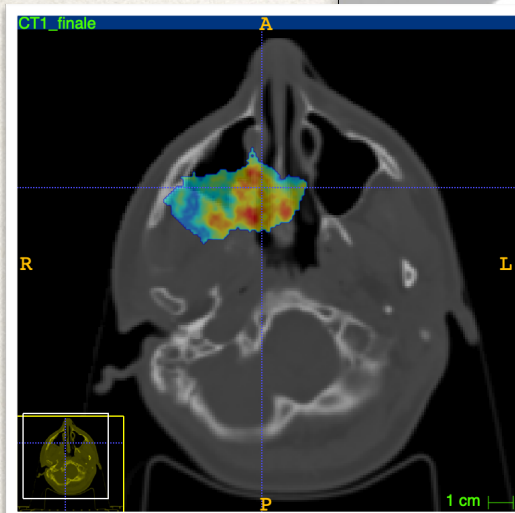
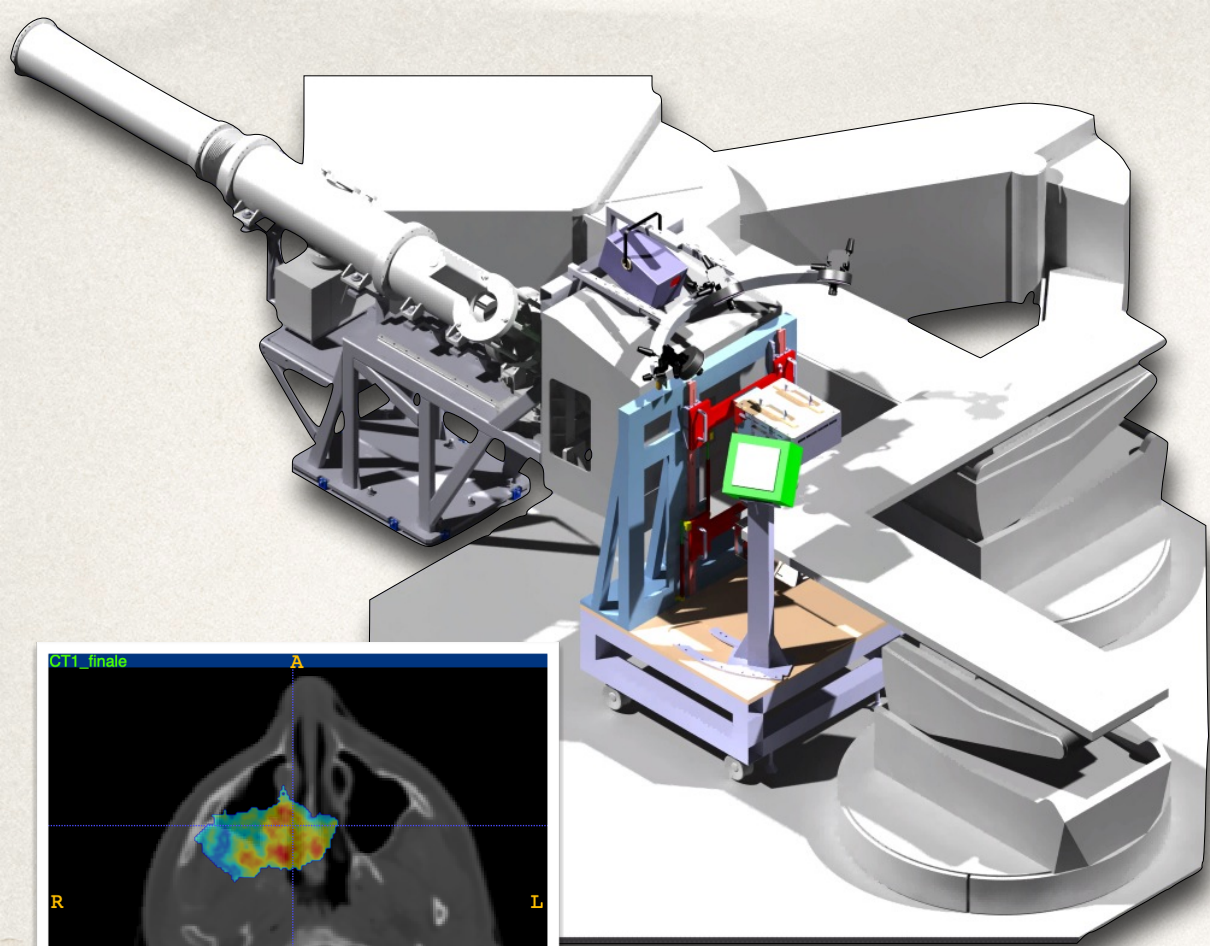
- ❖ **FRIDA** (Flash Radiotherapy with high Dose-rate particle beams): CALL CSN5 (INFN)



- ❖ **SHERPA** (Scintillating HETerostructures for high Resolution fast PET imAging): **PRIN2020**, PI Angelo Monguzzi (Università degli Studi Milano Bicocca)

<https://www.mur.gov.it/it/atti-e-normativa/decreto-direttoriale-n-2435-del-20-10-2021>





Grazie per l'attenzione



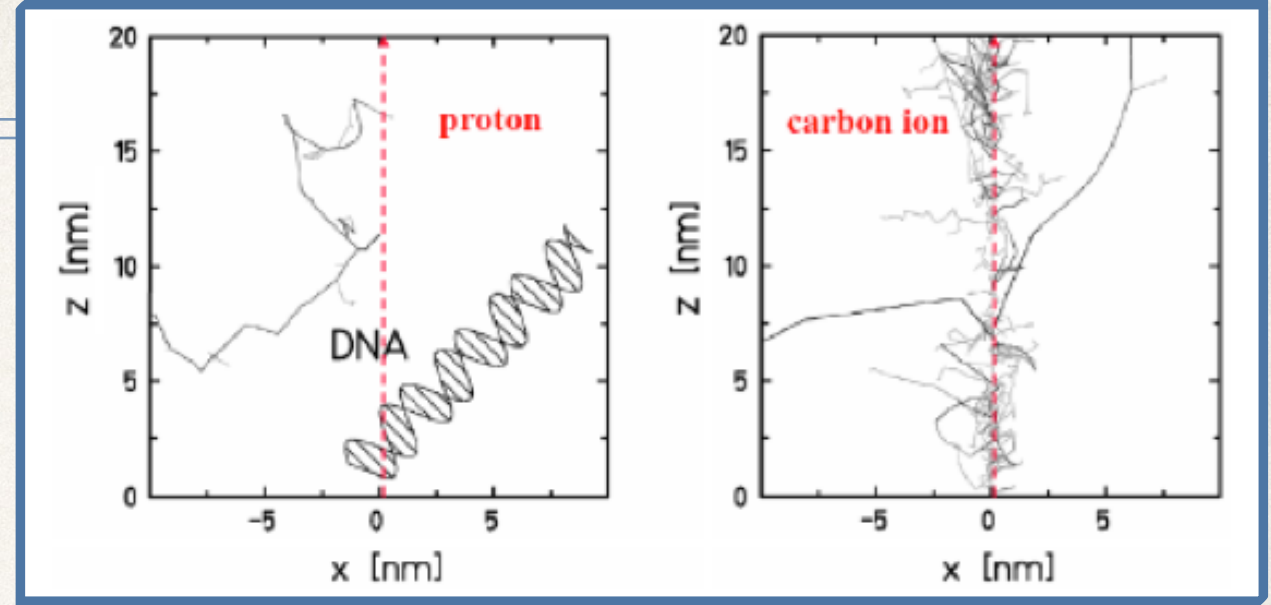
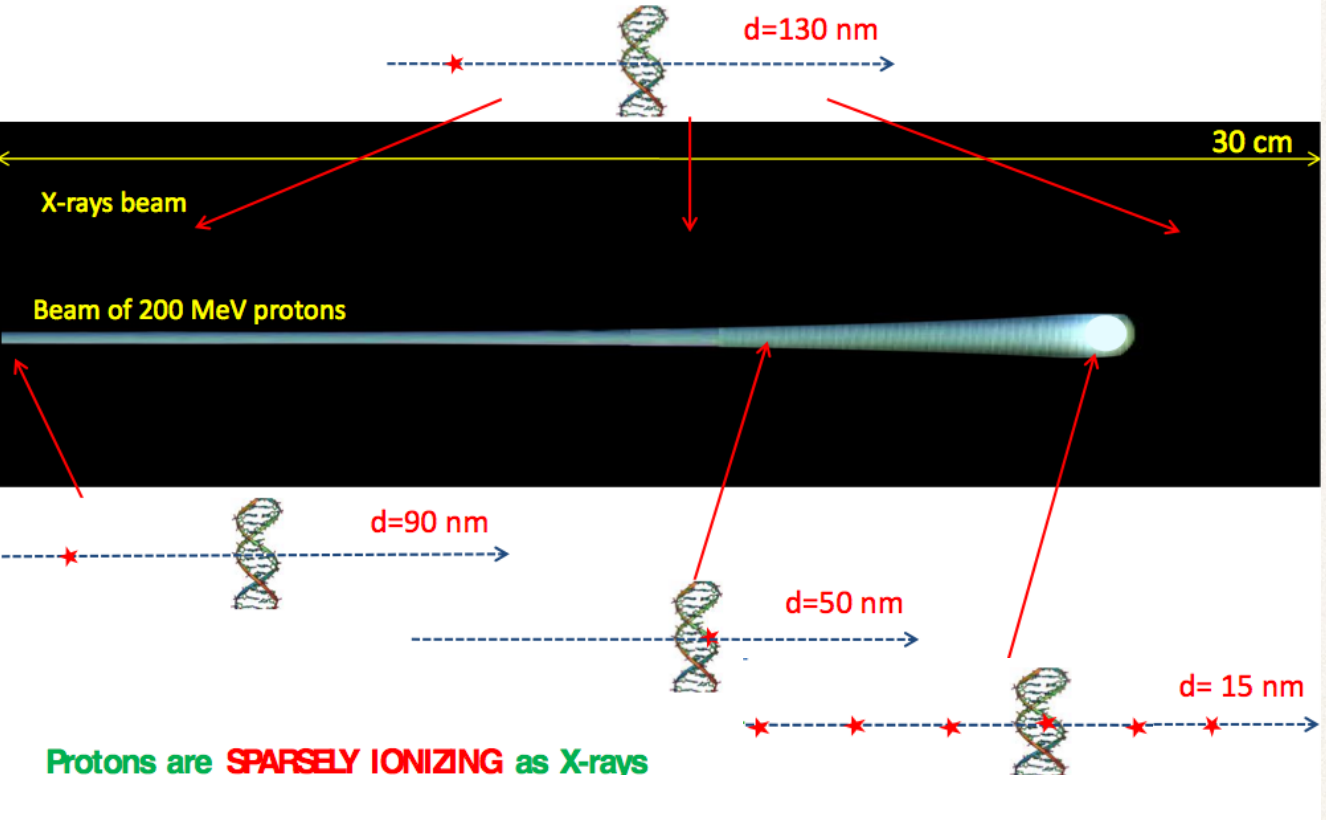
ilaria.mattei@mi.infn.it

SPARES

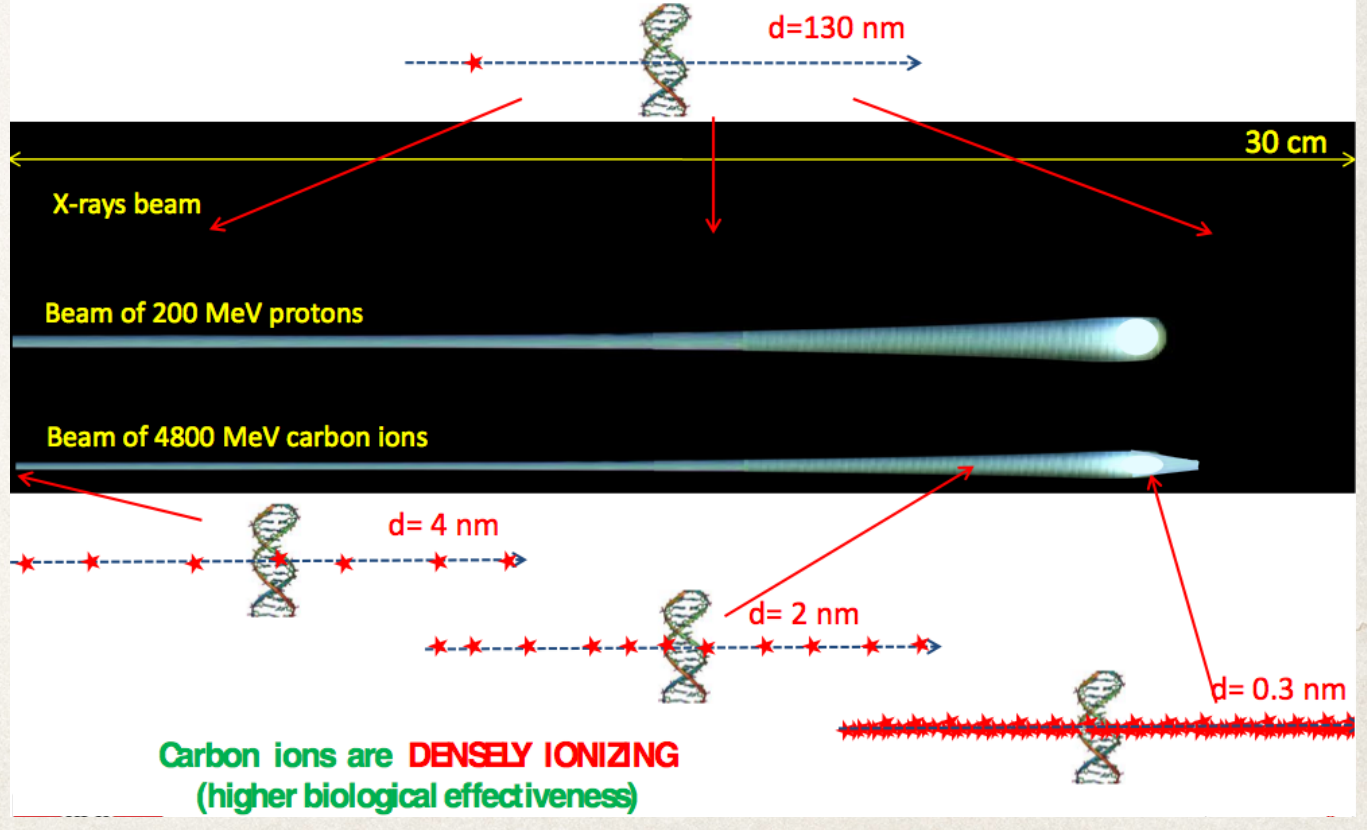
Protons vs ^{12}C

❖ Ionization density (LET)

Protons: 1. more favorable dose 2. same 'indirect effects'



Carbon ions: 1. more favorable dose 2 'direct effects'

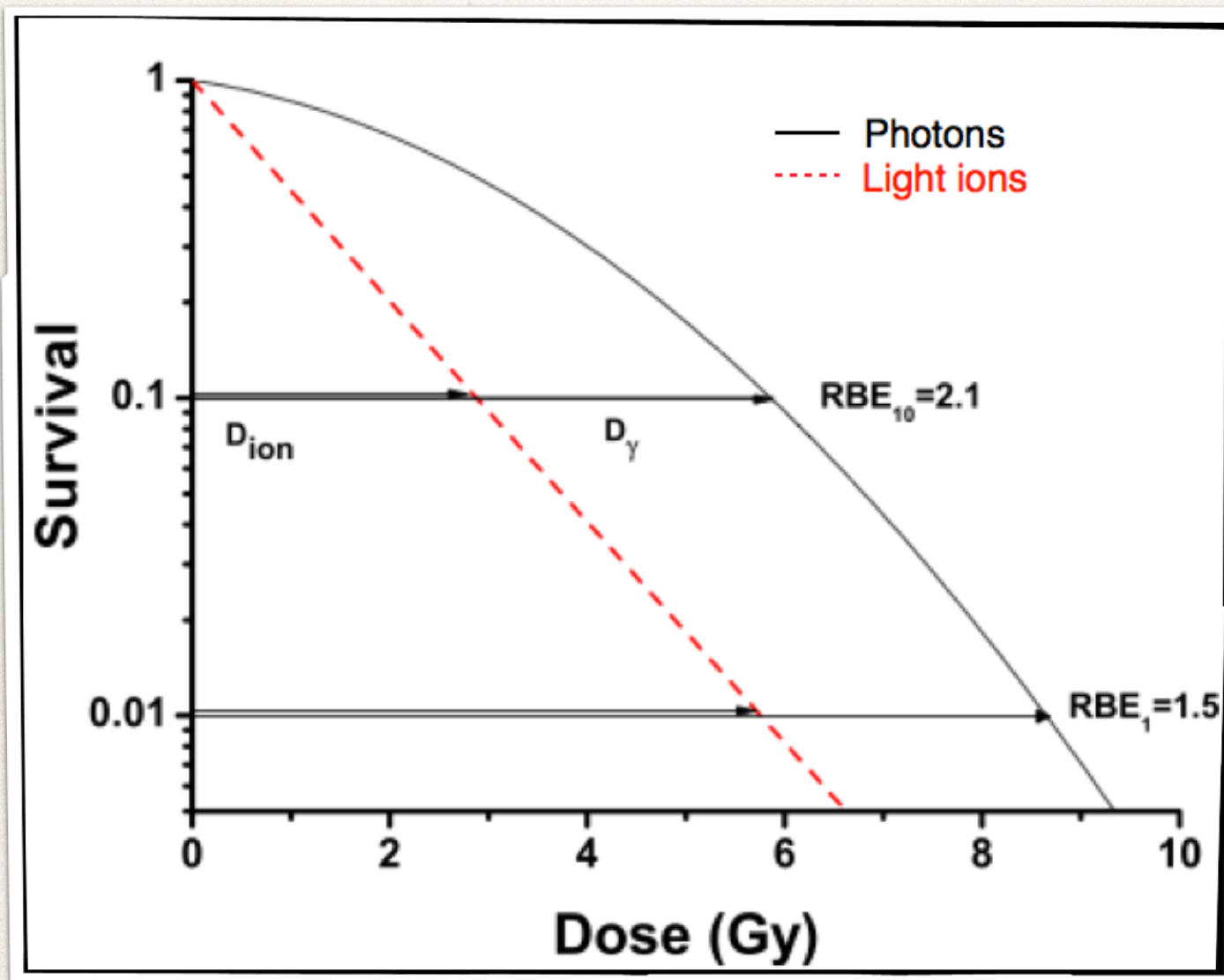
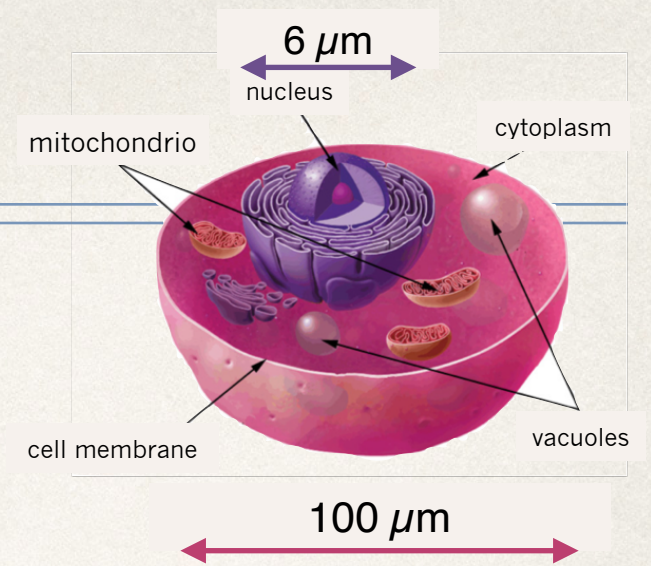


For the beam delivery techniques:
MS is exploited for PROTONS (passive) but NOT for heavier ions (fragmentation=>active)

RBE

❖ Survival Fraction

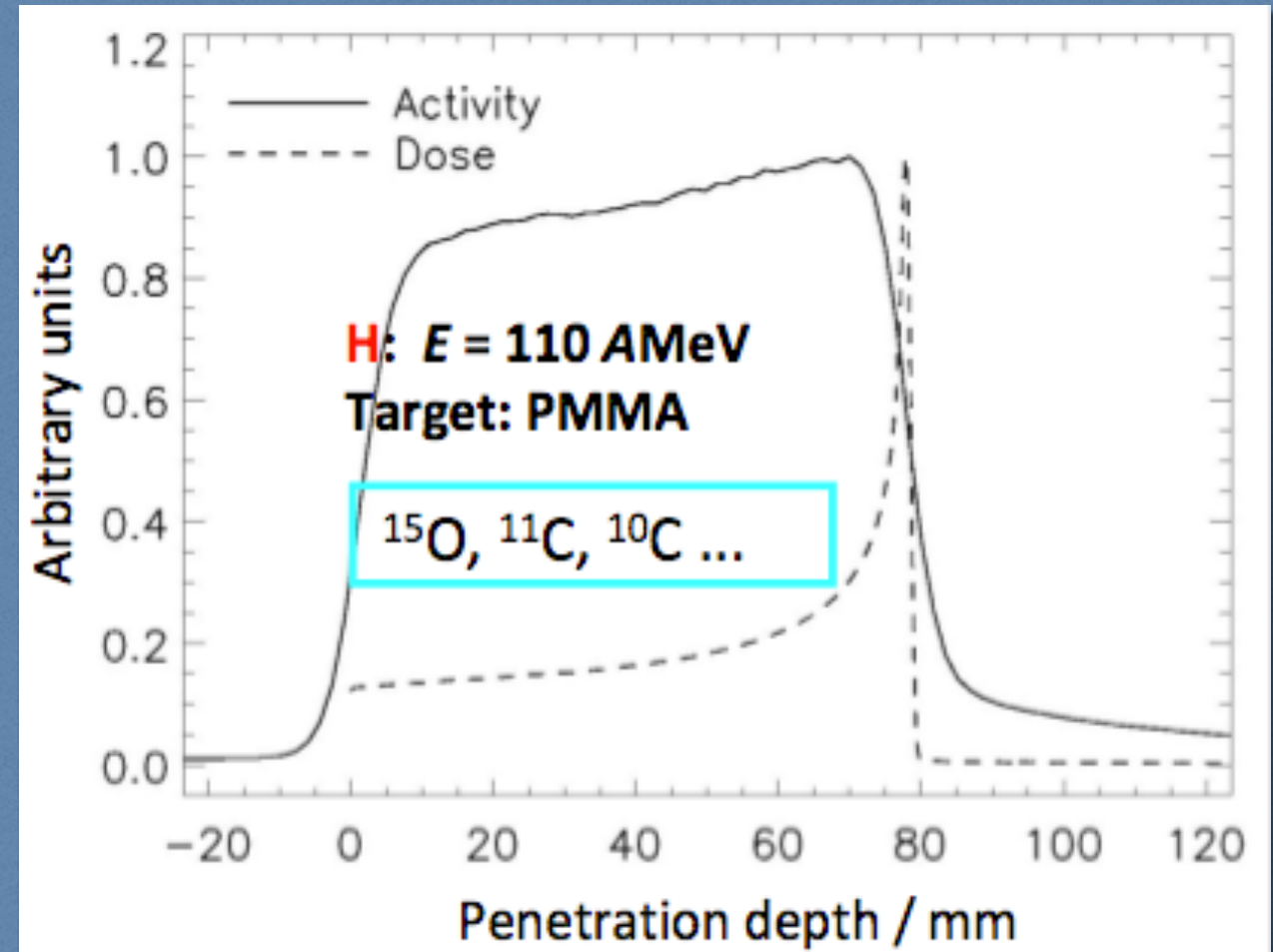
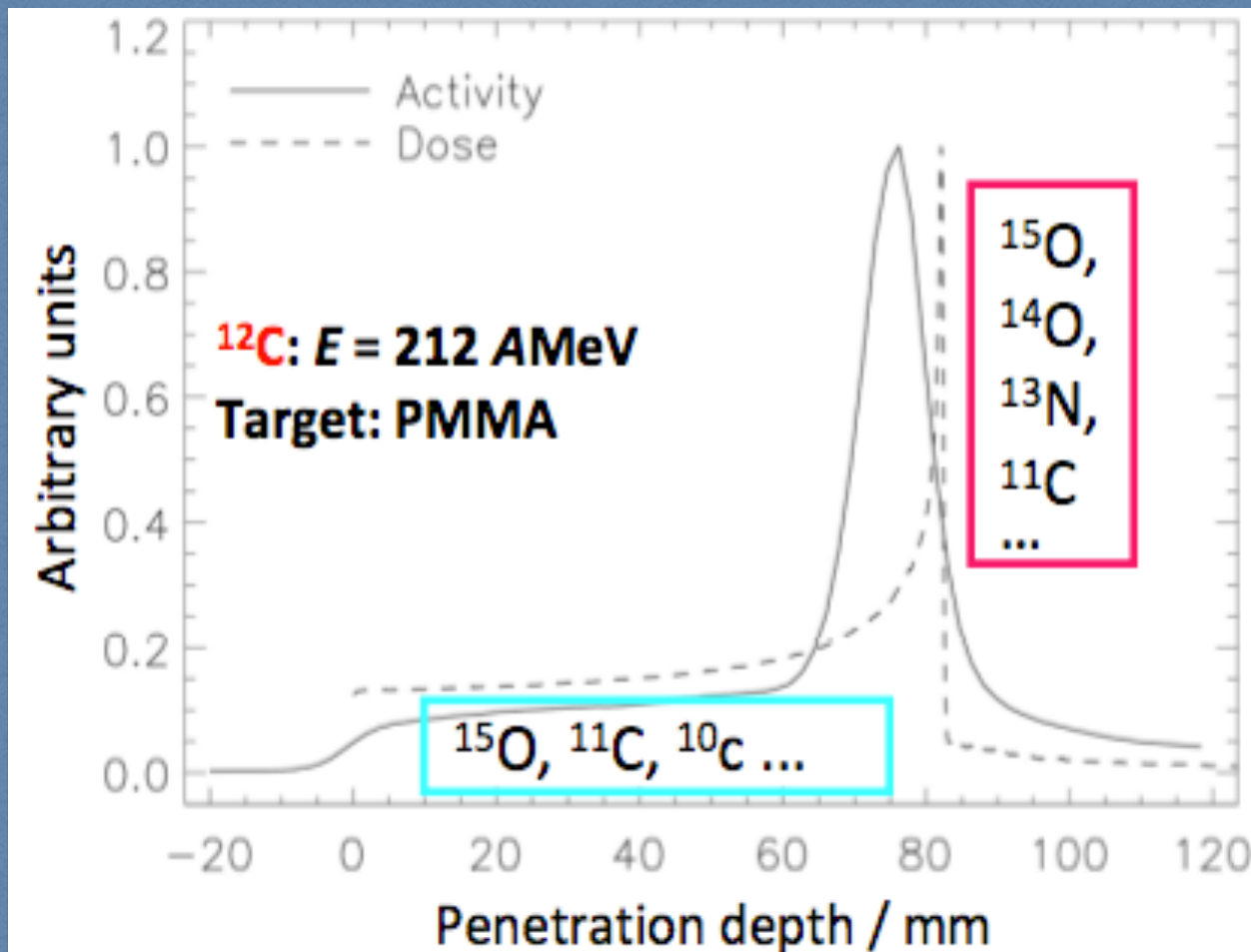
$$S = \frac{N_{surv}}{N_{seed}} = e^{-(\alpha D + \beta D^2)}$$



❖ Relative Biological Effectiveness

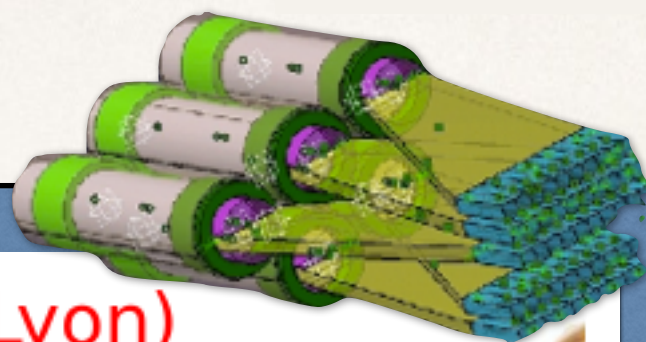
$$RBE = \frac{D_\gamma}{D_{ch}} \Big|_{iso}$$

Dose Monitoring: PET- γ

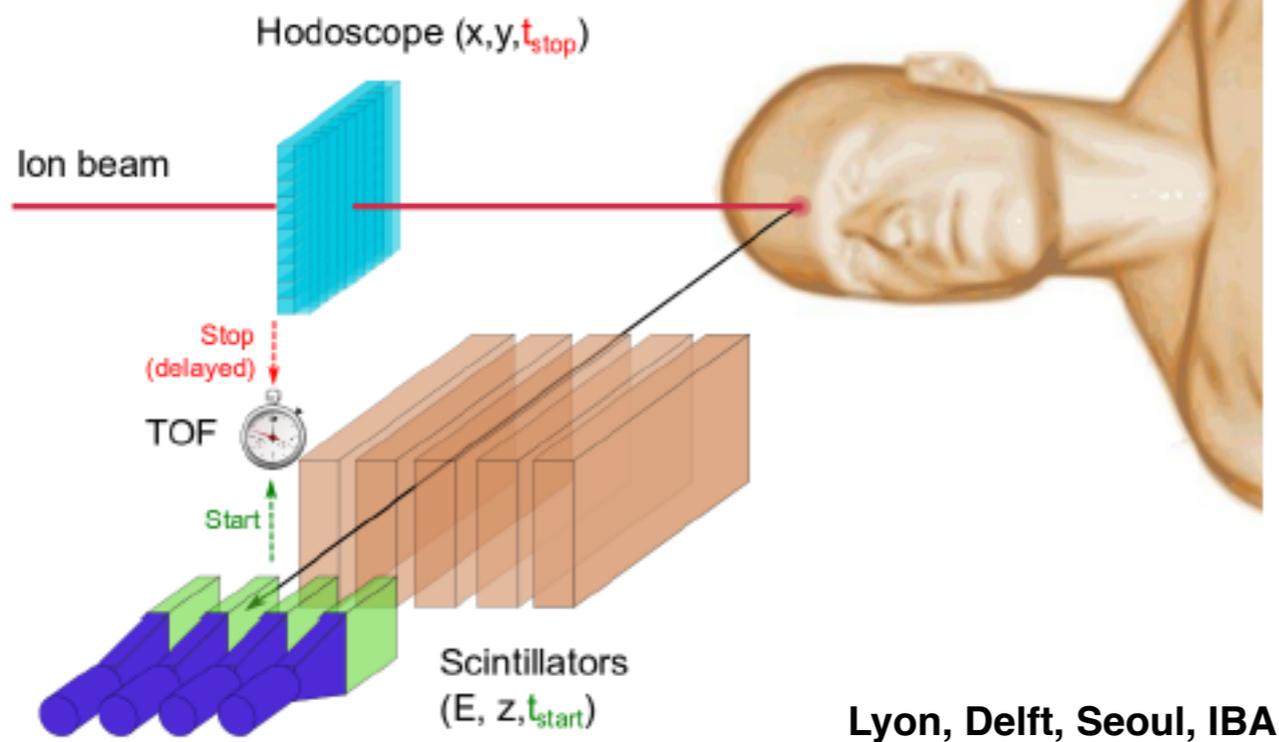


The β^+ activity emission shape is correlated with the dose distribution (and to the Bragg Peak position). The β^+ emits a positron that produces two (back-to-back) 511 keV photons during its annihilations.

Dose Monitoring: Prompt- γ



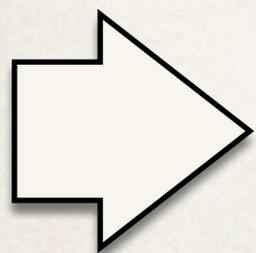
Multi-slit camera (Lyon)



- Difficult to stop and collimate prompt photons (large energy spectrum: 1-10MeV)
- Huge neutron background
- Abundant Secondaries

Balance of promptly emitted particles outside the target:

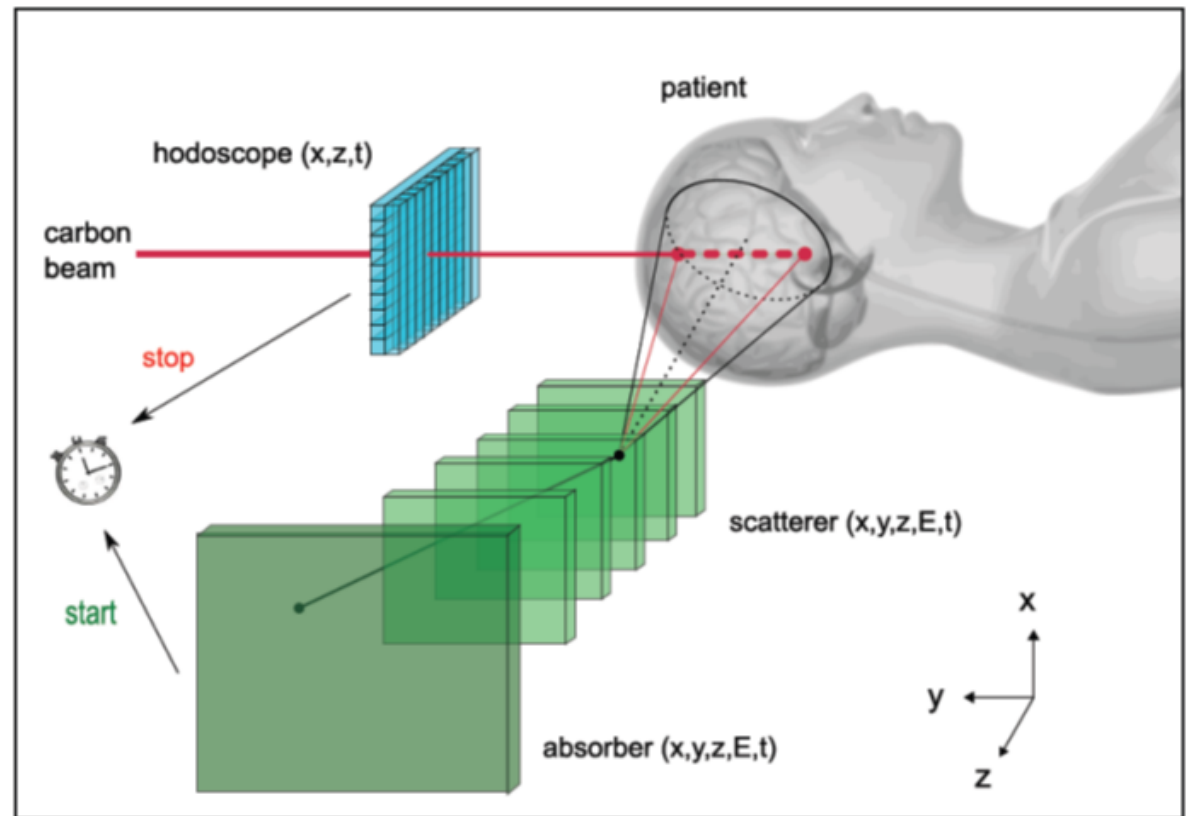
Incident protons:	1.0	($\sim 10^{10}$)
γ -rays:	0.3	($3 \cdot 10^9$)
Neutrons:	0.09	($9 \cdot 10^8$)
Protons:	0.001	($1 \cdot 10^7$)
α -particles:	$2 \cdot 10^{-5}$	($2 \cdot 10^5$)



Millimetric range-control at the pencil-beam scale for protons

Dose Monitoring: Prompt- γ

Compton Camera



- No collimation: potentially higher efficiency
- Potentially better spatial resolution ($< 1\text{cm}$ PSF)
- If beam position known simplified reconstruction
- 3D-potential imaging (several cameras)

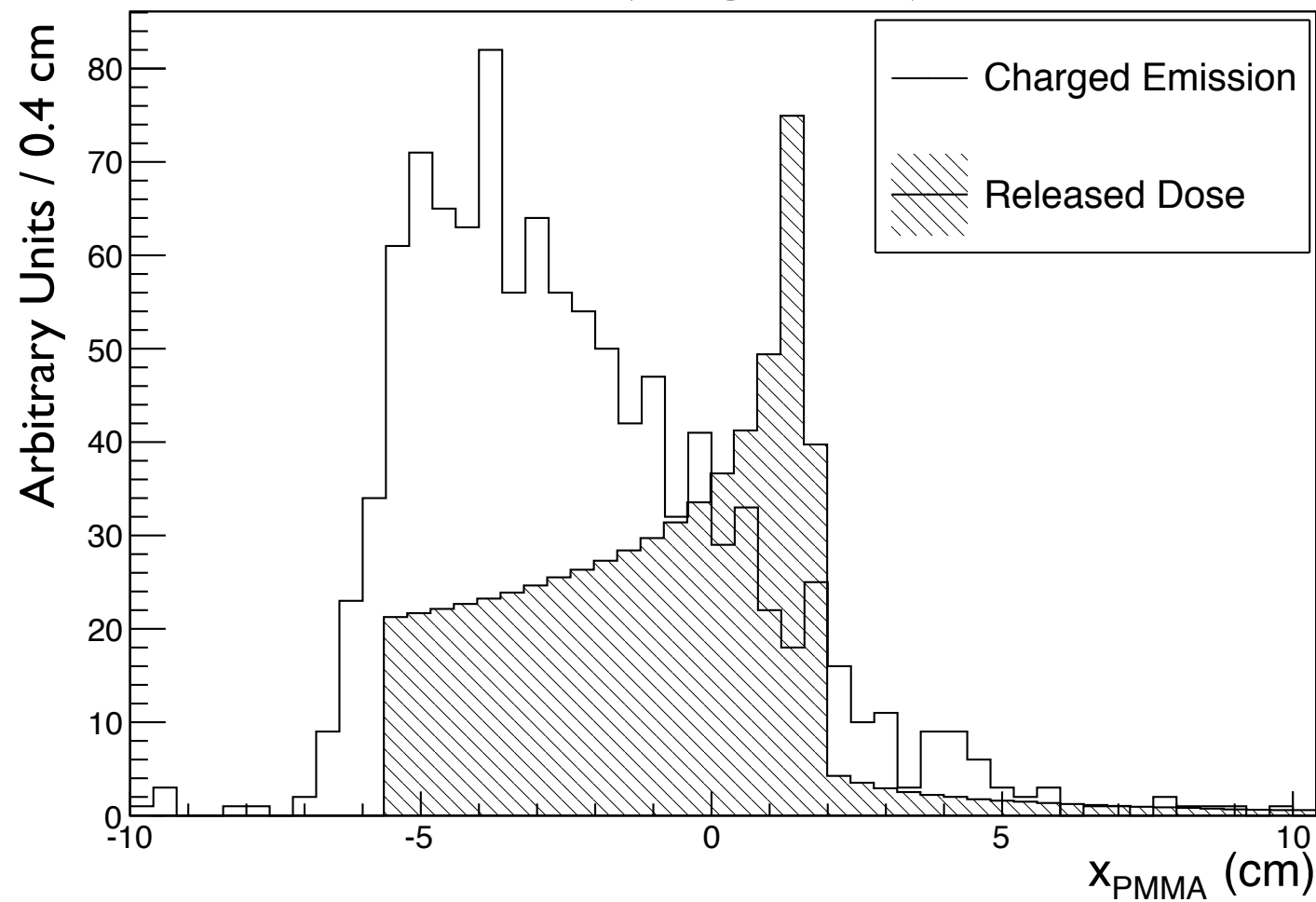
➔ Main issue: necessity to work at reduced intensity

Courtesy of D.Dauvergne PET symposium 2014

Dose Monitoring: Charged Fragments

Charged secondary particles: protons, deuterons and tritons..

Measured emission profile (^{12}C @PMMA)



Charged secondary particles are mainly produced before the Bragg Peak. The emission shape can be correlated with the BP position.

Dose Monitoring: Charged Fragments

Charged secondary particles: protons, deuterons and tritons..

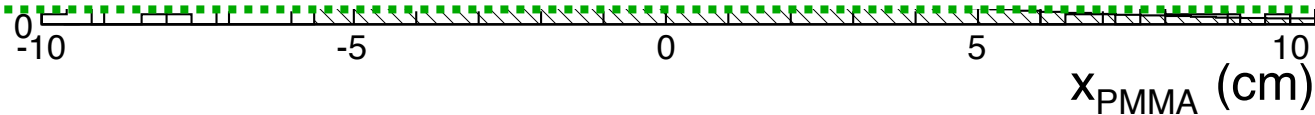
Measured emission profile (^{12}C @PMMA)



Charged secondary particles
a... before

FEATURES

- The detection efficiency is very high;
- Can be easily back-tracked to the emission point => the distribution of the emission points can be correlated to the beam profile;
- They are not so many;
- Energy threshold to escape $\sim 50\text{-}100$ MeV;
- They suffer multiple scattering inside the patient -> worsen the back-pointing resolution;



Charged Fragments: Detection Angle

The main contributions to the uncertainty of the emission point determination of secondary charged particles are:

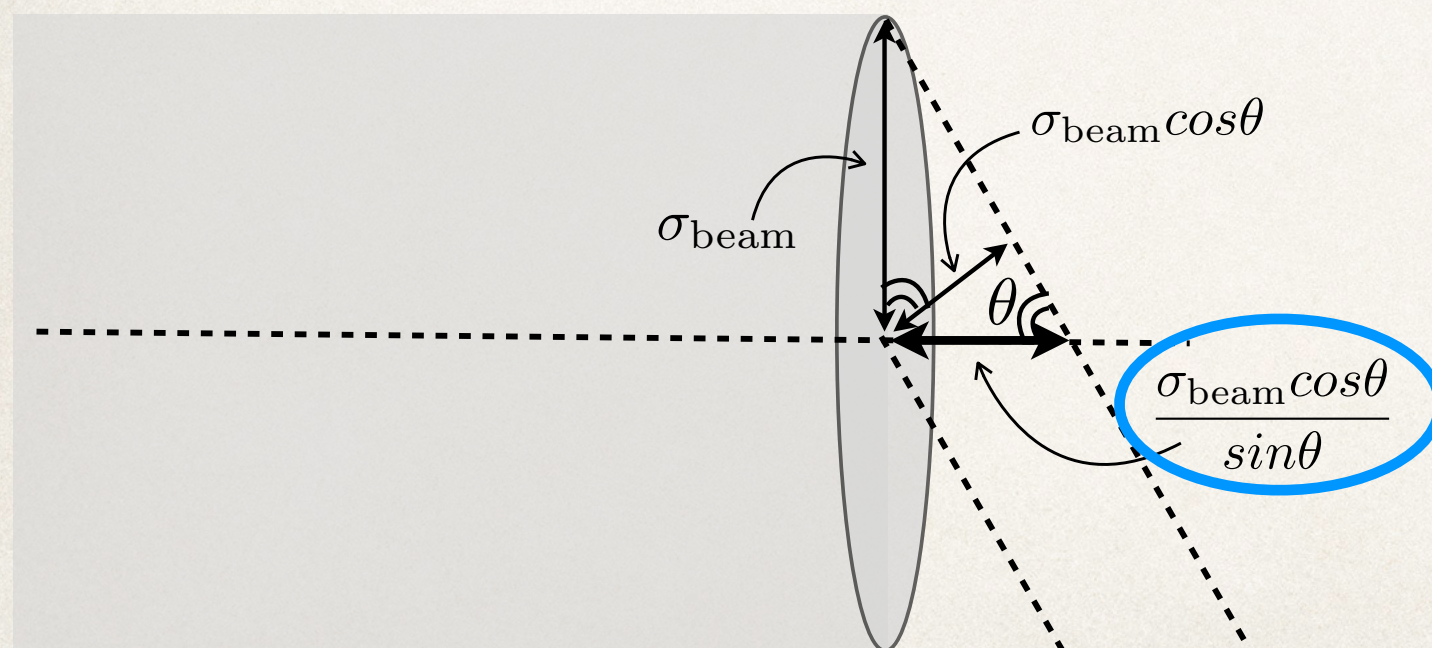
- ❖ the Multiple Scattering inside the target ($\propto \sqrt{x}, E^{-1}$)
- ❖ the statistics ($\propto \vartheta$)
- ❖ The DCH resolution (to the beam line)
- ❖ the beam spot dimension ($\sim 2 \text{ mm} - 1.5 \text{ cm}$)

COMPENSATION:

Low ϑ (high stat)

Large $E \Rightarrow$ Low MS

Large $x \Rightarrow$ Large MS



**LOWERED AT
LARGE
ANGLES**

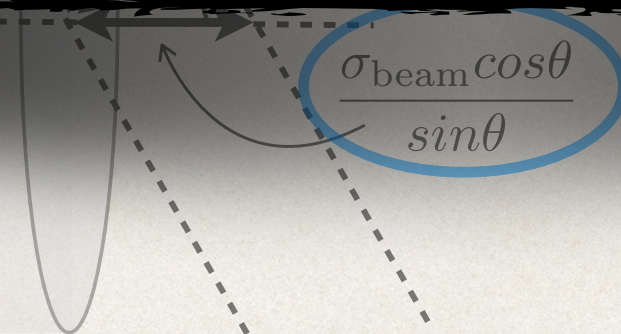
Charged Fragments: Detection Angle

The main contributions to the uncertainty of the emission point determination of secondary charged particles are:

- ❖ the Multiple Scattering inside the target ($\propto \sqrt{x}, E^{-1}$)

COMPENSATION:

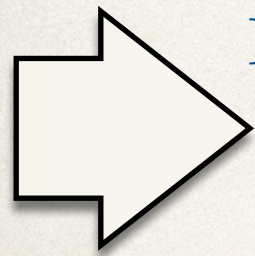
- ❖ In a treatment room, very often the positions at low ϑ are not available to a monitor
- ❖ device, in particular in the treatment configuration where the patient body is aligned with the beam axis.



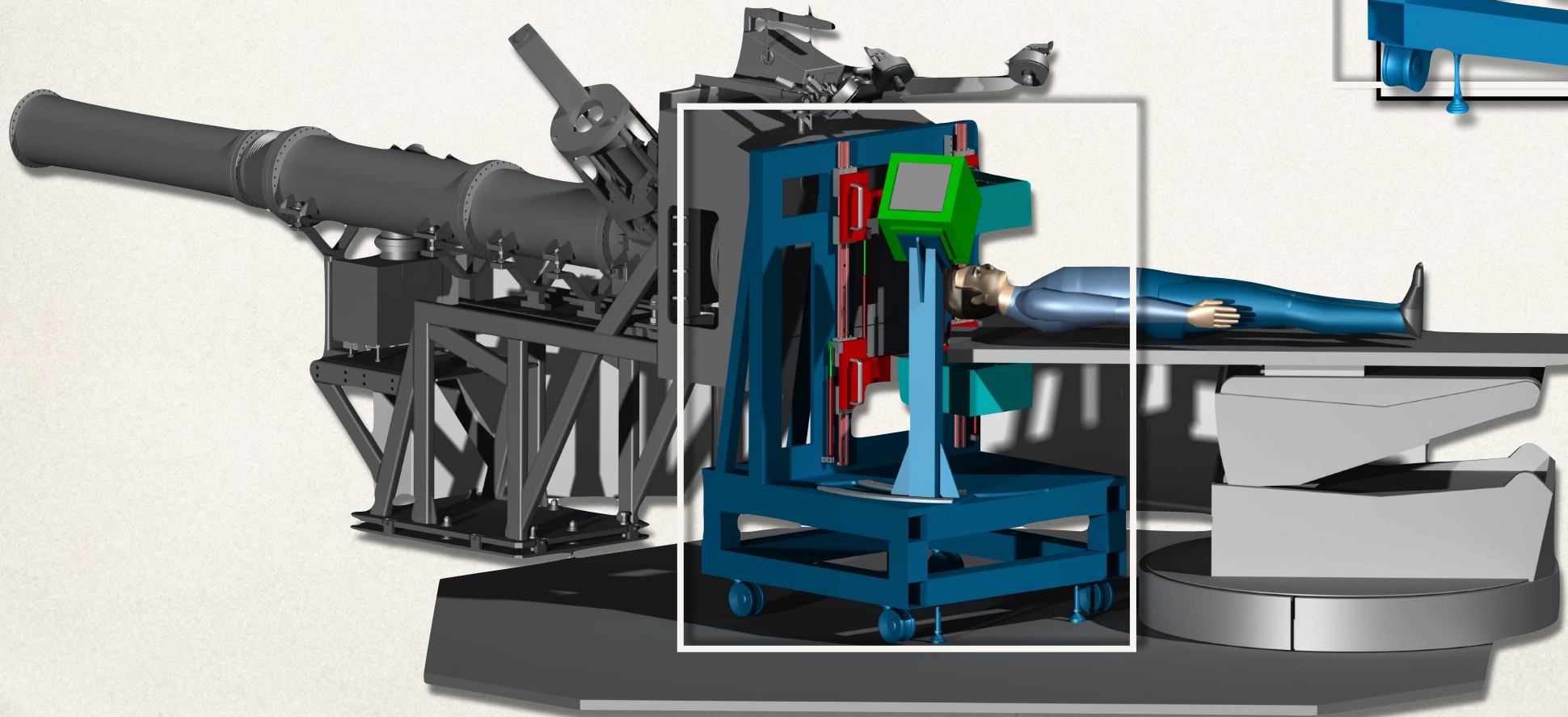
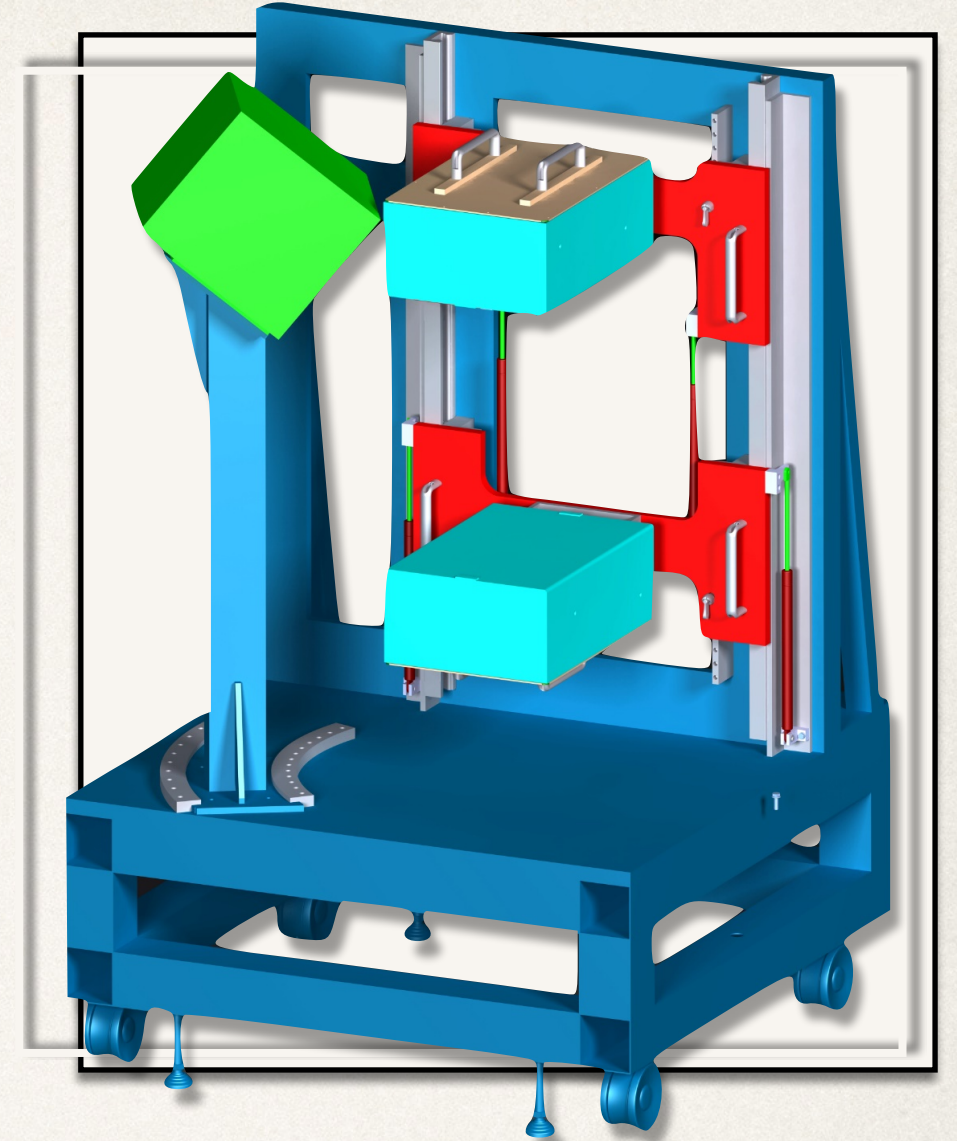
**LARGE
ANGLES**

The INSIDE Project

The project addresses the dose monitoring on line problem: two PET-heads to β^+ activity measurements and a Dose Profiler for the reconstruction of the charged secondary particles emission distribution.

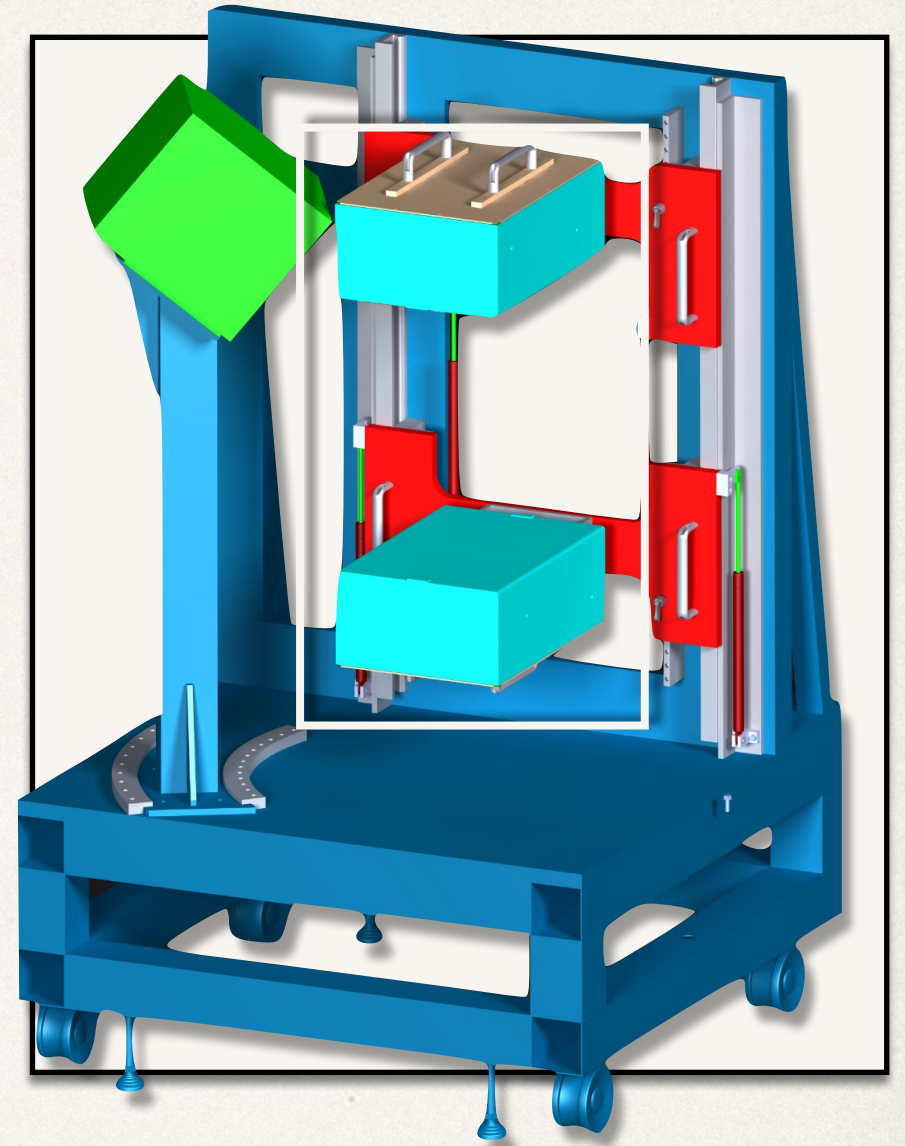


For the CNAO measurements we design a cart in order to hold up the detectors minimizing the interferences with therapy procedures



The INSIDE Project

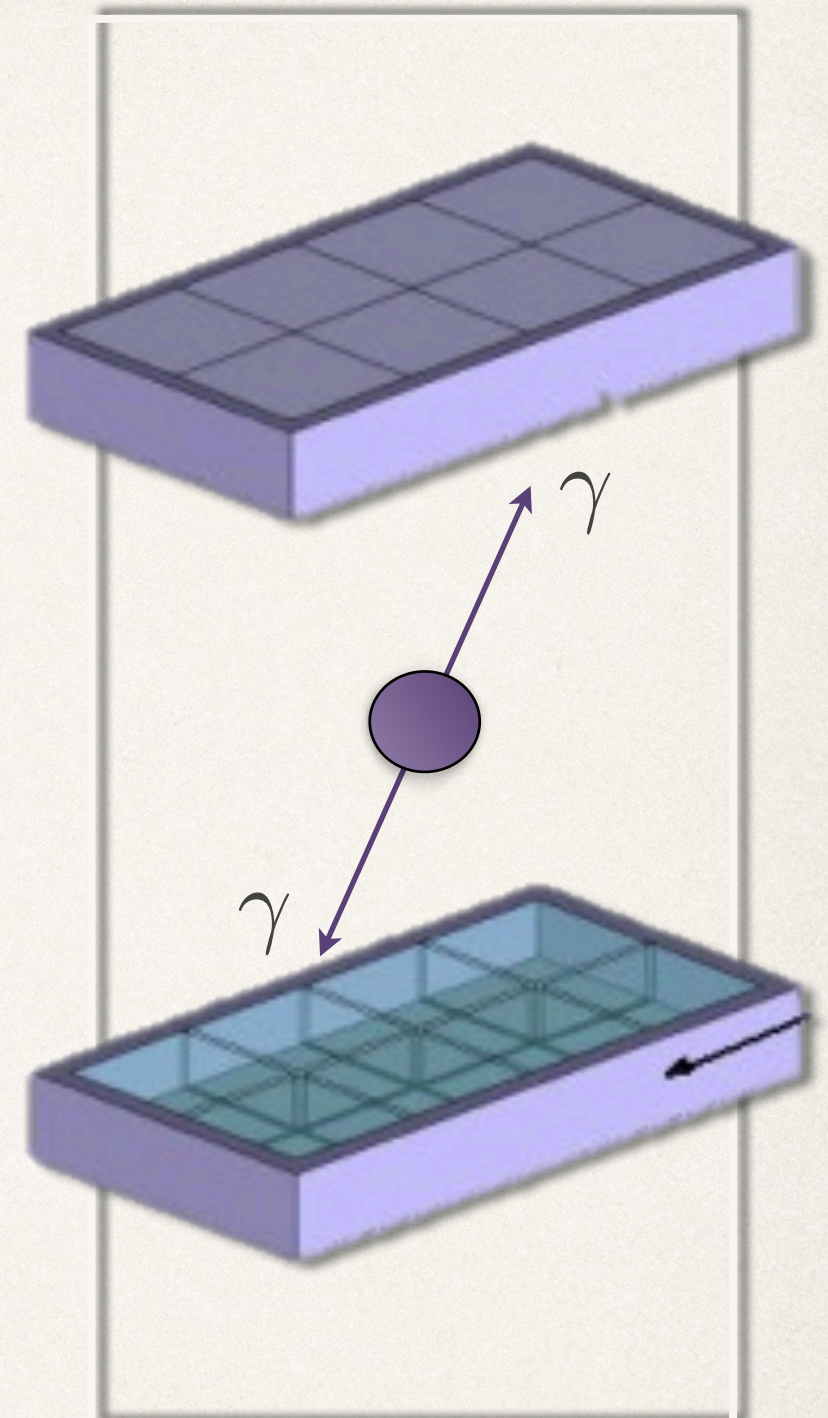
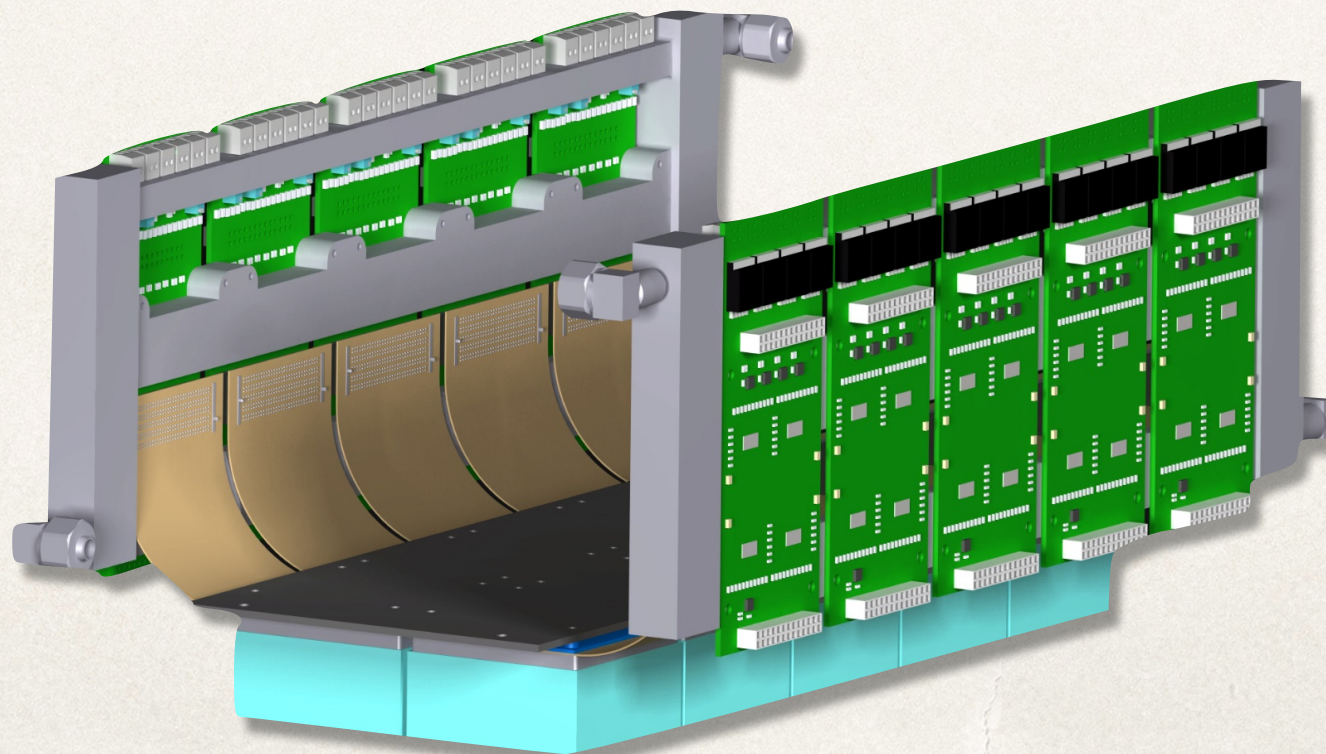
- ❖ Detectors to measure the 511 keV photons in order to reconstruct the β^+ activity map;
- ❖ Full in-beam PET system able to sustain annihilation, prompt photon and neutron rates during the beam irradiation (in-beam and inter-spill);



Total sensitive area of a module: 5 cm x 5 cm

The INSIDE Project

- ❖ Detectors to measure the 511 keV photons in order to reconstruct the β^+ activity map;
- ❖ Full in-beam PET system able to sustain annihilation, prompt photon and neutron rates during the beam irradiation (in-beam and inter-spill);
- ❖ Two planar panels: 10 cm x 20 cm wide => 2 x 4 detection modules;



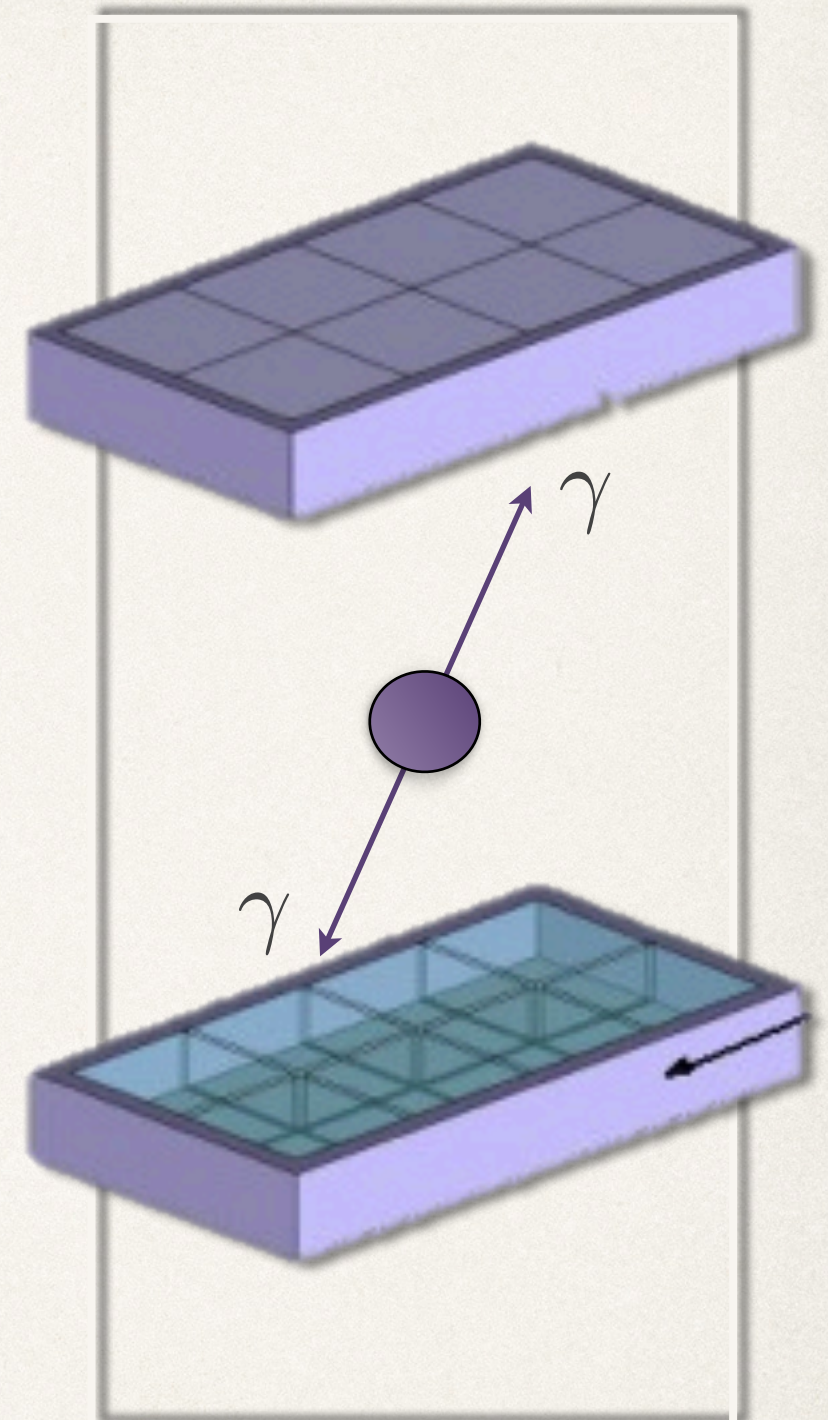
=> 511 keV back-to-back

The INSIDE Project

- ❖ Detectors to measure the 511 keV photons in order to reconstruct the β^+ activity map;
- ❖ Two planar panels: 10 cm x 20 cm wide => 2 x 4 detection modules;

- Each module is composed of a pixelated LYSO matrix 16 x 16 pixels, 3 mm x 3 mm crystals (pitch 3.1mm);
- LYSO matrix readout: array of SiPM (16x16 pixels) coupled one-to-one.

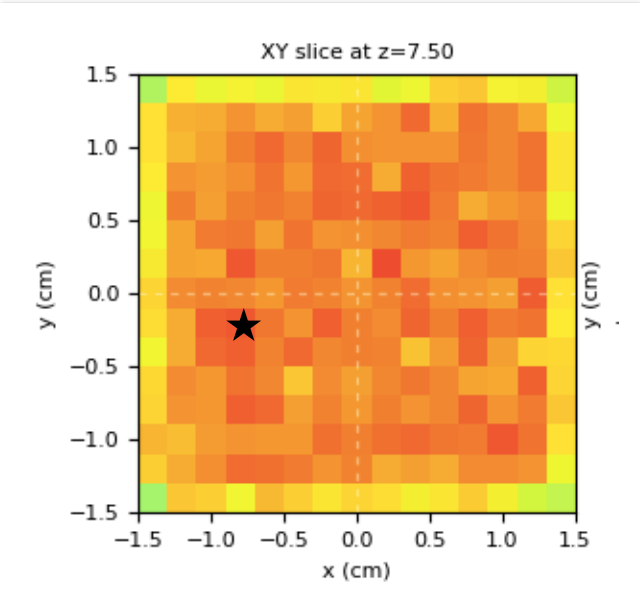
The **resolution** of the two PET heads system in the β^+ activity reconstruction map is expected to be between 1 and 2 mm (FWHM) in beam direction.



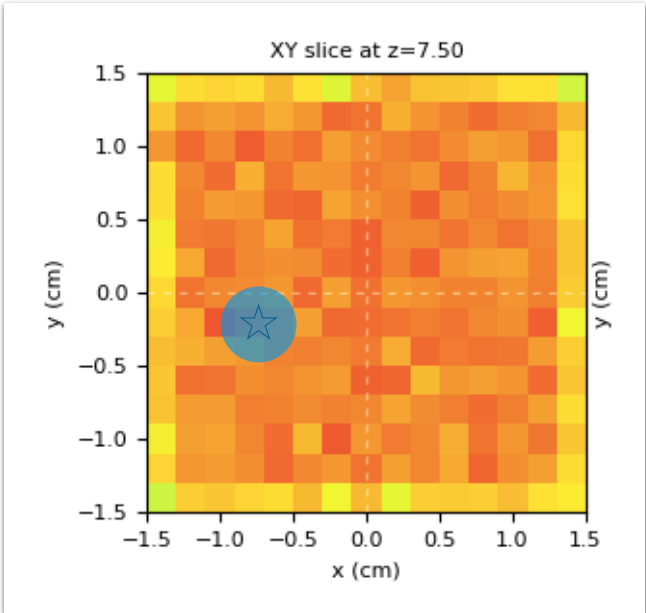
=> 511 keV back-to-back

Gamma index analysis

First Map



Second Map



γ -index 2mm/3%

$$\Gamma(\vec{r}_e, \vec{r}_r) = \sqrt{\frac{|\vec{r}_e - \vec{r}_r|^2}{\Delta d^2} + \frac{[D_e(\vec{r}_e) - D_r(\vec{r}_r)]^2}{\Delta D^2}}$$

D= dose (D_r of the reference map, D_e of the evaluation map)

r = position of the evaluated point (r_r of the reference map, r_e of the evaluation map)

$$\gamma(\vec{r}_r) = \min\{\Gamma(\vec{r}_e, \vec{r}_r)\} \forall \{\vec{r}_e\}$$

$\gamma \leq 1$ = test passed

$\gamma > 1$ = test NOT passed

pass rate $\geq 92\%$
clinical acceptance

